Circum-Pacific Seismic Potential
1989-1999

S.P. Nishenko

Final Report to
Agency For International Development
Office of U.S. Foreign Disaster Assistance
under PASA BOF-0000-P-IC-4051-00
"Comparative Earthquake and Tsunami Potential
for Zones in the Circum-Pacific Region"

U.S. Geological Survey Open File Report 89-86

Table of Contents

(p.v follows)

Acknowledgements

A review and synthesis of this scope could not have been completed without the advice and support of numerous experts and friends in the circum-Pacific community. Thanks go to Brian Atwater, Sue Beck, Tom Boyd, Ray Buland, Doug Christensen, Jim Dewey, Bob Engdahl, Al Espinosa, Klaus Jacob, Paul Krumpe, Bob Massé, Bill McCann, Karen McNally, Carlos Mendoza, Dave Perkins, Enrique Silgado, Krishna Singh, Lynn Sykes, Rick Terman, Randy White, Mary Ellen Williams, and last, but not least, my fellow members of the Working Group on California Earthquake Probabilities. The additional task of reviewing this manuscript fell on Ray Buland, Jim Dewey, Al Espinosa, and Bill Spence. Their comments were invaluable in improving the overall presentation.

(p. vii follows)

Glossary of Terms, Symbols, and Abbreviations

A .... Area of fault dislocation or earthquake rupture zone.
Aftershock .... Secondary, smaller magnitude earthquakes following a mainshock.
Aseismic slip .... The occurrence of fault motion without earthquakes.
Asperity .... Area of geometric complexity, or increased strength, on a fault surface.
Body wave .... Seismic waves transmitted through the interior of the Earth, e.g. P and S waves.
^{14}C .... Radioactive isotope of Carbon used for radiometric dating.
Characteristic earthquake .... An earthquake which repeatedly ruptures a fault segment, and whose dimensions define that fault segment.
Coefficient of variation .... The ratio of the standard deviation, σ, to the mean, μ.
Conditional probability .... Probability of an event to occur within a specific time interval, conditional upon the event not having occurred prior to the beginning of that time interval.
Convergent margin .... Zone of plate collision, resulting in subduction, earthquakes, volcanism, and mountain building.
Coseismic displacement .... Amount of movement on a fault surface during an earthquak
COR .... Compressional outer-rise earthquake.
Dendrochronology .... Tree ring dating.
Earthquake cycle .... The process of strain accumulation bewteen two characteristic earthquakes.
Forecast time window .... $\pm 90\%$ confidence interval about T_{exp}.
Great earthquake .... Earthquake with $M_S, M_W \geq 7.7$.
IDNDR .... International Decade of Natural Disaster Reduction.
Interplate earthquake .... Earthquake occurring along the edge of a plate boundary.
Intraplate earthquake .... Earthquake occurring in the interior of a plate.
Large earthquake .... Earthquake with $7.0 < M_S < 7.7$.
Lognormal distribution .... Probability distribution that is normally distributed about the mean in log space.
MM Intensity .... Modified Mercalli intensity, a subjective scale with ratings from I to XII, which describes the effects of an earthquake.
Magnitude .... A measure of energy release in an earthquake.
m_b .... Body-wave magnitude.
M_S .... Surface-wave magnitude.
M_t .... Tsunami-wave magnitude.
M_W .... Seismic moment magnitude.
Major earthquake .... An earthquake with $M_S \geq 7.0$.
M_O .... Seismic moment.
μ .... Shear modulus.
μ_D .... Mean of lognormal distribution.
Plate .... One of the mechanically independent lithospheric segments comprising the outermost layer of the Earth.
Poisson distribution .... Probability distribution that is exponentially distributed about the mean.

Repeat time	Time interval between two events of similar location, mechanism, and magnitude.
Seismic gap	Segment of a simple plate boundary with a history of either large or great earthquakes, and no similar occurrence within the last 30 years.
Seismic potential	Estimate of conditional probability for a seismic gap.
σ_B	Variability of median recurrence estimates.
σ_D	Intrinsic, global variability of recurrence times, μ_D=0.215.
σ_M	Total variability of recurrence estimate, $\sigma_M^2 = \sigma_D^2 + \sigma_B^2$.
T	Individual recurrence interval for a fault segment.
$\overline{T}$	Median recurrence interval.
T_{ave}	Average recurrence interval for a fault segment.
t_o	Date of last earthquake.
T_{exp}	Estimated recurrence time.
T_{pred}	Predicted date of recurrence.
^{230}Th	Radioactive isotope of Thorium used for radiometric dating.
Time-dependent	Earthquake recurrence models which account for the time since the last event.
Time-independent	Earthquake recurrence models which do not account for the time since the last event.
Time-Predictable model	Earthquake recurrence model where the repeat time is proportional to the size of the preceeding event.
Transform margin	Zone of horizontal motion between plates.
TOR	Tensional outer-rise earthquake.
U	Average coseismic displacement.

Executive Summary

The International Decade of Natural Disaster Reduction comes at a time when many nations are faced with the inevitability of natural disasters and the harsh realities of restricted economic resources. The prudent development of disaster mitigation and reduction programs for specific locations, within socially beneficial time frames, requires an understanding of when and where natural disasters are to occur.

In the past 30 years, great strides have been made in the fields of seismology and geophysics towards understanding the nature of large and great earthquake occurrence along simple plate boundaries. More recently, these advances have led to the development of long-term earthquake forecasts for specific fault zones. Proof that these techniques and ideas are applicable to at least some areas of the circum-Pacific region was demonstrated by the successful forecast of the great (M_S 7.8) 1985 Valparaiso, Chile earthquake (Nishenko, 1985). The locations of other successful earthquake forecasts and predictions since 1940 are shown in Figure 1. At present, national earthquake prediction programs in the United States (Parkfield, California) and Japan (Tokai district) have identified these specific areas for intensive study based on regularities in the pattern of historic earthquake occurrence and the expectation of similar sized events in the near future. On a broader scale, The Working Group on California Earthquake Probabilities (1988) report represents one of the first national probabilistic forecasts for earthquake activity.

This report summarizes the known seismic history for more than 119 seismic gaps around the circum-Pacific region, and describes the potential for future large and great earthquake activity in terms of conditional probability for the next 10 years (1989-1999). These results are presented in the map "Seismic Potential of the Circum-Pacific, 1989-1999" (Plate 1.) The level of reliability associated with these forecasts varies from region to region, and is influenced by the completeness of the historic earthquake record and our present understanding of the mode of earthquake rupture in these regions. Presenting these data in a probabilistic framework accounts for individual variations in recurrence time along a specific fault segment, as well as errors in our determination of the *repeat time*, and provides a basis for uniform comparison of seismic hazard between segments which have differing recurrence times.

One advantage of studying such a broad and diverse area is that many seismic regions have relatively short recurrence times. The short observed recurrence times, 20 to 60 years, compared to 100 to 200 year intervals observed at many other plate boundaries, allows for the evaluation of earthquake forecasts in a relatively small amount of time. This rapid "turn around" time for scientific evaluations in turn can lead to a better understanding of longer-term processes occurring at other regions and the overall improvement of strategies for implementing disaster mitigation programs.

Based on our assessment of the seismic potential of more than 119 gaps around the circum-Pacific region, we have compiled a list of the sites most likely to experience a large or great earthquake within the next 10 years (see Table 1). Large or major refers to those earthquakes with surface wave magnitudes (M_S) between 7.0 and 7 3/4. Great earthquakes are those events with seismic moment-magnitudes (M_W) larger than 7 3/4. The southwest Pacific region, including the islands of New Guinea, Vanuatu, and Tonga, presently contains the majority of high probability gaps. High potential gaps near population centers presently include Jama, Ecuador and southeastern Guatemala. This list does not preclude large or great earthquakes occurring in other segments with lower probabilities, however. Many segments of Central America have gaps, that while presently assigned intermediate probabilities for the next 5 years, will become areas of high concern within the next 10 or 20 years. Table 2 lists all of the high (i.e. $\geq$ 50%) probability regions for a 20 year window (1989-2009) and is of use for long-term planning. The 30 highly ranked gaps in Table 2 represent 1/4 of the total number of gaps studied. Many of these gaps are near urban centers and represent a potential future threat. The Appendix contains a list of all of the gaps studied, their coordinates, the date and magnitude of the most recent large or great earthquake, and probability estimates for 5, 10, and 20 year windows (i.e. 1989-1994, 1989-1999, and 1989-2009).

The assessment of long-term seismic hazard for the simple plate boundaries of the circum-Pacific region is an active and rapidly developing field. The time-dependent nature of these forecasts necessitate that these results be regularly updated. In addition, new data for other seismogenic regions and improvements in the model on which these assessments are based will lead to revision and refinement of the seismic hazard forecasts presented here. Development of reliable intermediate-term forecasts, which cover time intervals of years to months, will also need to be included in this assessment. These intermediate-term data can narrow the earthquake forecast time window, and provide additional motivation for increased awareness and action.

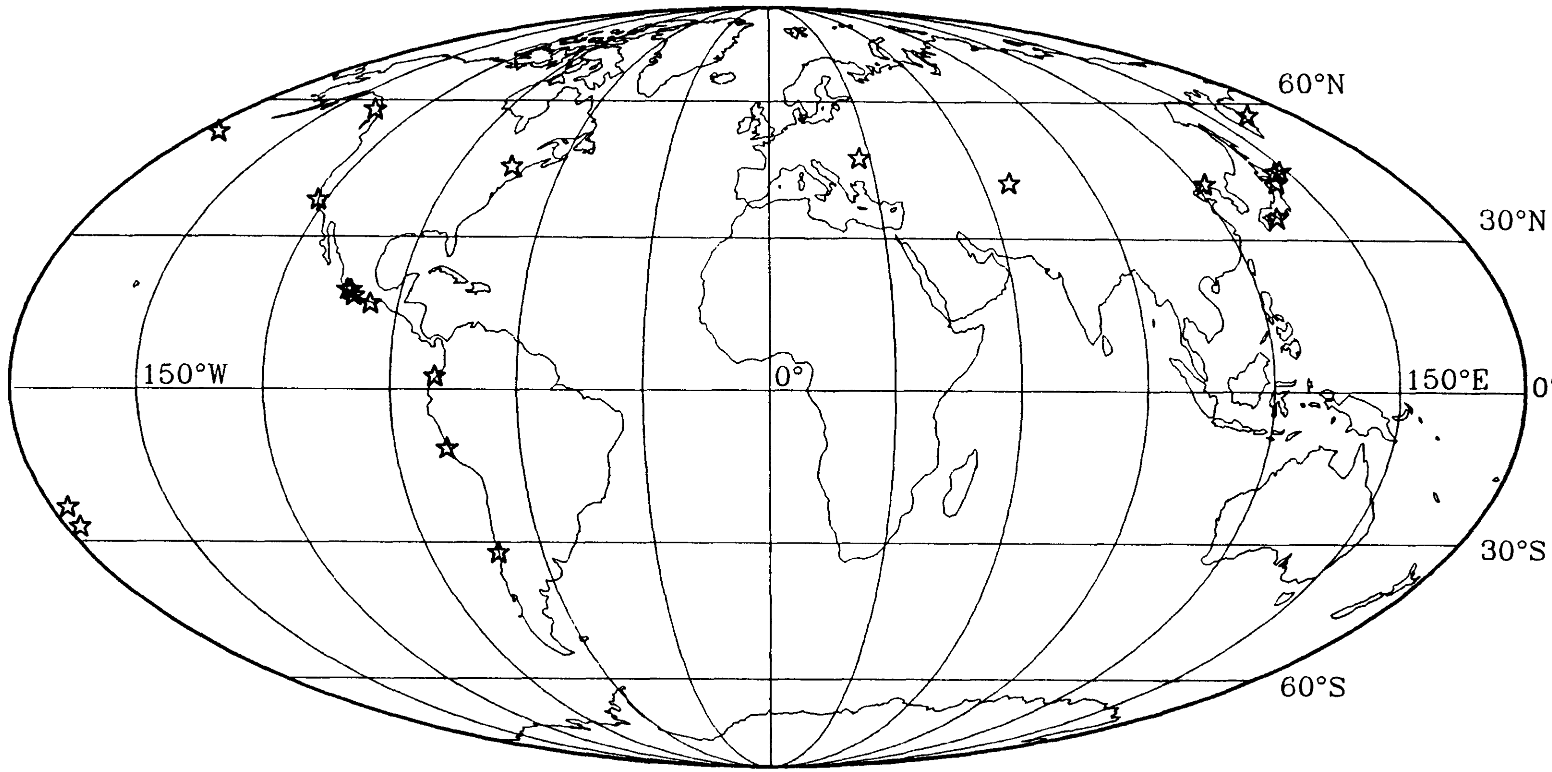

Figure 1. Successful earthquake forecasts and predictions. Stars show the location of successful earthquake forecasts and predictions from 1940 through 1986. While events in both intra- and interplate environments are shown, the majority of successful forecasts have been associated with interplate, or simple plate boundary, earthquakes (after Nishenko, 1989).

Table 1. Top Seismic Gaps
Gaps with $\geq$ 50% Conditional Probability for
Recurrence During 1989-1999

	Location	Magnitude	Last Event	Probability
1.	Parkfield, California	m_b 6.0	1966	93%
2.	Delarof Is., Aleutians	M_S 7.5	1957	(85%)
3.	Vankolo Is., Vanuatu	M_S 7.5	1980	83%
4.	Jama, Ecuador	M_S 7.7	1942	(66%)
5.	S. Santo Is, Vanuatu Is.	M_S 7.1	1971	60%
6.	E. New Britain, New Guinea	M_S 8.0	1971	59%
7.	W. New Britain, New Guinea	M_S 8.0	1945	(58%)
8.	Central Tonga	M_S 8.0	1948	58%
9.	N. Bougainville, New Guinea	M_S 8.0	1971	53%
10.	S.E. Guatemala	m_b 7.5	1915	51%

Probability values in parentheses reflect less reliable estimates.

Table 2. Top Seismic Gaps
Gaps with $\geq$ 50% Conditional Probability for
Recurrence During 1989-2009

	Location	Magnitude	Last Event	Probability
1.	Parkfield, California	m_b 6.0	1966	$\geq$99%
2.	Vankolo Is., Vanuatu	M_S 7.5	1980	99%
3.	Delarof Is., Aleutians	M_S 7.5	1957	(98%)
4.	Nicoya, Costa Rica	M_S 7.4	1978	93%
5.	Jama, Ecuador	M_S 7.7	1942	(90%)
6.	E. New Britain, New Guinea	M_S 8.0	1971	92%
7.	S. Santo Is, Vanuatu	M_S 7.1	1971	91%
8.	N. Bougainville, New Guinea	M_S 8.0	1971	90%
9.	Central Tonga	M_S 8.0	1948	84%
10.	W. New Britain, New Guinea	M_S 8.0	1945	(84%)
11.	Santa Cruz, Vanuatu	M_S 8.1	1966	82%
12.	Loyalty Is., Vanuatu	M_S 7.2	1980	80%
13.	SE Guatemala	m_b 7.5	1915	79%
14.	Shumagin Is., Alaska	M_S 7.7	1917	75%
15.	Ometepec, Mexico	M_S 7.3	1950	74%
16.	C. Oaxaca, Mexico	M_S 7.8	1928	(72%)
17.	Guadacanal, Solomons	M_S 7.5	1988	71%
18.	San Cristobal, Solomons	M_S 8.0	1931	(71%)
19.	E. Oaxaca, Mexico	M_S 7.8	1965	70%
20.	Unimak Is., Alaska	M_S 7.4	1946	(67%)
21.	Fox Is., Aleutians	M_S 7.4	1957	(67%)
22.	Colima, Mexico	M_S 7.5	1973	66%
23.	West Oaxaca, Mexico	M_S 7.4	1968	64%
24.	Kamchatsky Pen., U.S.S.R.	M_S 7.5	1971	61%
25.	S. Valparaiso, Chile	M_S 7.5	1906	59%
26.	Papagayo, Costa Rica	M_S 7.5	1916	(55%)
27.	Tokai, Japan	M_S8.0	1854	(53%)
28.	Urup Is., Kuriles	M_S 8.5	1963	(52%)
29.	C. Guerrero, Mexico	M_S 7.8	1899-1911	(52%)
30.	C. Guatemala	M_S 7.9	1942	50%

Probability values in parentheses reflect less reliable estimates.

(p. 7 follows)

Introduction

It is generally known which population centers and sites of critical facilities around the circum-Pacific region have experienced destructive large (M_S 7.0-7.7) and great (M_W 7.7-9.3) earthquakes in the historic past. These same localities are also candidates for the inevitable recurrence of similar earthquakes and tsunamis at some time in the future. Hence, while it is of academic interest to know *how long* it has been since a prior destructive earthquake at a particular location; it is more important from a societal perspective to know when the *next* damaging event will occur. In an attempt to address these social concerns, the utilization of recent advances in seismology and geophysics have enabled the identification of specific areas around the circum-Pacific region that are thought to be the most likely sites of large and great earthquakes in the immediate future. This report represents, for the first time, a comprehensive survey of the likelihood of 119 seismic gaps around the circum-Pacific region to produce either large or great earthquakes during the next 10 to 20 years. The 10 year interval (1989-1999) overlaps the International Decade of Natural Disaster Reduction (IDNDR).

The portrayal of seismic hazards around the circum-Pacific region involves comparison of many fault segments, or portions of plate boundaries, that exhibit varying recurrence times, earthquake magnitudes, and tectonic regimes. Presenting these data in terms of a probabilistic earthquake forecast, which describes the conditional probability for an event to occur within some future time window (i.e. the next 5, 10, or 20 years) provides a framework for this type of global comparison. While not funded under this contract, this report also includes results, using the same statistical methodology, for the western and northern coasts of North America. We have incorporated these additional results to present a comprehensive survey of seismic potential in the circum-Pacific region.

Methodology

In this study, we have attempted to quantitatively describe the seismic hazards associated with the future recurrence of large and great earthquakes along segments of the circum-Pacific seismic zone. These events are termed interplate earthquakes and reflect motion at the boundary of and between crustal plates. Most of the cumulative seismic energy release, seismic moment, and cumulative seismic slip along major plate boundaries occurs in large or great earthquakes. The strain energy that is released in shallow large or great earthquakes is believed to be built up slowly along simple plate boundaries for tens to hundreds of years. This strain comes from the movement of the plates, which varies from 2 to 12 cm/yr for the major plate boundaries discussed here. Friction along plate boundaries prevents many major seismic zones from moving continuously on a scale shorter than tens to hundreds of years. Once stresses build to a critical level, the plate interface moves suddenly about 1 to 20 m during the rupture associated with a large or great earthquake. The other class of earthquakes, not covered in this report, are intraplate earthquakes, which reflect deformation within plate interiors.

Many analyses of earthquake hazards around the circum-Pacific region have been based on the seismic gap hypothesis, i.e. the idea that segments of simple plate boundaries that have not ruptured in a large or great earthquake in many decades are the most likely sites of future large or great events (Fedotov, 1965; Mogi, 1968; Sykes, 1971; Kelleher et al., 1973; McCann et al., 1979; Nishenko and McCann, 1981). For a segment of a plate boundary to be considered a seismic gap, it must have a history of prior large or great earthquakes and not have ruptured in a large or great event in at least 3 decades (McCann et al., 1979). Given the present large number of seismic gaps around the circum-Pacific, additional information is necessary to differentiate between those gaps which may be sites of large or great shocks in the immediate future (i.e. the next 5 to 10 years) and those which may remain dormant for longer time intervals. Hence, in addition to knowing when the last event occurred at a particular location, information on the *repeat times* of large and great earthquakes, the local rates of fault motion and strain accumulation, and the size of the expected earthquake are essential for completely describing the seismic hazard.

Descriptions of interplate seismic potential are presented in terms of estimates of the expected *repeat time* for large and great earthquakes in this region, and the corresponding time-dependent conditional probability for time intervals of 5, 10 and 20 years duration from the present (i.e. 1989–1994, 1989–1999 and 1989–2009). Estimates of earthquake *repeat times* are based on 1) recurrence intervals from the historic and instrumental record, 2) radiometric dating (i.e. ^{14}C and ^{230}Th) of uplifted marine terraces, coral heads, and offset Holocene deposits, and 3) direct estimates based on the size of the most recent earthquake and the local rate of plate motion. Presenting these data in a probabilistic framework accounts for variations in recurrence time along a specific fault segment, as well as errors in our determination of the *repeat time*, and provides a basis for the comparison of seismic hazard between segments which have differing recurrence times. The flow chart in Table 3 presents the procedure used to estimate seismic potential or conditional probability.

Table 3. Flowchart of Earthquake Recurrence Time and Conditional Probability Calculations

HISTORIC	GEOLOGIC	DIRECT
Dates of historic earthquakes	Dates of prehistoric earthquakes$\pm\sigma_i^A$	Estimates of coseismic displacement & rates of fault motion $\pm\sigma_i^B$
$\Downarrow$	$\Downarrow$	$\Downarrow$
Observed Average Repeat Time T_{ave}	Observed Average Repeat Time T_{ave}	Estimated Repeat Time $\overline{T}$
$\Downarrow$	$\Downarrow$	$\Downarrow$

Compute $\overline{T}$ and T_{exp}^C

$\Downarrow$

Date of last event (t_o)

$\Downarrow$

$T_{pred} = (t_o + T_{exp})$

$\Downarrow$

Year and window length for probability estimates

$\Downarrow$

Lognormal Distribution

$\Downarrow$

Conditional Probability Estimates

Notes:

A. For prehistoric earthquakes, σ_i is a measure of ^{14}C dating uncertainties and other errors if known.

B. For direct estimates, σ_i is a measure of the uncertainties in coseismic displacement (σ_1) and rates of fault motion (σ_2), where $\sigma_i = \sqrt{\sigma_1^2 + \sigma_2^2}$.

C. $\ln\overline{T} = \ln(T_{ave}) + \mu_D$, and $T_{exp} = \overline{T}e^{(\mu_D + \sigma_M^2/2)}$, where $\mu_D = 0.0099$, $\sigma_D = 0.215$, and $\sigma_M = \sqrt{\sigma_B^2 + \sigma_D^2}$. See text for additional details.

The individual steps in this procedure will be explained more fully in the following sections.

One approach to probabilistic hazards assessment has been to lump all known recurrence information for a specific magnitude class into one data set for analysis of regional recurrence statistics. Pooling data from large regions is necessary because well determined or robust estimates of recurrence times and probabilities require more data than are usually available for individual fault segments. This approach, of pooling the available data, was attempted by Rikitake (1976) for a number of individual seismic zones using a Weibull function as the preferred statistical distribution. The amount of time elapsed since a prior large or great shock in each segment is an intrinsic factor for the hazards estimate. The probability, or likelihood for a large or great earthquake is low immediately following the occurrence of a similar sized event, and grows as a function of the time elapsed since the last event. This approach to hazards forecasting is termed time-dependent, and is fundamentally different from approaches that assume random or Poisson distributions of earthquake recurrence times (see Figure 2). In the latter case, the Poisson model leads to estimates of conditional probability that are independent of the amount of time elapsed since the last event. In both cases, averaging recurrence information over a geographic and seismically diverse region usually results in a reduced ability to differentiate distinct segments, each of which may have their own characteristic recurrence behavior.

In an attempt to rigorously describe the time-dependent recurrence behavior of individual fault segments, Nishenko and Buland (1987) used the ratio T/T_{ave} for a number of segments along simple plate boundaries with well known recurrence histories. For each individual fault segment, T_{ave} is the observed average recurrence interval and T is the observed individual recurrence interval. By utilizing *a priori* information about the underlying distribution of earthquake recurrence intervals, more accurate descriptions of recurrence behavior are possible than using a few available data alone.

Probability density functions for earthquake recurrence time, $f(t)$, where t is the time elapsed since the last characteristic earthquake, form the basis of the time-dependent probability approach. These density functions and their associated measures of variability - the standard deviation, σ, and the coefficient of variation, $\sigma/mean$, define the degree of temporal resolution and hence, the information content of the recurrence interval data. An important result of the T/T_{ave} analysis of Nishenko and Buland (1987) is that the standard deviation of the lognormal distribution appears to be a fixed fraction of the recurrence interval. The coefficient of variation of the lognormal recurrence distribution, $\sigma_D = 0.215$ and is approximately constant over a wide range of recurrence times and seismic moments in a variety of tectonic environments. It is this property, when used in a normalized time frame, that permits a "generic " description of the underlying probability density function for earthquake recurrence studies and calculations of conditional probability. The marginal time-dependent probability density function, $f(T)$, defined by Nishenko and Buland (1987) and Buland and Nishenko (1989), and used in this study is:

$$f(T) = \frac{1}{T\sigma_M\sqrt{2\pi}} e^{-(ln(T/\overline{T}) - \mu_D)^2/2\sigma_M^2} \qquad (1)$$

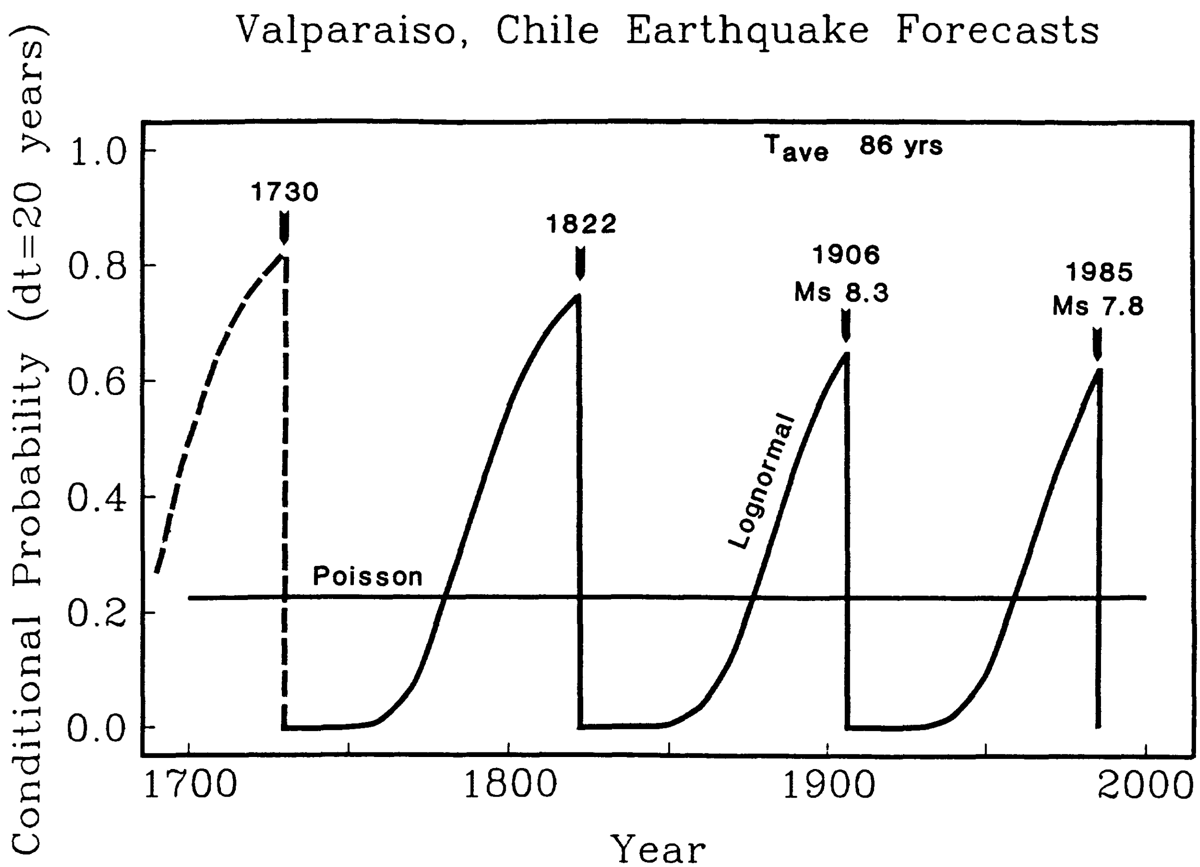

Figure 2. Comparison of time-dependent and time-independent conditional probability estimates. Curves compare the lognormal (time-dependent) and Poisson (time-independent) conditional probabilty estimates for the Valparaiso, Chile seismic zone. Time-dependent models, which account for the regularity in characteristic earthquake occurrence, are low immediately following a large or great earthquake and grow as a function of the time elapsed since the last event. In contrast, Poisson models, which assume random earthquake recurrence behavior, are constant as a function of the time elapsed and are time-independent.

where $\ln\overline{T} = \ln(T_{ave} + \mu_D)$. The mean and standard deviation of $f(T)$ are μ_D = -0.0099 and $\sigma_M = \sqrt{\sigma_B^2 + \sigma_D^2}$, respectively. The standard deviation, σ_D, defines the intrinsic variability of recurrence intervals based on the global analysis of Nishenko and Buland (1987) discussed above and is equal to 0.215, the second standard deviation, σ_B, describes the uncertainty in our estimates of the median recurrence interval. The complete joint probability density function, which describes the variability in the actual recurrence time, and our estimates of the median recurrence time is shown in Figure 3.

For historic earthquakes, values of T_{ave}, $\overline{T}$ and σ_B are estimated from observations of T, the individual recurrence times. How well the median recurrence time can be estimated is described by σ_B , and depends on both the number and quality of observations of T. In other words,

$$\sigma_B^2 = \sum_{i=1}^{N} \frac{1}{\sigma_i^2/T_i^2 + \sigma_D^2} \tag{2}$$

In equation 2, the σ_i^2/T_i^2 term, where the subscript i denotes an individual recurrence interval, accounts for the uncertainty in measuring a recurrence time. For historical data, there is generally little or no uncertainty as to when the events in question occurred and this term is set equal to 0. Hence, σ_B is only a function of the number of historical recurrence intervals observed and the intrinsic variability of those intervals. For geologically based estimates, the σ_i/T_i term is included in equation 2 to account for the additional uncertainties in the geologic data (i.e. the $\pm 1\sigma$ values for the ^{14}C dates). Hence, the resolution in estimating recurrence times from geologic data is a function of both the errors in dating previous events and the intrinsic variability of the recurrence intervals, the latter being independent of age-dating uncertainties. For direct estimates of recurrence time, the σ_i/T_i term in equation 2 is used to account for the the $\pm 1\sigma$ uncertainties in the rate of fault motion and coseismic displacement, and the direct recurrence time estimate itself is set equal to $\overline{T}$.

The expected recurrence time, T_{exp}, is based on a number of observations of T for a specific fault segment and is given by,

$$T_{exp} = \overline{T} e^{(\mu_D + \sigma_M^2/2)} \tag{3}$$

The predicted date of occurrence of the next event (T_{pred}) is simply the sum of the date of the last earthquake (t_o) with either the average or estimated recurrence time of the next earthquake (T_{exp}), (i.e., $T_{pred} = t_o + T_{exp}$). The above recurrence time estimate can also be presented in terms of a forecast or prediction time window. Following Nishenko and Buland (1987), the forecast time window used in this study is defined as the time interval $[T_{pred} - \eta,\ T_{pred} + \eta]$, where η is defined as the 90% confidence interval for the estimate of T_{exp} and is equal to 1.645 var $[T_{exp}]^{1/2}$, where var$[T_{exp}] = {\sigma_M}^2 T_{exp}^2$.

In addition to estimating the recurrence time for a specific fault segment, we can also estimate the conditional probability or the likelihood for the event to occur in a given

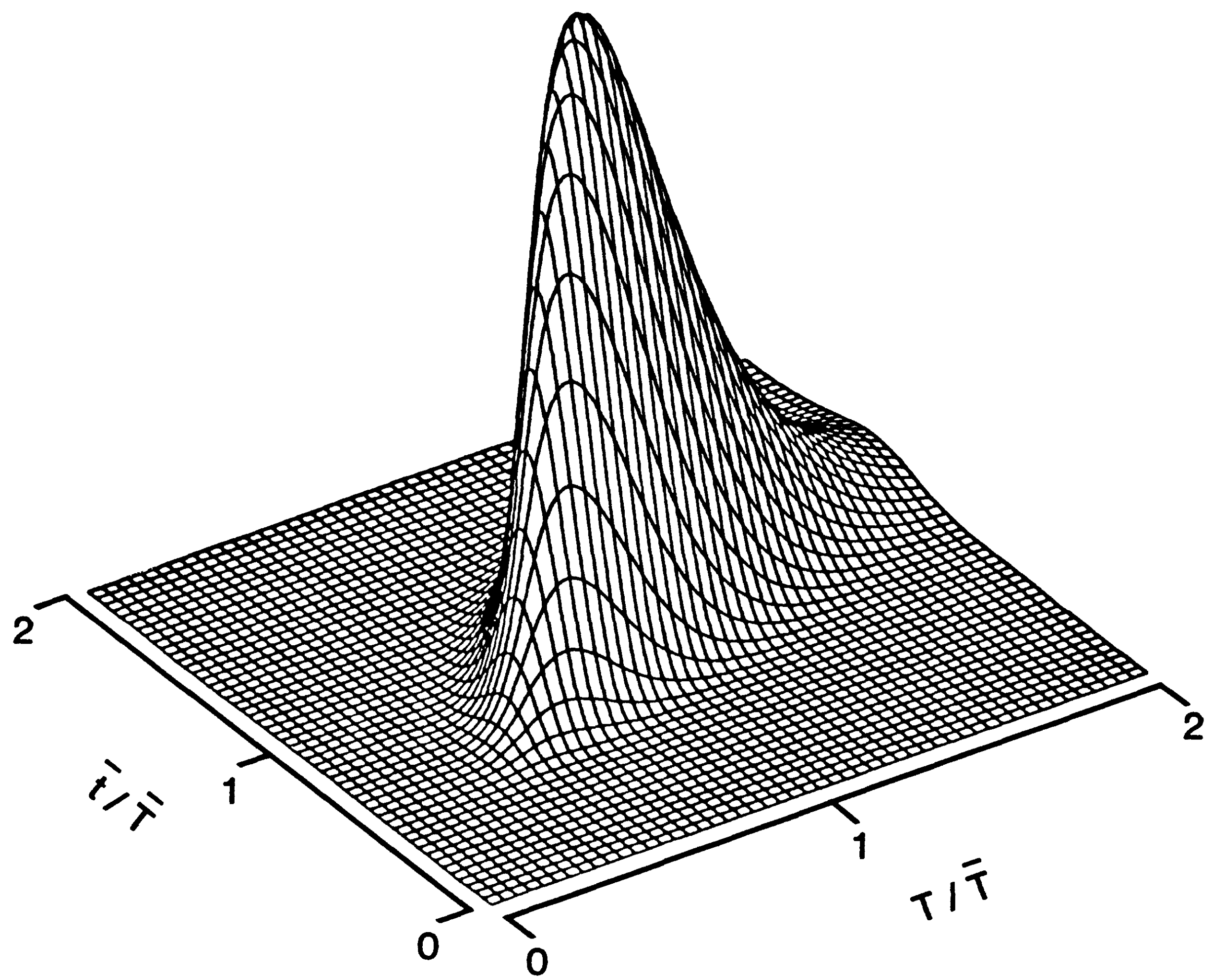

Figure 3. Three-dimensional representation of the lognormal joint probability density function. Joint probability density amplitude is shown as a function of the variation in $T/\overline{T}$ (the ratio of individual recurrence time for a fault segment, T, to our best estimate of the median recurrence time, $\overline{T}$) on the X-axis and the variation of $\bar{t}/\overline{T}$ (the ratio of a realization of the median recurrence interval, $\bar{t}$, to our best estimate of the median recurrence interval, $\overline{T}$) on the Y-axis. The coefficient of variation for the random variable ln $(t/\overline{T})$ is 0.2 (from Buland and Nishenko, 1989).

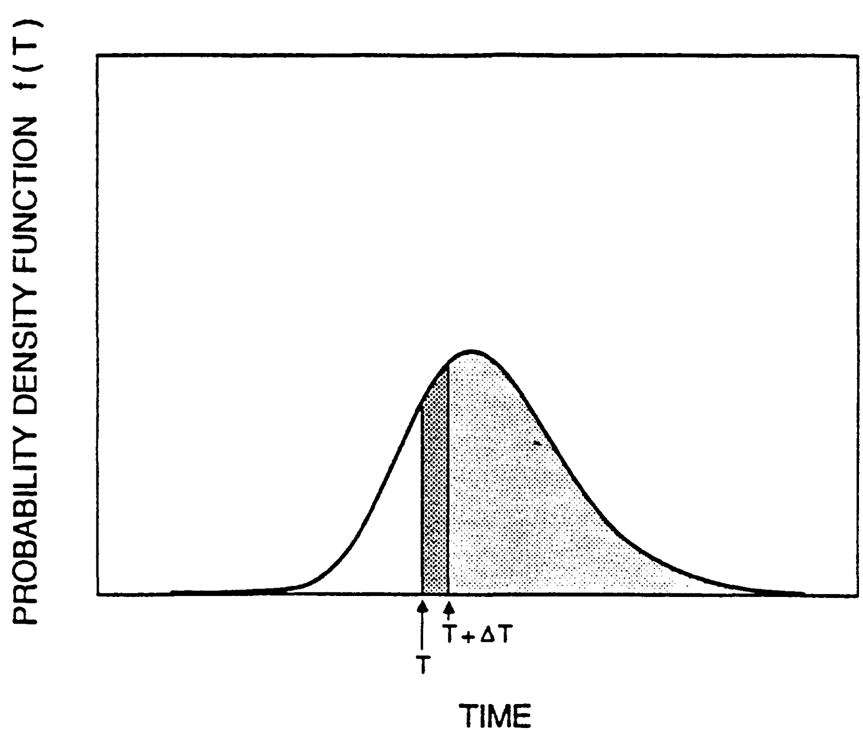

Figure 4. Conditional probability for earthquake occurrence. The probability for an earthquake in the interval T, $T + \Delta T$, is given by the area of dark shading under the probability density curve. The probability, conditional on the earthquake not having occurred prior to T, is the ratio of the area of dark shading to the sum of the areas with dark and light shading.

time interval $t + \Delta t$. This probability is computed from the the ratio of areas under the lognormal distribution in equation 1 for two different time intervals and is of the form:

$$P_C = \frac{\int_{t_1 - t_0}^{t_2 - t_0} f(T/\overline{T})dT}{\int_{t_e - t_0}^{\infty} f(T/\overline{T})dT} \tag{4}$$

and is conditional on knowing both the expected recurrence time, and that the event has not happened by time t_e (see Figure 4). By implicitly incorporating the uncertainties in T_{exp} into the probability distribution, the functions in equations 1 and 4 become more broadly distributed with increasing uncertainty in the data and dampen changes of probability as a function of time. Overall conditional probability values are dependent on the above uncertainties, and the width of the time window, Δt, chosen for an individual forecast. In other words, for a given seismic gap, the conditional probabilities for a 20 year window are always larger than those for a 10 or 5 year window. The comparison of probability estimates among various gaps must be done using the same time interval.

The following sections describe the different types of basic data sets used in estimating the segmentation, recurrence times, and probabilities for the simple plate boundaries of the circum-Pacific region.

Historical/Instrumental Observations

Initial investigations of the seismicity and tectonic setting of the circum-Pacific region relied on the aftershock distributions of prior large and great earthquakes and historical descriptions of damage and felt intensities to define rupture zones and segmentation along the strike of simple plate boundaries (Fedotov, 1965; Mogi, 1968; Kelleher et al., 1973; Sykes, 1971; McCann et al., 1979; Nishenko and McCann, 1981). The above earthquake data provide the basic seismological foundation for defining the recurrence behavior of individual fault segments in this analysis and will be discussed in more detail in the later sections. Overall, the limited number of available observations make it difficult to define the recurrence characteristics for many of the segments around the circum-Pacific.

For individual fault segments, the penalty for few recurrence observations is a large uncertainty in the estimated recurrence time and associated conditional probability, as indicated by the 90% confidence limits of T_{exp} and the corresponding range of probabilities for a particular exposure time. For one recurrence interval, the standard deviation, $\overline{\sigma}$ is taken to be 21% of $\overline{T}$. As discussed in the previous section, and shown in equation 2, more recurrence observations can reduce this uncertainty. Overall, the uncertainties in using historic data are smaller than those in other data sets (i.e. geologic and direct estimates, see following sections).

Geologic Investigations

Radiometric dating of geologic features produced or altered by coseismic displacements in previous great earthquakes have greatly extended the recurrence history along sections of the circum-Pacific seismic zone. Unfortunately, these features have only been identified and studied in a few areas. In Alaska, studies of offset Holocene moraines along the Fairweather fault (Plafker et al., 1978) and uplifted, wave-cut marine terraces on Middleton Island and the Cape Yakataga-Yakutat Bay region (Plafker, 1986) have helped constrain the rates of plate motion and the size and timing of prehistoric great earthquakes in this region. Radiometric dating of uplifted coral heads on the Vanuatu Islands (Taylor et al., 1988) has extended the seismic history for this region of the southwest Pacific. In the northeast Pacific, study of subsided coastal terrains along the coast of Washington and Oregon (Atwater, 1988) have begun to document the potential for a large or great earthquake in that region. The offset of sediments during large and great earthquakes on the San Andreas fault in southern California (Sieh et al., 1989) and the Chixoy-Polochic fault in Guatemala (Schwartz, 1985) have been invaluable in documenting the behavior of major transform faults within the study area.

By taking into account the $\pm 1\sigma$ uncertainties in the radiometric dates for individual earthquakes, as well as the intrinsic variability of recurrence intervals, geologic data can be included with and compared to recurrence estimates based on historic data or direct calculations as shown in equation 2 (see also Nishenko and Buland [1987] and Buland and Nishenko [1989] for further details and examples).

Direct Estimates

For those fault segments lacking either a historic or geologic record of prior events, we have estimated recurrence times based on the size of the most recent large or great earthquake along that fault segment. The principal assumption in this type of calculation is that the most recent large or great event reflects the typical or characteristic size of earthquakes in a given seismic gap from cycle to cycle. These direct estimates of recurrence time are determined by dividing the coseismic displacement, or amount of fault slip, of the most recent earthquake by the long-term rate of fault motion and assume that no aseismic slip is occurring. These direct estimates of recurrence time assume the time-predictable model of Shimizaki and Nakata (1980). For some events, only the instrumentally measured long-period seismic moment (M_O) is known. For older earthquakes, we can also estimate the seismic moment by using observations of tsunami wave heights (see Figure 5). In both cases, average coseismic displacements are calculated using estimates of the rupture area from aftershock of felt area studies, where U, the displacement $= M_O/\mu A$, μ is the shear modulus and A is the fault area. For strike-slip faults, observations of coseismic surface offsets can be compared to estimates of displacement based on the seismic moment. In both cases, the degree of resolution in our forecasts of recurrence time and magnitude is dependent on knowing the distribution of coseismic displacement along the fault surface. Within a single rupture zone, subsegments that have smaller amounts of displacement may repeat sooner or more often than those segments with greater amounts of displacement. In some cases, detailed investigations have outlined heterogeneous slip distributions, so recurrence estimates can also be attempted for subsections of larger ruptures, as well.

The major sources of uncertainty in our direct calculations of recurrence time are the rates of plate motion and the amount of coseismic displacement. Overall, the uncertainty

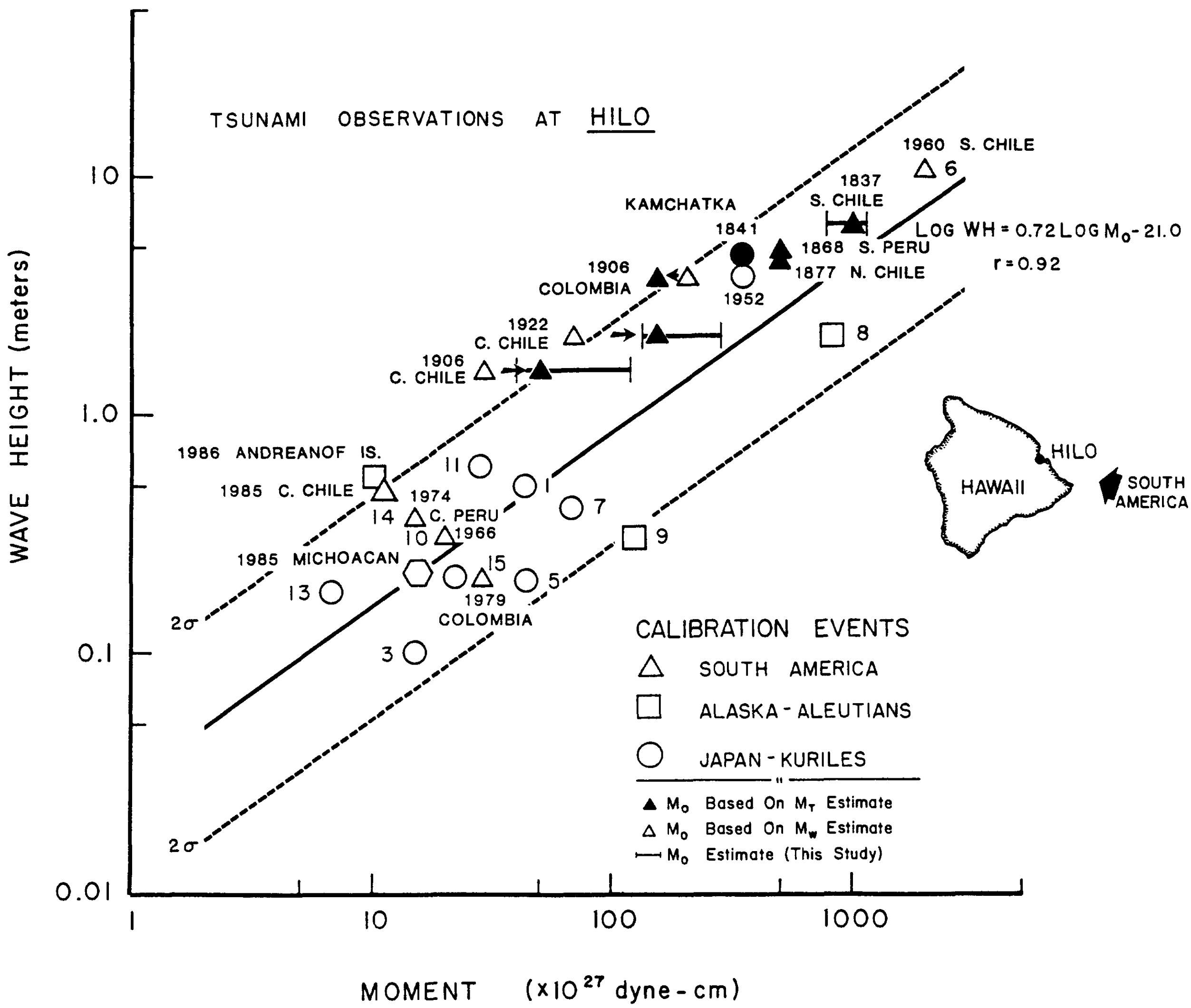

Figure 5. Tsunami observations at Hilo, Hawaii. Tsunami wave heights, recorded at Hilo, Hawaii are plotted as a function of seismic moment (M_O) for a set of calibration events (open, numbered symbols). A least squares fit for the calibration events (Log (Wave Height) = 0.72 Log M_O - 21.0) and $\pm$ 2 σ limits, is shown as solid and dashed lines respectively. This calibration allows estimation of the seismic moment of older, non-seismographically recorded earthquakes and provides a rapid estimate of wave heights at Hilo, Hawaii for recent earthquakes (after Nishenko, 1985).

in the relative rates of plate motion are at the 3 to 8% level (Minster and Jordan, 1978; Chase, 1978). In this study we use a conservative estimate of 10%. What is more uncertain however, is the amount of aseismic slip that may be occurring along any one fault segment. All of the direct recurrence time calculations presented assume no aseismic slip, and hence represent minimum *repeat time* and maximum probability estimates. Where available, the historic record provides a comparison for estimating the amount of aseismic slip. Estimates of coseismic displacement vary by a greater amount than the rates of plate motion, and reflect both the inherent uncertainty in the methods used to measure displacement as well as the variability in displacement along a fault surface. For each segment, we have used a variety of displacement estimates (where available) to help bracket the recurrence time. The variation in displacement (and to a lesser extent relative plate motion) define the σ_i/T_i values in equation 2. These estimates tend to have the largest ranges in probability, reflecting the greater uncertainty in the recurrence time estimates.

Figure 6. Seismic potential of the Chilean seismic zone: 1989-1999. Colors portray the level of conditional probability for occurrence of great (M_S 7.7 and larger) earthquakes during the next 10 years, 1989-1999, and range from dark blue, 0-20%; green, 20-40%; yellow, 40-60%; and red, 60-100%. Light blue regions are those areas with no historic record of large or great earthquakes. Specific dates and magnitudes refer to areas with incomplete historic records. Base map from the Plate Tectonic Map of the Circum-Pacific Region (1985), see legend at right for additional symbols and information.

CIRCUM-PACIFIC COUNCIL FOR ENERGY AND MINERAL RESOURCES
Michel T. Halbouty, Chairman and President

CIRCUM-PACIFIC MAP PROJECT
John A. Reinemund, Director
Warren O. Addicott, General Chairman
George W. Moore, Deputy Chairman for Marine Geoscience
Maurice J. Terman, Special Consultant for East Asia Tectonics and Resources

PLATE-TECTONIC MAP OF THE CIRCUM-PACIFIC REGION

PACIFIC BASIN SHEET

KENNETH J. DRUMMOND
Chairman, Northeast Quadrant Panel
CHIKAO NISHIWAKI
Chairman, Northwest Quadrant Panel
JOSE CORVALAN
Chairman, Southeast Quadrant Panel
H. FREDERICK DOUTCH
Chairman, Southwest Quadrant Panel
CAMPBELL CRADDOCK
Chairman, Antarctica Panel

TECTONIC ELEMENTS
George W. Moore, U. S. Geological Survey, Menlo Park, California 94025
José Corvalán, Departamento de Geología, Universidad de Chile, Santiago, Chile
Campbell Craddock, Department of Geology and Geophysics, University of Wisconsin-Madison, Madison, Wisconsin 53706
H. Frederick Doutch, Bureau of Mineral Resources, Canberra, ACT 2601, Australia
Kenneth J. Drummond, Mobil Oil Canada, Ltd., Calgary, Alberta, Canada T2P 2J7
Chikao Nishiwaki, 2-2-8, Nishinogawa, Komae-shi, Tokyo, 201 Japan
Tamotsu Nozawa, Geology Department, University of Shimane, Matsue, 690 Japan
Gordon H. Packham, Department of Geophysics, University of Sydney, Sydney 2006, Australia
Seiya Uyeda, Earthquake Research Institute, Tokyo University, 113 Japan

MAGNETIC LINEATIONS
Xenia Golovchenko, Marathon Oil Company, Littleton, Colorado 80160
Roger L. Larson, University of Rhode Island, Kingston, Rhode Island 02881
W. C. Pitman III, Lamont-Doherty Geological Observatory, Palisades, New York 10964
Nobuhiro Isezaki, Department of Earth Sciences, Kobe University, 657 Japan

GEOMAGNETIC POLARITY TIME SCALE
Roger L. Larson, Xenia Golovchenko, and W. C. Pitman III

PLATE-MOTION VECTORS
George W. Moore

HOLOCENE VOLCANOES
Tom Simkin and Lee Siebert, Museum of Natural History, Smithsonian Institution, Washington, D. C. 20560

SEISMIC EPICENTERS
Wilbur A. Rinehart, World Data Center A for Solid Earth Geophysics, National Oceanic and Atmospheric Administration, Boulder, Colorado 80303

Lambert Azimuthal Equal-Area Projection
(Map center point: Equator, 160°W.)

1985

NEIC

CIRCUM—PACIFIC SEISMIC POTENTIAL 1989—1999

Prepared by
U. S. Geological Survey
National Earthquake Information Center
with support from
Office Of U. S. Foreign Disaster Assistance
Agency For International Development

1989

Stuart P. Nishenko
NEIC

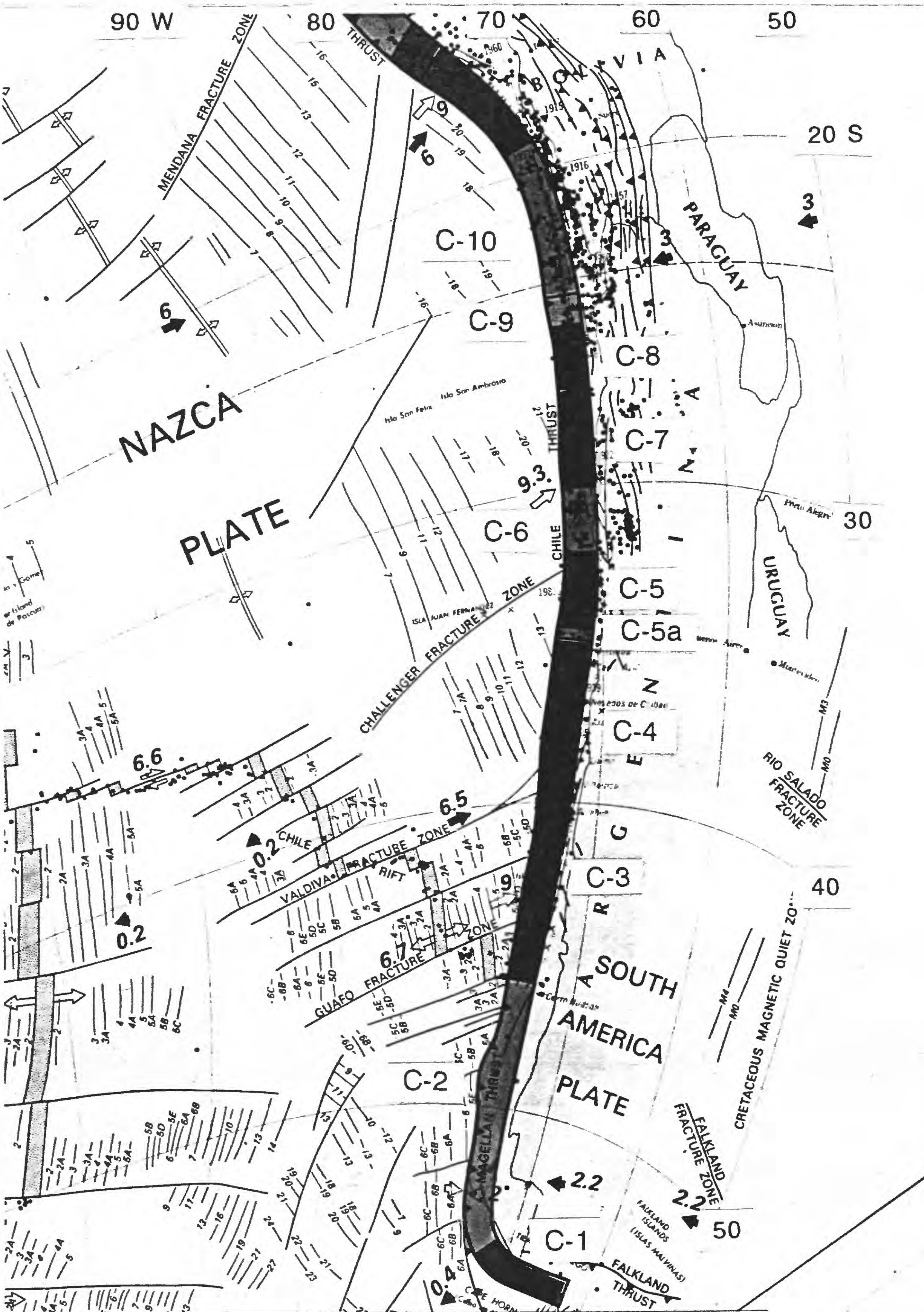

South American Seismic Zone

Chile

EXPLANATION

MOTION VECTORS

8.6 — 7 — 6 — 10

Relative plate motion In cm/yr at strike-slip, converging, and diverging plate boundaries, with the entire rate assigned to the principal plate boundary where the movement is distributed over several faults; chiefly after the model of Minster and Jordan (1978), a computerized best fit of 330 worldwide measurements of rate from seafloor spreading, and direction from transform faults and earthquake first-motion analyses

Absolute motion Chiefly after Minster and Jordan (1978) and derived from the relative-motion model controlled by a best fit of rates and directions from traces of active hotspots

ACTIVE HOTSPOT

Trace of present movement Circle shows approximate location, bar shows movement with respect to associated plates during past 10 m.y. based on the absolute-motion model of Minster and Jordan (1978)

INTRAPLATE STRUCTURES

Inactive spreading ridge Dashed where approximately located; also includes minor active spreading ridges

Major intraplate faults Arrows show displacement of strike-slip fault; barbs on upper plate of thrust fault; dashed where approximately located

MAGNETIC LINEATIONS

2 — 3

Magnetic anomalies Labels show correlation with geomagnetic polarity time scale

ACTIVE PLATE BOUNDARIES

Active transform fault The principal fault at broad strike-slip plate boundaries, and arbitrarily drawn where the boundary is covered by uncoupled crustal slabs; dashed where approximately located

Subduction zone The surface trace of a Benioff seismic zone, a dipping layer of earthquake foci believed to mark the upper surface of a descending lithospheric plate; barbs on upper plate; dashed where approximately located

Active spreading ridge Pattern shows oceanic crust formed during past 1 million years; dashed where approximately located

Complex transform fault boundary With elements of dilation

VOLCANIC CENTERS

Active in historic time Generally within past 1,000 yr, and documented during or soon after eruption; volcano named in color if active 1964 through 1983

Active in Holocene time Within past 10,000 yr; not documented historically

Holocene activity uncertain Includes solfataras and volcano-related thermal springs; no direct evidence for Holocene eruption. Volcano data chiefly from Simkin and others (1981)

EARTHQUAKE EPICENTERS

Depth (km): 0, 70, 300, 700

1906 ▼ • — 1916 ▼ • — 1904 ▼ •

Focal depth Colored dots indicate 1964 through 1979 magnitude 5.0 through 7.4 events; triangles of matching colors labeled by date indicate 1899 through 1982 events of magnitude 7.5 or greater (generally surface-wave magnitude)

CONDITIONAL PROBABILITY

1989 - 1999

60 - 100%

40 - 60%

20 - 40%

0 - 20%

No Historic Record of Great Earthquakes

Incomplete Historic Record — Date and Magnitude of Most Recent Earthquake: 1919, M_S 8.2

Discussion Of Individual Regions

The following sections summarize the basic earthquake data for the simple plate boundaries of the circum-Pacific region covered in this report. Individual segments or source zones are identified by number, name and either latitudinal or longitudinal extent. Each section contains a description of the previous earthquake history, our estimates of the average *repeat time*, and the conditional probability for recurrence in the next 10 years (1989-1999). Estimates for additional time windows (i.e. 5 and 20 years, 1989-1994 and 1989-2009) can be found in the Appendix.

SOUTH AMERICA

Chile

The Chilean seismic zone marks the zone of interaction between the South American, Antarctic (south of 46°S), and Nazca (north of 46°S) plates along the west coast of South America. The rates of plate convergence range from 2 cm/yr in the south (South America/ Antarctic convergence) to 9 cm/yr farther north (South America/ Nazca convergence). Variations in the tectonic regime, as evidenced by gaps in active Quaternary volcanism and changes in the attitude of the intermediate depth seismic zone, are influenced by intersections of bathymetric features on the subducted Nazca plate and differences in the age of subducted sea floor (Barazangi and Isacks, 1976). These various tectonic regimes also influence the size and recurrence times of large and great earthquakes that occur along the Chilean margin. The following section summarizes the basic earthquake data for 10 segments of the Chilean subduction zone, and is an update of Nishenko (1985). Estimates of conditional probability for 1989-1999 are shown in Figure 6.

C-1. *Tierra del Fuego*, 65°-72° W. Previous large or great earthquakes that are documented for this region include 2 February 1879 and 17 December 1949 (2 M_S 7.7 events within 8 hours). Both the 1879 and 1949 events produced Modified Mercalli (MM) intensities of VII in Punta Arenas. While details are lacking for both events, it is assumed that both represent rupture along the Magellan fault system (the transform plate boundary between the South American and Scotian plates). Field studies of the 1949 events indicate rupture extended from the western end of the Brunswick Peninsula (near Punta Arenas) to Policarpo (Tierra del Fuego), and suggest an overall fault length of about 450 km (Winslow, 1982). Based on these length estimates, the combined 1949 events rank as one of the largest strike-slip earthquakes in the 20th century.

If the 70 year recurrence indicated by the historic record is characteristic for this segment, the probability for the recurrence of a great earthquake in the next 10 years is at the 11% level. In spite of these low estimates, however, more work is needed in this region to document the earthquake history for a better understanding of the seismic regime.

C-2. *Chilean Archipelago*, 46°-52° S. South of the intersection of the Chile Ridge with the South American plate at 46°S, the Antarctic plate is being subducted beneath

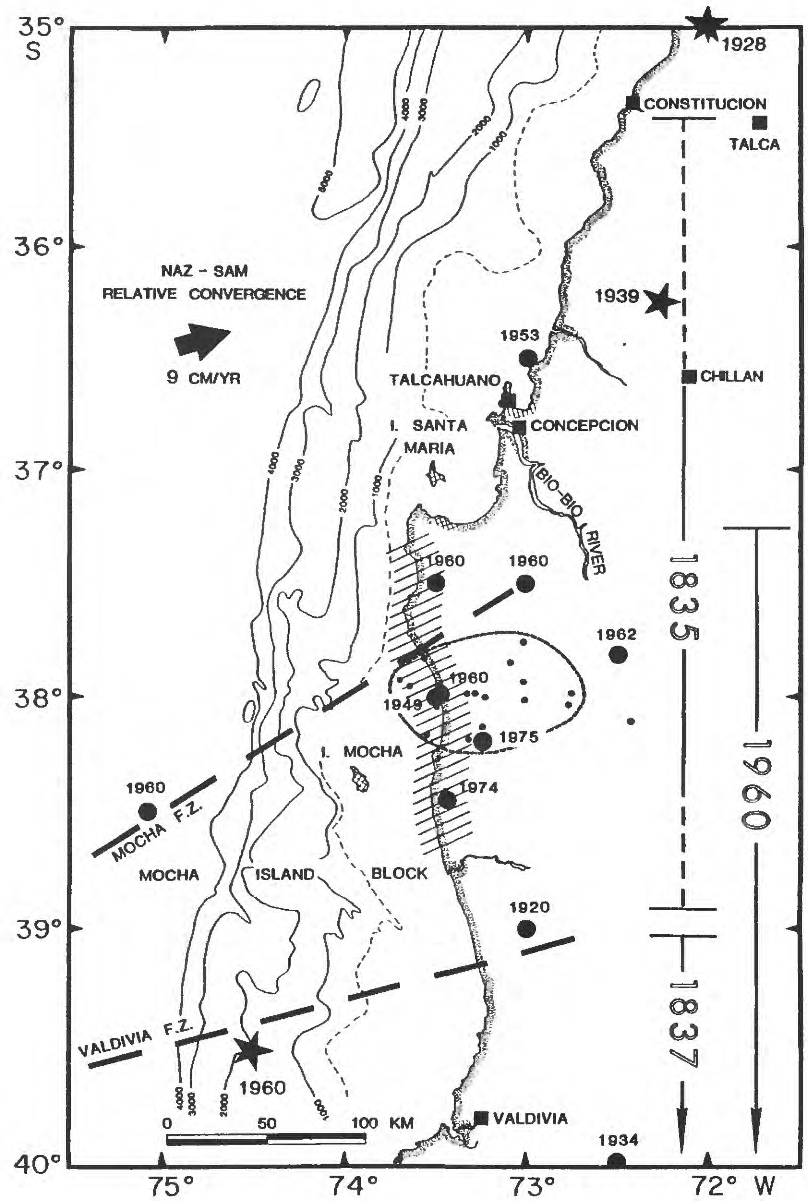

Figure 7. Recent and historic earthquakes in the Concepcion- Valdivia, Chile area. Rupture lengths for great earthquakes in this area (1835, 1837, and 1960) are solid where known and dashed where inferred. Cross-hachured areas of the coast are areas of observed coastal uplift associated with the 1835 Concepcion earthquake and include Mocha Island, Santa Maria Island, and the Talcahuano-Concepcion area. Larger hachuring is the zone of uplift associated with the 21 May 1960 earthquake (after Plafker and Savage [1970]). Overlap of uplifted areas suggests that the 21 May 1960 'foreshock' to the great 22 May 1960 earthquake may have been a repeat of the 1835 earthquake in this area (after Nishenko, 1985). Coastal outline and bathymetry (contour interval 1000 m) after Prince et al. (1980). Projection of the Mocha and Valdivia fracture zones from Herron (1981).

the western coast of South America at about 2 cm/yr. This region is characterized by a sediment filled trench, a low level of seismicity, and no history of large or great earthquakes. In view of the low convergence rate, *repeat times* for large and great earthquakes may be a few hundred years. At present, no data are available to estimate a recurrence time or conditional probability for this segment.

C-3. *Southern Chile*, 40°-46° S. Previous great earthquakes that have ruptured this segment of the Chilean margin include: 16 December 1575; 24 December 1737; 7 November 1837 (M_t 9.2); and 22 May 1960 (M_W 9.4). The 1960 event presently ranks as the largest earthquake in the instrumental record. All of the events in this segment are estimated to have rupture lengths between 700 and 1000 km long. Based on the historic record, the average *repeat time* for this region is 128 ± 16 years, and the probability for recurrence over the next 10 years is considered negligible (i.e. $\leq$1%) due to the recency of the last event.

C-4. *Concepcion*, 35°-40° S. Previous great earthquakes located in this zone include: 8 February 1570; 15 March 1657; 25 May 1751; 20 February 1835; 1 December 1928 (M_S 7.9); 25 January 1939 (M_S 8.3); and 21 May 1960 (M_S 7.9). Comparison of 20th century earthquakes with those in preceding centuries suggests a variable mode of rupture for this region. In other words, previous events appear to have ruptured the entire segment at one time, while the most recent episode which began in either 1928 or 1939 has taken 20+ years to complete. The 21 May 1960 event is included in this zone rather than zone C-3, based on similarities with observations of the 1835 event. Both events produced uplift on the Arauco Peninsula and on Mocha Island (see Figure 7). Previously, the 21 May event had been identified as a 'foreshock' of the great 22 May 1960 earthquake (zone C-3). Consideration of the closely coupled behavior of both zones (which historically have ruptured within less than a few years of one another), and the above noted similarity in coseismic uplift suggests that the rupture of the Concepcion segment was completed on 21 May 1960. Accordingly, the average *repeat time* for this segment is about 95 ± 10 years, and the conditional probability for the recurrence of a great earthquake in the next 10 years appears to be at the $\leq$ 1-3% level.

C-5 & 5a. *Valparaiso and Pichilemu - Llico*, 32°-35° S. Previous earthquakes in this segment occurred on: 13 May 1647; 8 July 1730; 19 November 1822; 16 August 1906 (M_S 8.3); and 3 March 1985 (M_S 7.8). Prior to 1985, Nishenko (1985), using the methods described in this study, had forecast the Valparaiso region as the most likely site along the Chilean margin for a great earthquake in the next 20 years (1984-2004). This forecast was dramatically confirmed by the 3 March 1985 event. The average *repeat time* for great earthquakes along this segment of the margin is 85 ± 9 years. The small standard deviation of these *repeat times* (± 9 years or ± 11%) is remarkable, compared to a global compilation (± 21%, Nishenko and Buland, 1987) and especially in light of new evidence that the rupture lengths (and hence, magnitudes) of these events have varied by a factor of 2 to 3 over the last 300+ years (Compte et al., 1986).

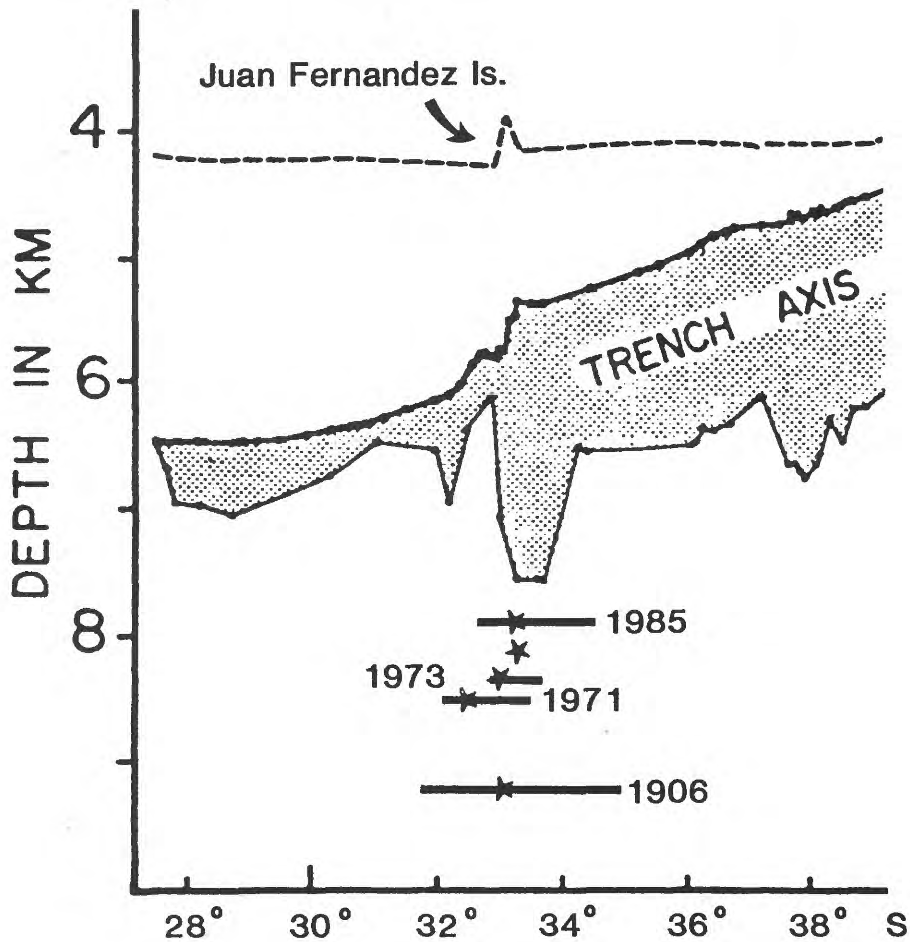

Figure 8. Comparison of basement relief along the Chile trench and earthquake rupture zones in the Valparaiso, Chile area. Maximum depth to basement along the Chile trench is shown by solid line, stippled area represents depth of sediment fill. Dashed line at top of figure represents the regional depth of the Nazca plate at a distance of 300 km from the trench axis (from Schweller et al., 1981). Stars are earthquake epicenters and horizontal bars depict length of rupture for large and great earthquakes during this century. Note that all epicenters appear to cluster near the trench axis high at 33° S which is inferred to be related to the intersection of the Juan Fernandez Islands. Foreshocks to the 3 March 1985 earthquake were also located in this region. This spatial coincidence suggests that this tectonic feature, or its downdip extension, has an important influence on large and great earthquake occurrence in this area.

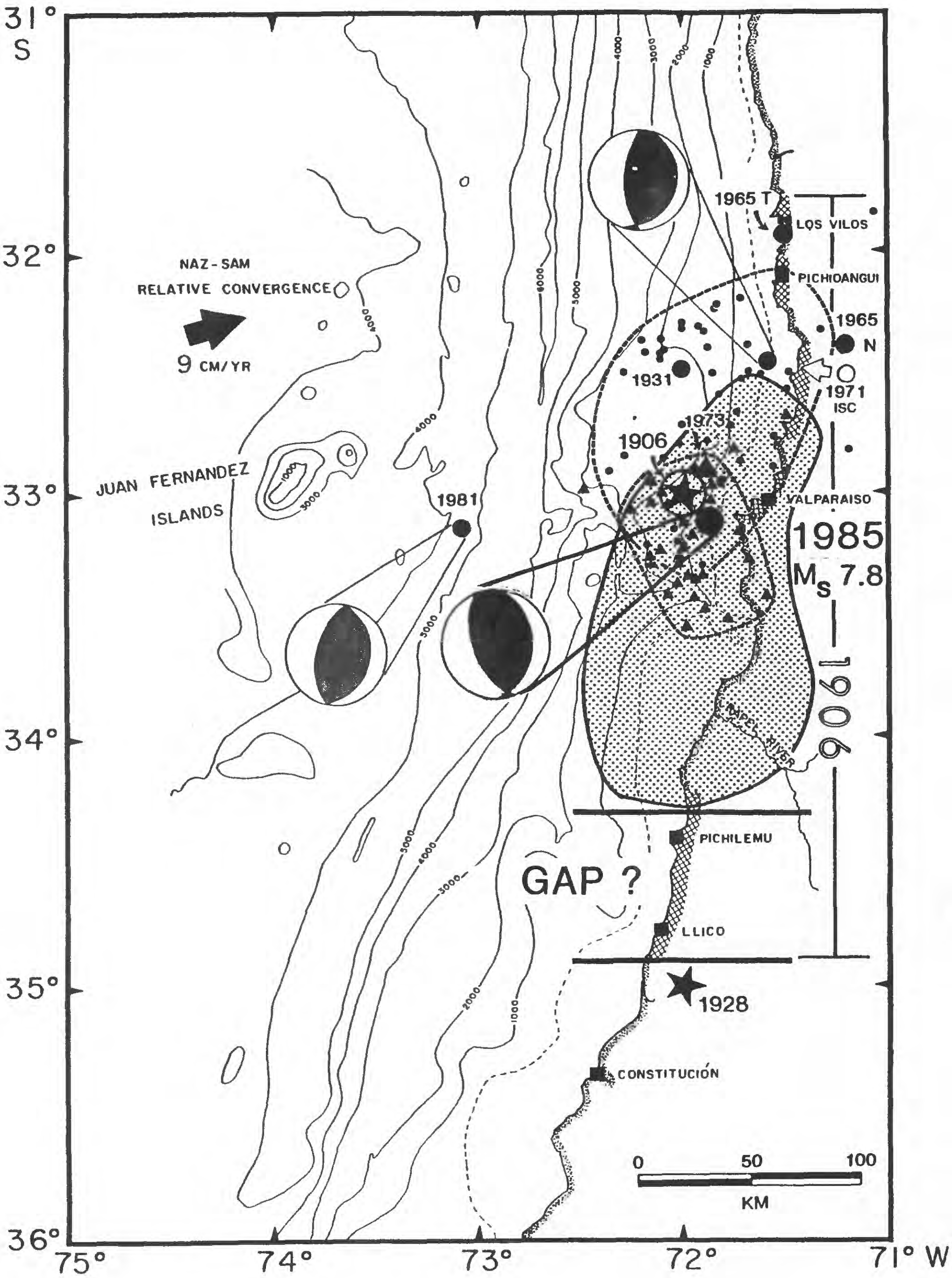

Figure 9. Recent earthquakes near the Valparaiso, Chile region. Rupture zone of the 3 March 1985, M_S 7.8 event shown as shaded region. Note the close spatial proximity of the 1906, 1973 and 1985 epicenters. The 1981 earthquake is an outer rise event that indicated the existence of compressional stresses in the region prior to the 1985 rupture. Cross-hachured area along the coast is the area of uplift associated with the 1906 earthquake. At present, the region between 34.5° and 35° S labelled GAP ? has been unruptured since 1906, may be the site of a future large event in this region (Compte et al., 1986).

Both the 1730 and 1985 earthquakes were preceeded by a series of pronounced foreshocks. The 1985 foreshock sequence is located offshore, near the postulated intersection of the Juan Fernandez Islands with the Chile trench and a sharp offset in the depth to basement in the Chile trench (see Figure 8). If the occurrence of small earthquakes in this particular area is a characteristic phenomena prior to great earthquakes in this segment, their future identification will be vital for short-term earthquake prediction.

While the probability for the Valparaiso region appears to be presently low, due the recency of faulting (assuming the 1985 is the gap filling event), the 1985 event did not fill in the same area as the 1906 rupture (see Figure 9). The region between 34.5° and 35° S (segment C-5a, Pichilemu-Llico) has remained unruptured since 1906 and may be the site of a future large event (Compte et al., 1986). The corresponding probability for this subsegment is at the 33% level for the next 10 years.

C-6. *Coquimbo-Los Vilos*, 30°-32° S. Previous great earthquakes that have occurred along this segment of the margin include: 8 July 1730; 15 August 1880; and 6 April 1943 (M_W 8.2). Note that the 1730 event also ruptured zone C-5. There is no information concerning events between 1730 and 1880. Both the 1880 and 1943 events appear to be similar in size, however, and the 63 year recurrence time appears to be the most reasonable estimate for this zone at this time. Based on these data, the probability for recurrence in the next 10 years is at the 24% level.

C-7. *Atacama* 26°-30° S. While this area has experienced a number of large events in the 18th, 19th and 20th centuries, only the 30 March 1796 and 10 November 1922 (M_S 8.2-8.5), events appear to be great earthquakes that ruptured all or most of this segment. This region lies within the megatectonic element of the Chilean margin that is characterized by a shallow dipping, intermediate depth seismic zone and an absence of Quaternary volcanism (Barazangi and Isacks, 1976). The epicenter of the 1922 event is located about 100 km inland, and is unusual in that it produced a great tsunami (M_t 8.5). Most tsunamigenic earthquakes tend to be located at or near the coast. Gutenberg (1939) suggests, however, that the tsunami may have been triggered by submarine landslides (similar to the suggested mechanism for the 1946 Unimak Island, Aleutian tsunami [see Alaska section]). Lomnitz (1970) indicates that the 1796 event may have been similar to the 1922 event, but no tsunami was generated by the former. If the 1922 tsunami was landslide related, differences between the two events are diminished, and the time interval 1922-1796, or 126 years is a reasonable recurrence time estimate. For comparison, direct calculation of a recurrence time for the 1922 event, based on the magnitude and estimates of coseismic slip average 104 years. Both estimates indicate low probabilities (4–11%) for the recurrence of a great earthquake in the next 10 years.

C-8 *Taltal-Copiapo*, 25°-27° S. As well as being involved in the great earthquakes that originate in zone C-7, this segment has independently produced a number of large and great earthquakes during the last two centuries. Events in 3 April 1819; 26 May 1851; 5 October 1859; 4 December 1918 (M_S 7.6); 2 August 1946 (M_S 7.1); and 4 October 1983

(M_S 7.4) all produced localized damage. This region lies within the rather diffuse tectonic boundary between 'normal' subduction to the north, with associated active Quaternary volcanism, and the shallow dipping, intermediate depth Benioff zone to the south (zone C-7). In addition, the boundary between these two tectonic regimes may be coincident with the abrupt change in trench axis depth at 27° S (Schweller et al., 1981). Given that the last large earthquake occurred in 1983, we estimate the probability for a future large event to be at the $\leq 1\%$ level for the next 10 years.

C-9. *Paposo* 25°-24° S. This small segment, located between the 1966 Taltal and the great 1877 Arica-Antofagasta earthquake, has no prior history of large or great events. The 1877 earthquake (discussed below) may have ruptured into this segment, but no reports are available to confirm this suggestion. Additionally, estimates of tsunami source region for the great 1877 earthquake terminate in the vicinity of Antogfagasta (based on data in Milne, 1880). Hence, the seismic hazard for this segment of the Chilean margin is not well understood at this time, with the exception of noting that this region may have the potential for participating in a large or great earthquake that may initiate from either the north or the south.

C-10. *Arica-Antofagasta* 19°-24° S. This segment is distinguished by the great (M_t 9.0) 9 May 1877 earthquake which, in addition to producing shaking damage along the Chilean coast, also produced a destructive tsunami throughout the entire circum-Pacific basin. Information about previous great earthquakes in this region are not presently known, partially due to low population density and the late development of this area at the end of the 19th century. Lacking any further information, the best recurrence estimate we can provide is based on tectonic analog with the Southern Chile segment (Zone C-3) and the adjacent Arica segment in Peru (see Peru discussion). Based on comparison with zone C-3 (128 year *repeat time*) the probability for recurrence is at the 20% level for the next 10 years. If however, this zone is more analogous to the adjacent 1868 zone in Peru (264 year *repeat time*), the resultant probabilities are even lower over the next 10 years. The uncertainty in recurrence times for this segment, however, and the potential threat to the entire circum-Pacific community underscores the need for more research to be done in this segment of the Chilean margin.

Peru

The Peruvian seismic zone marks the boundary between the South American and Nazca plates, and the continuation of the Peru-Chile trench system along the west coast of South America. In addition to having rates of plate convergence similar to those in Chile (9 cm/yr), Peru also exhibits a number of seismo-tectonic features that are similar to those in Chile. The absence of active Quaternary volcanism in Central Peru (2°-15° S) and a shallow dipping intermediate depth seismic zone is similar to the Atacama region in central Chile (27°-33° S; Barazangi and Isacks, 1976). The Peruvian margin can be divided into three major segments based on the patterns of historic seismicity and the presence of

Figure 10. Seismic potential of the Peru-Ecuador-Colombia seismic zone: 1989-1999. Colors portray the level of conditional probability for occurrence of great (M_S 7.7 and larger) earthquakes during the next 10 years, 1989-1999, and range from dark blue, 0-20%; green, 20-40%; yellow, 40-60%; and red, 60-100%. Light blue regions are those areas with no historic record of great earthquakes. Specific dates and magnitudes refer to areas with incomplete historic records. See Figure 6 for additional symbols and information.

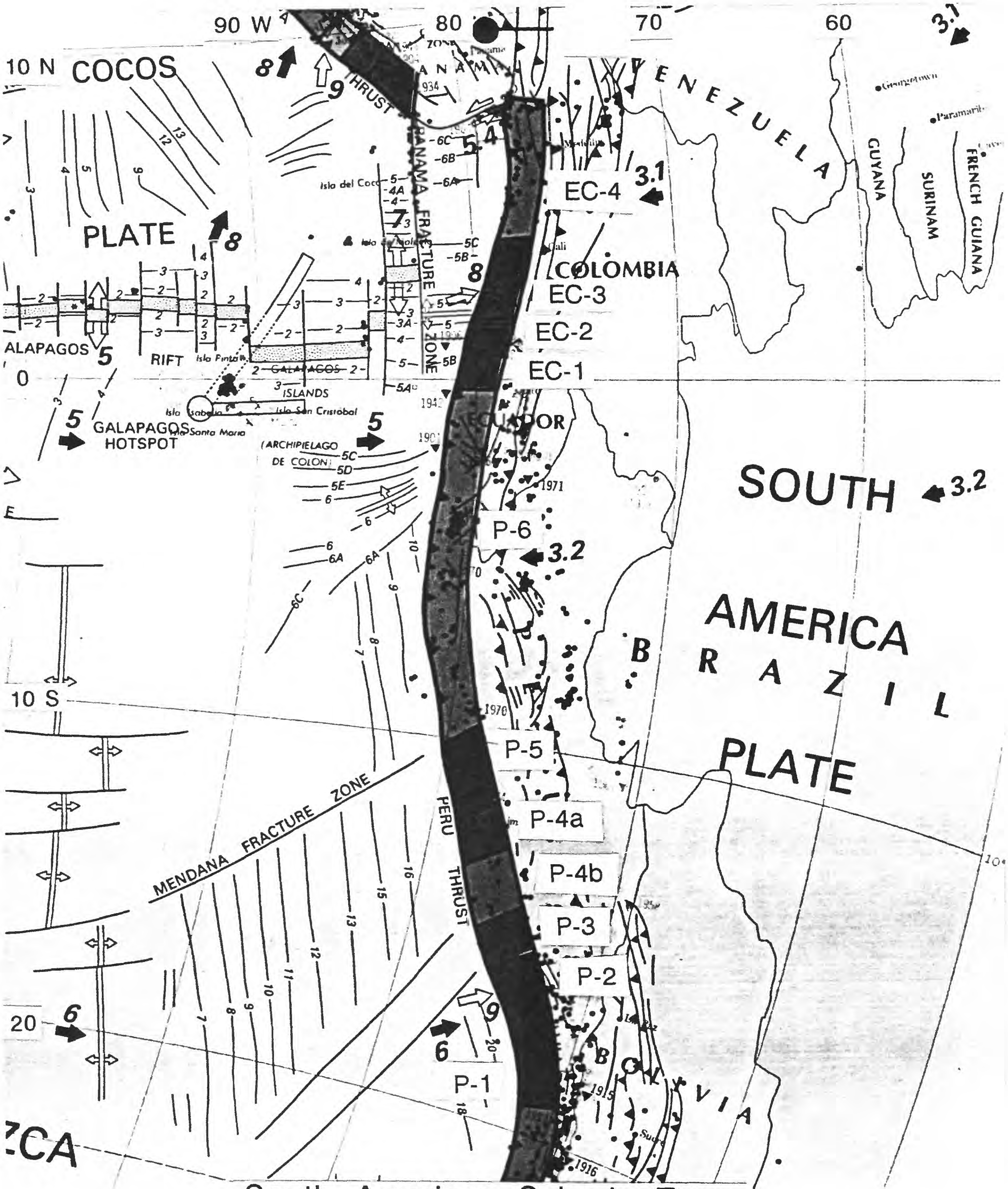

South American Seismic Zone
Peru - Ecuador - Colombia

(p. 33 follows)

major tectonic elements along the convergent margin. These segments are defined by the intersection of the Carnegie Ridge, the Mendana fracture zone, and the Nazca Ridge with the Peru trench. Estimates of conditional probability for 1989-1999 are shown in Figure 10.

P-1. *Arica*, 19°-16.6° S. The only known prior great tsunamigenic earthquakes in this segment occurred on 24 November 1604 and 14 August 1868 (M_t 9.0). The latter event is one of the most widely documented 19th century South American earthquakes. Comparison of intensities in Peru for both events indicate similar rupture zone lengths (approximately 400 km in Peru, see Figure 11). Unfortunately, comparable data does not exist in Chile for the 1604 event, and the southern boundary of the 1604 earthquake is unconstrained. The long recurrence interval between these events, 264 years, is enigmatic when compared to similar sized earthquakes in southern Chile (see previous discussions for Chilean segments C-3 and C-10). Using the single, historic recurrence time of 264 years, the probability for a M_t 9.0 earthquake appears to be negligible (i.e. 1%) for the next 10 years. If we use the recurrence history from southern Chile as a estimate for this segment, the probabilities increase to the 23% level for the next 10 years.

P-2. *Camana*, 16.6°-15.8° S. Prior destructive earthquakes that have affected the Camana region of the Peru margin occured in 1590; 27 March 1725; 10 July 1821; and 6 August 1913 (M_S 7.8). The average *repeat time* is 108 ± 13 years, and the probability for another great earthquake in this region appears to be at the 13% level for the next 10 years.

P-3. *Nazca*, 15.8°-14° S. At present, with the exception of the 12 May 1664 Ica earthquake, no predecessor is known for the 24 August 1942 Nazca (M_W 8.2) earthquake. The 1942 event is located at the intersection of the Nazca ridge with the Peru trench. Preliminary analysis of body waves for the 1942 event (S. Beck, personal communication, 1988) indicates this to be a complex earthquake and about twice the size of the 1940 Lima event (see section P-5). The 1664 earthquake destroyed Ica and caused great damage in Pisco. Unfortunately, no reports are available southeast of Ica, and we could not directly compare the extent of damage in 1942 and 1664. As discussed in the next section, the 20 October 1687 double earthquake, appears to have ruptured the segment of the plate margin between Lima and Pisco/Ica. The 23 year interval between 1664 and 1687 appears to be too short an interval to accumulate the necessary strain for a great earthquake in the same segment of plate boundary. Hence, we presently assume that the 1664 event ruptured the plate boundary east of Ica including the Nazca Ridge intersection. Accordingly, our best recurrence time estimate for this segment is 278 years (i.e 1942-1664). In other locations around the circum-Pacific, the collision of bathymetric features at convergent zones is suggested to locally modify the subduction process, resulting in longer than average recurrence times (Kelleher and McCann, 1976). Based on the historic 278 year interval, the probabilities for a great earthquake in the Nazca segment for the immediate future are at the $\leq$ 1% level.

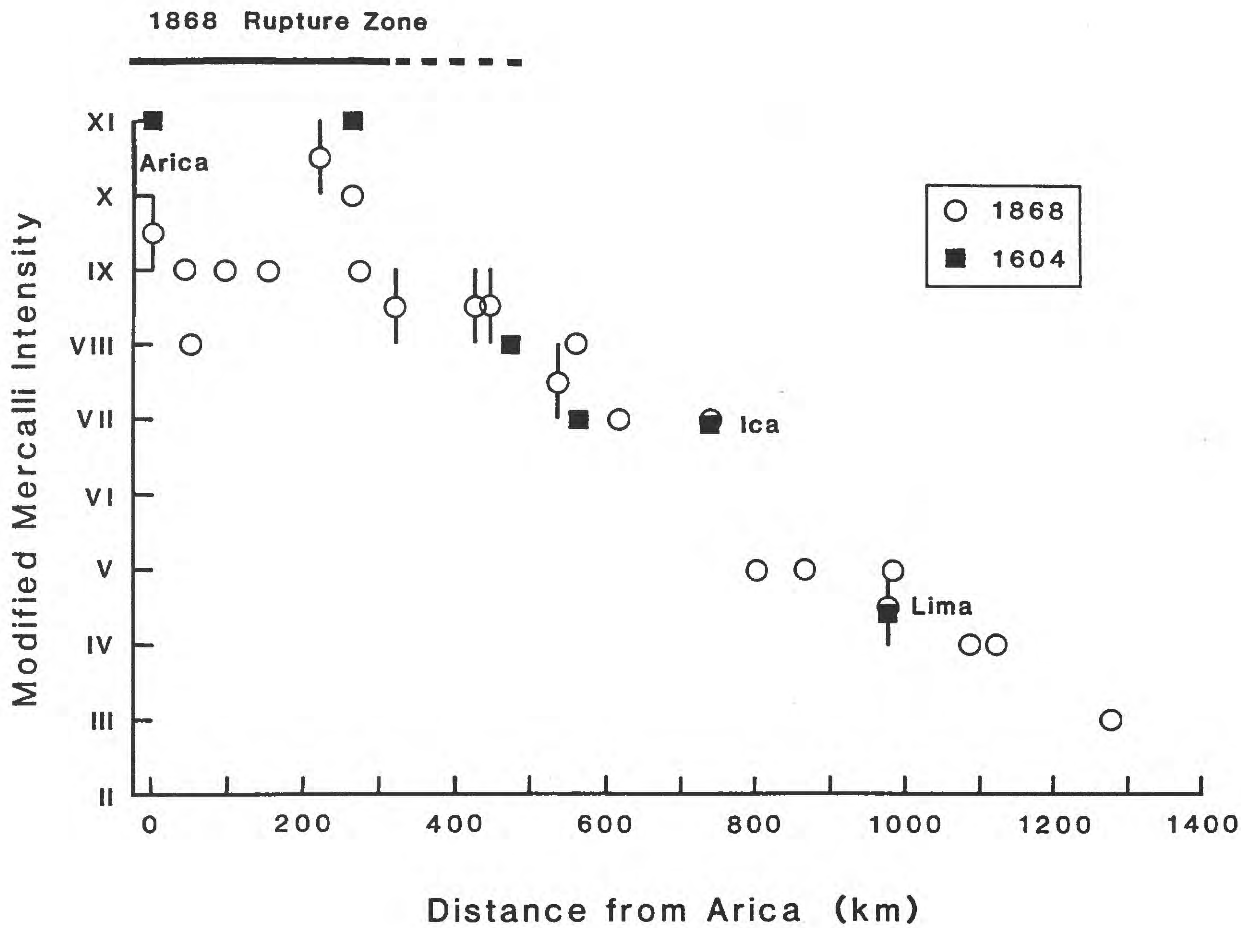

Figure 11. Comparison of felt intensities for the 24 November 1604 and 14 August 1868 Arica, Peru earthquakes. Modified Mercalli intensities in Peru for the 1604 (solid squares) and 1868 (open circles) earthquakes are plotted as a function of distance from Arica, Peru (based on intensity data from Silgado [1985]). Line at top of figure shows the estimated rupture zone for the 1868 earthquake (dashed where inferred). The similarity in the decay of intensity with distance suggests that these two events ruptured equivalent portions of the plate margin in Peru. Unfortunately, comparable data does not exist in Chile for the 1604 earthquake and the southern boundary of the 1604 earthquake is presently unconstrained.

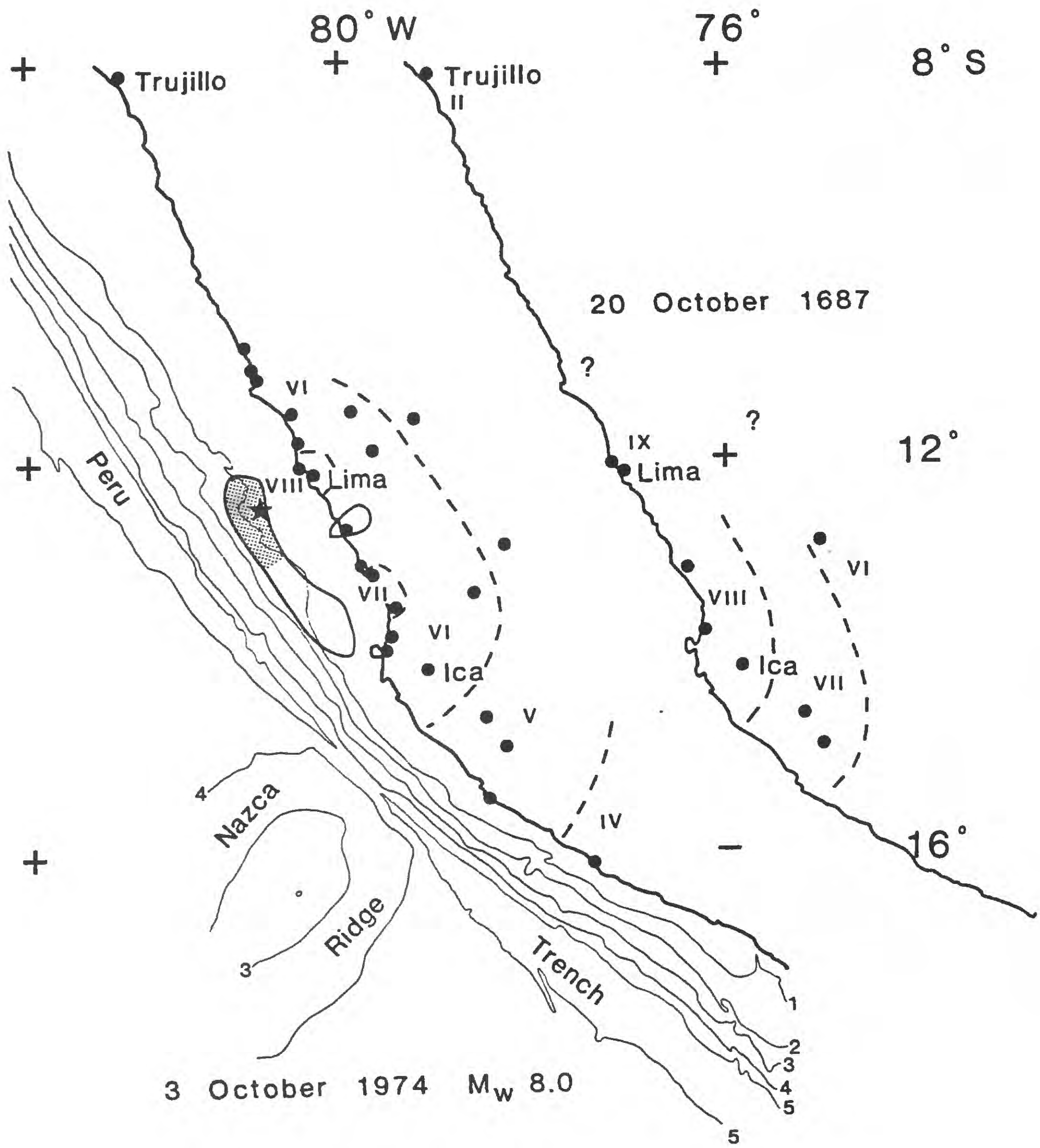

Figure 12. Comparison of 1687 and 1974 Peru earthquakes. Modified Mercalli intensities for the 20 October 1687 (combined effects of 2 earthquakes, 2 hours apart) and 3 October 1974 earthquakes from Espinosa et al. (1975, 1977) and Silgado (1985). Aftershock zone and epicenter (star) of the 1974 earthquake from Dewey and Spence (1979). Stippled region inside the aftershock zone represents the area of major seismic moment release in 1974 (from Beck and Ruff, 1989). In general, the combined felt area of both 1687 earthquakes is larger than that of the 1974 event, and suggests that the southern portion near Ica may represent a seismic gap that was not ruptured in 1974 (from Beck and Nishenko, 1989). Bathymetry from Prince et al. (1980), contour interval: 1000 m.

P-4a,b. *Lima-Pisco and Pisco-Ica*, 12°-14° S. This and the adjoining Chimbote-Lima segment of the Peru margin are defined by the intersection of the Mendana fracture zone at 10° S and the Nazca Ridge at 15° S. Both segments have exhibited considerable variation in the mode of earthquake rupture during the last 250+ years (Beck and Nishenko, 1989). On 20 October 1687, 2 earthquakes, approximately 2 hours apart, caused widespread shaking and tsunami damage from Lima to Ica. Reports and intensity data, however, are not detailed enough to determine which portion of the margin ruptured in which event. Comparison of these events with the more recent 3 October 1974 (M_W 8.0) earthquake indicates that the combined effects of the 1687 events covered a much larger area (see Figure 12). The 1974 event involved two dominant asperities, in close proximity, southwest of Lima (Beck and Ruff, 1989), and the maximum damage is located near Lima (Espinosa et al., 1975, 1977) . While the 1974 aftershock zone of Dewey and Spence (1979) extends to the Pisco area, low intensities and low aftershock activity near Pisco and Ica indicate that this southern area apparently did not rupture in the same manner as in 1687. Based on the high intensities near Ica and Pisco in 1664 and 1687, we believe this area to be a presently unbroken seismic gap. Previous events in 1687 and 1813 suggest that a 126 year *repeat time* may be appropriate for this region. Accordingly, probabilities for the southeastern portion of this segment, near Pisco, may be as high as 28% for the next 10 years, and this region deserves further attention. The portion of this segment that ruptured in 1974 (segment P-4a) presently has a $\leq$1% probability in the next 10 years.

P-5. *Chimbote-Lima*, 10°-12° S. The largest known earthquake along this segment of the Peru trench occurred on 28 October 1746 (M 8.4). Since then, no earthquake along this segment of the coast has been as large or has produced the same pattern of damage. Analysis of the sequence of great underthrust events on 24 May 1940 (M_W 8.2) and 17 October 1966 (M_W 8.1) have provided some insight into the nature of fault rupture along this segment (Beck and Ruff, 1989; Beck and Nishenko, 1989), and may explain the marked difference in the mode of rupture. Both the 1940 and 1966 events are characterized as relatively simple events which ruptured discreet asperities northwest of Lima. Comparison of the highest felt intensities for 1746, 1940 and 1966 earthquakes indicate that while the shaking and damage in 1746 is one to two Modified Mercalli values higher than 1940 or 1966, all occupy similar areas along the coast (see Figure 13). Beck and Nishenko (1989) suggest that the 1746 earthquake may have ruptured both the 1940 and 1966 asperities in one single event. Studies of multiple asperity earthquakes (e.g. see Ecuador-Colombia section) indicate that they are much larger, and more devastating, than the sum of single asperity earthquakes, even though they rupture the same segment of plate boundary. Based on the historic record of great earthquakes in 1746, 1828, and 1940-1966, we tentatively estimate the *repeat time* to be about 91 years, and estimate the probability for future great earthquakes in this segment to be at the $\leq$1-8% level for the next 10 years.

P-6. *Chimbote-Guayaquil*,2°-10° S. This segment of the Peru Trench is defined by the

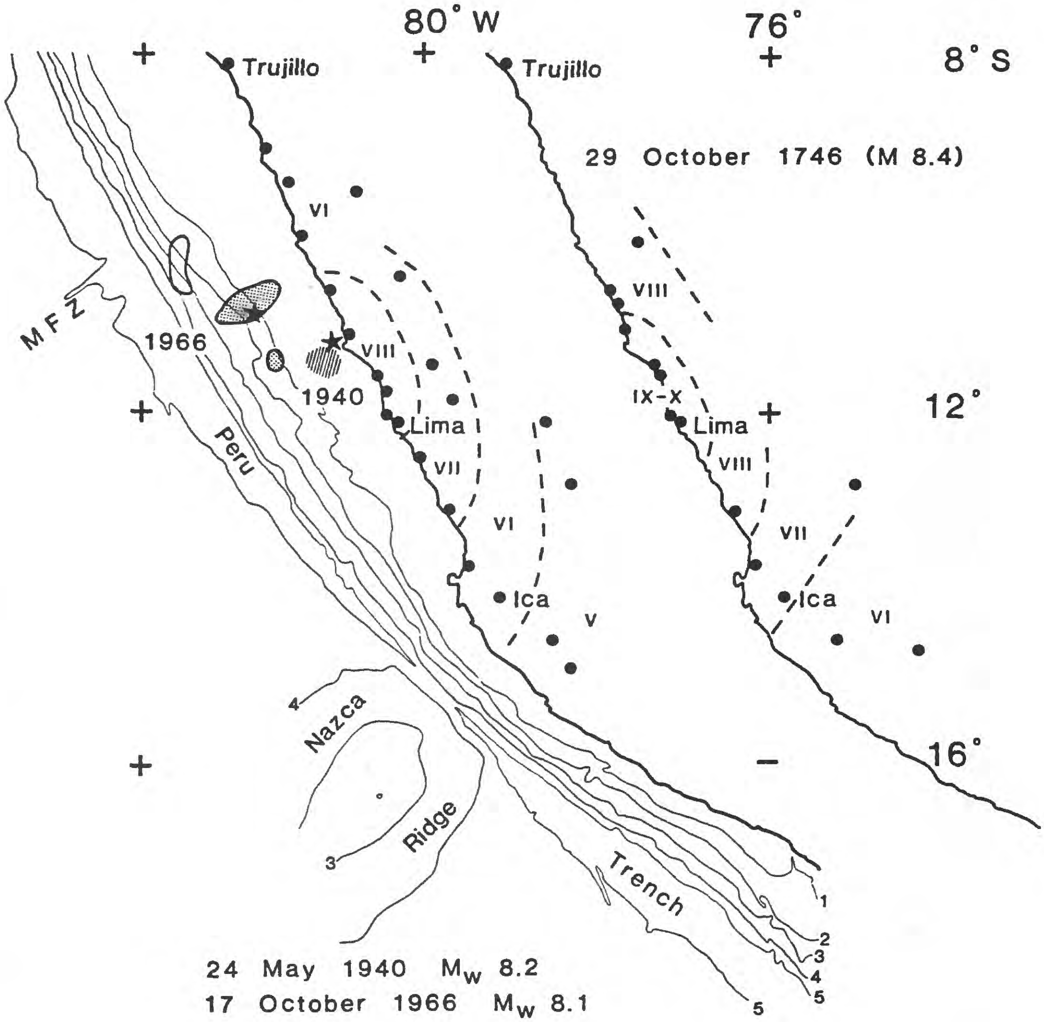

Figure 13. Comparison of 1746, 1940, and 1966 Peru earthquakes. Modified Mercalli intensities for the 29 October 1746, 24 May 1940, and 17 October 1966 earthquakes from Askew and Algermissen (1985) and Silgado (1985). Aftershock zone and epicenter (star) of the 1966 earthquake from Dewey and Spence (1979). Stippled regions represents the areas of major seismic moment release in 1966 (from Beck and Ruff, 1989). Hachured area for 1940 earthquake represents the estimated area of principal seismic moment release. MFZ is the Mendana fracture zone. Based on the spatial coincidence of areas of high shaking in 1746, 1940, and 1966, it is proposed that the 1746 earthquake simultaneously ruptured the same areas that subsiquently ruptured individually in 1940 and 1966 (from Beck and Nishenko, 1989). Bathymetry from Prince et al. (1980), contour interval: 1000 m.

intersection of the Carnegie Ridge and the Mendana fracture zone. In contrast to the other segments of the Peru-Chile Trench, the area between Chimbote and Trujillo is characterized by infrequent large earthquakes and no record of great underthrust earthquakes for the past 300 years (Kelleher, 1972). Subduction of the massive Carnegie Ridge complex could be responsible for greater than average *repeat times* in this region. At present we have no data with which to quantitatively evaluate the potential of this region.

Ecuador-Colombia

The Ecuador-Colombia seismic zone marks the boundary between the Nazca and South American plates in northwestern South America. The rate of convergence along this margin is about 8 cm/yr. Based on the patterns of seismicity over the last 100 years, the Ecuador-Colombia margin is comprised of 4 major segments. During the last 80 years, 3 out of 4 segments have ruptured in a series of large and great earthquakes. The mode of rupture, however, was not similar in all cases (Kanamori and McNally, 1982; Mendoza and Dewey, 1984; Beck and Ruff, 1984). The great 31 January 1906 earthquake (M_W 8.8) ruptured an estimated 500 km length of the Ecuador-Colombia coast. Following this great earthquake, events on 14 May 1942 (M_S 7.9), 19 January 1958 (M_S 7.8), and 12 December 1979 (M_S 7.7) ruptured subsegments of the 1906 zone (see Figure 14). At this writing, the Buenaventura segment (4°-7.5° N) is distinguished as not having any history of large or great coastal events.

Given the variable earthquake history, and the sparse settlement along the coast of Ecuador and Colombia in the 19th century, recurrence time estimates based on the historic record are difficult. The 4 February 1797 earthquake, suggested by Heaton and Hartzell (1986) as a possible predecessor to the 1906 event, is now known to have occurred in the Andes near Quito (see Silgado, 1985). Lacking a complete historic record prior to 1906, calculations of coseismic displacement for the 1942, 1958 and 1979 earthquakes provide the primary estimates of recurrence time. These estimates can also be compared to the time intervals between the 1906 and subsequent earthquakes, assuming that these times are proportional to the characteristic *repeat time* for each segment.

EC-1. *Jama,* 0.5° S-1.2° N. The interval between the 1906 and 14 May 1942 event, 36 years, provides the only historic *repeat time* estimate for this segment. Based on this single 36 year estimate, the probability over the next 10 years is at the 66% level. Unfortunately, the segment with the highest potential is the one we presently know the least about, and deserves more investiagtion in the immediate future.

EC-2. *Esmeraldas,* 1.2°-1.7° N. As in the case of the 1942 event, the time between the 1906 and 14 January 1958 event, 52 years, provides the primary recurrence data for this segment. For comparison, the average slip in 1958, 2.3 meters (Kanamori and McNally, 1982), gives recurrence times of 29 years; while the maximum slip inferred from body wave inversion (Beck and Ruff, 1984), 3.75 meters, gives a recurrence time of 47 years, which

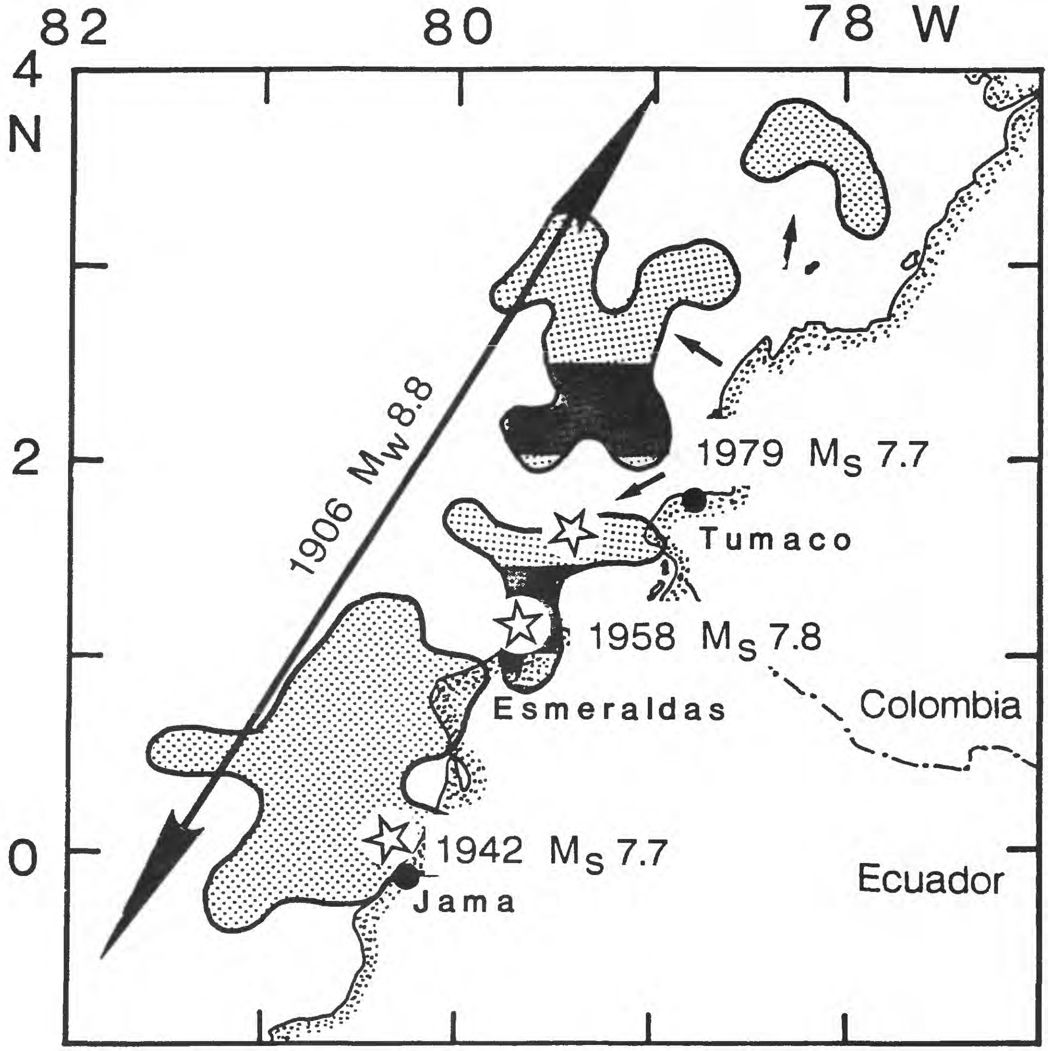

Figure 14. Comparison of recent earthquakes along the Ecuador-Colombia seismic zone. Relocations of aftershocks occurring within three months of the 14 May 1942, 19 January 1958, and 12 December 1979 earthquakes are shown by stippled zones (from Mendoza and Dewey, 1984). Epicenters are shown by stars. Darker shading highlights areas that generated the majority of seismic moment release in 1958 and 1979, and are suggested to represent the location of dominant asperities along the Ecuador-Colombia seismic zone (from Beck and Ruff, 1984). Line labelled 1906 represents the estimated rupture length of the great 31 January 1906 earthquake (from Kelleher, 1972). Note that the subsequent series of events in 1942, 1958, and 1979 all reruptured seperate portions of the 1906 zone and indicate the variable mode of great earthquake occurrence in this region.

is in better agreement with the historic record. Using the historic interval of 52 years indicates probabilities over the next 10 years at the 19% level.

EC-3. *Tumaco*, 1.7°-4° N. With the exception of the 1906 and 12 December 1979 events, there are no known predecessors for this segment of the Colombian subduction zone. Direct estimates of recurrence time, using the average and peak slip in 1979, 2.7 and 6 meters (Kanamori and McNally, 1982; Beck and Ruff, 1984), range from 34 to 75 years. The latter estimate is in good agreement with the amount of time elapsed between the 1906 and 1979 events. Using 73 years as the recurrence time estimate, the probability for the next 10 years is at the $\leq 1\%$ level.

EC-4. *Buenaventura*, 4°-7.5° N. At this writing, this segment of the Ecuador-Colombia seismic zone is distinguished by not having any history of large or great coastal earthquakes.

(p. 42 follows)

Figure 15. Seismic potential of the Central American seismic zone: 1989-1999. Colors portray the level of conditional probability for occurrence of large and great (M_S 7.0 and larger) earthquakes during the next 10 years, 1989-1999, and range from dark blue, 0-20%; green, 20-40%; yellow, 40-60%; and red, 60-100%. Light blue regions are those areas with no historic record of great earthquakes. Specific dates and magnitudes refer to areas with incomplete historic records. See Figure 6 for additional symbols and information.

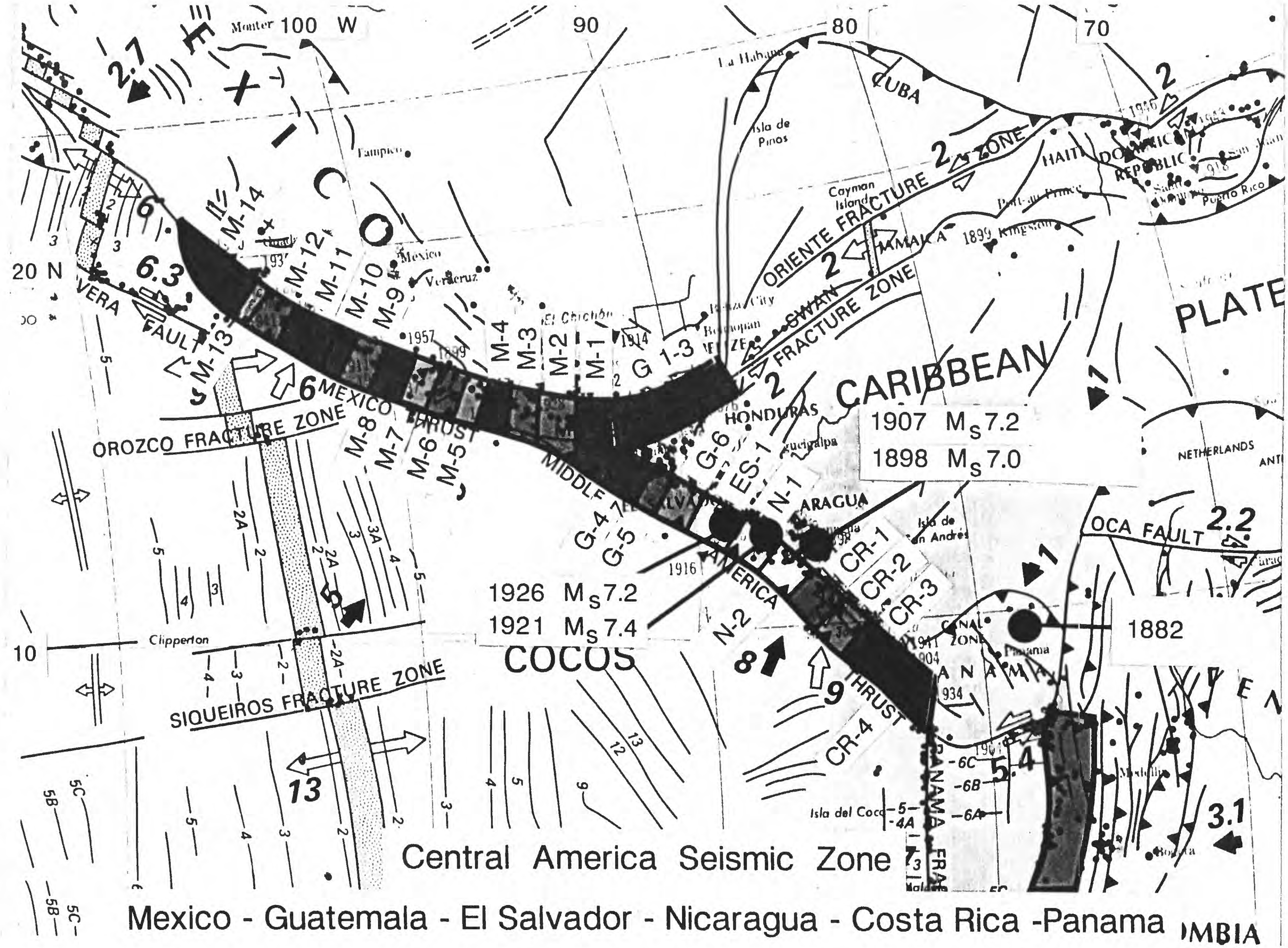
Central America Seismic Zone
Mexico - Guatemala - El Salvador - Nicaragua - Costa Rica -Panama
MEXICO
CARIBBEAN
PLATE
COCOS
CUBA
HAITI
DOMINICAN REPUBLIC
JAMAICA
HONDURAS
NICARAGUA
PANAMA
NETHERLANDS
Isla de Pinos
Cayman Islands
Isla de San Andrés
Clipperton
Isla del Coco
ORIENTE FRACTURE ZONE
SWAN FRACTURE ZONE
OROZCO FRACTURE ZONE
SIQUEIROS FRACTURE ZONE
MIDDLE AMERICA THRUST
MEXICO THRUST
OCA FAULT
VERA FAULT
M-1
M-2
M-3
M-4
M-5
M-6
M-7
M-8
M-9
M-10
M-11
M-12
M-13
M-14
G 1-3
G-4
G-5
G-6
ES-1
N-1
N-2
CR-1
CR-2
CR-3
CR-4
1907 M_S 7.2
1898 M_S 7.0
1926 M_S 7.2
1921 M_S 7.4
1882
100 W
90
80
70
20 N
10

CENTRAL AMERICA

The Central America seismic zone marks the boundary between the Cocos, Rivera, Caribbean, and North American plates along the Middle America and Mexican trenches. Rates of relative plate convergence between the Caribbean, North American, and Cocos plates range from 6 to 9 cm/yr, and are approximately 2 cm/yr between the Rivera and North American plates. The following discussion for the Panama, Costa Rica, Guatemala, and Mexican margins are based on work by Mendoza and Nishenko (1989), Montero (1986), White and Cifuentes (1989), and Nishenko and Singh (1987). Unfortunately, insufficent data exists at this present time for a quantitative analysis of seismic potential in El Salvador and Nicaragua. Estimates of seismic potential for the zones studied are shown in Figure 15 for the time interval 1989-1999.

Panama

The Panama region has been interpreted as a microplate located at the junction of the Cocos, Nazca, Caribbean, and South American plates (Adamek et al., 1988). Along the north or Caribbean coast of Panama, geologic evidence of north-south compression and the presence of a shallow, southerly dipping seismic zone indicate the existence of a convergent margin between Panama and the Caribbean. The lack of both active volcanism and seismicity deeper than 70 km, however, indicates that this is not a well developed subduction zone. The triple-junction between the Caribbean, Nazca, and South American plates exists in the eastern Panama/Colombia border region as a diffuse zone of faulting and seismicity. Along the southern coast of Panama, a diffuse left-lateral fault system between Panama and the Nazca plate has been suggested by Jordan (1975). The boundary between the Nazca and Cocos plates-the Panama fracture zone, and associated seismicity terminates near the Middle American Trench at the Panama-Costa Rica border.

In contrast to many of the adjacent countries in Central and South America, Panama is distinguished by relatively low levels of large and great earthquake activity(see Figure 16). During the 400 year historic record, only a few events stand out as causing widespread damage. One event, 7 September 1882, appears to have originated along the north coast of Panama (segment P-1). In addition to damaging the Panama-Colon railway line, this event produced a tsunami that washed away a number of towns along the San Blas Archipelago (see Figure 17). Current work by Mendoza and Nishenko (1989) is aimed at defining the location and size of this event. No other similar events are known from the historic record for this region. Hence, the lack of similar earthquakes along the north coast from 1600 to 1882 may indicate a recurrence time of approximately 300 years. Along the south coast of Panama, a large event on 2 May 1621 caused MM VIII damage in Veraguas province and MM VII damage in Panama City. Patterns of damage appear to be similar to those produced by events in 1845 and 1 October 1913 (M_S 7.5), suggesting similar tectonic origins. Too little is known, at present, to confidently assign recurrence time estimates for seismic zones in Panama, although we note, that relative to the north coast, both the east

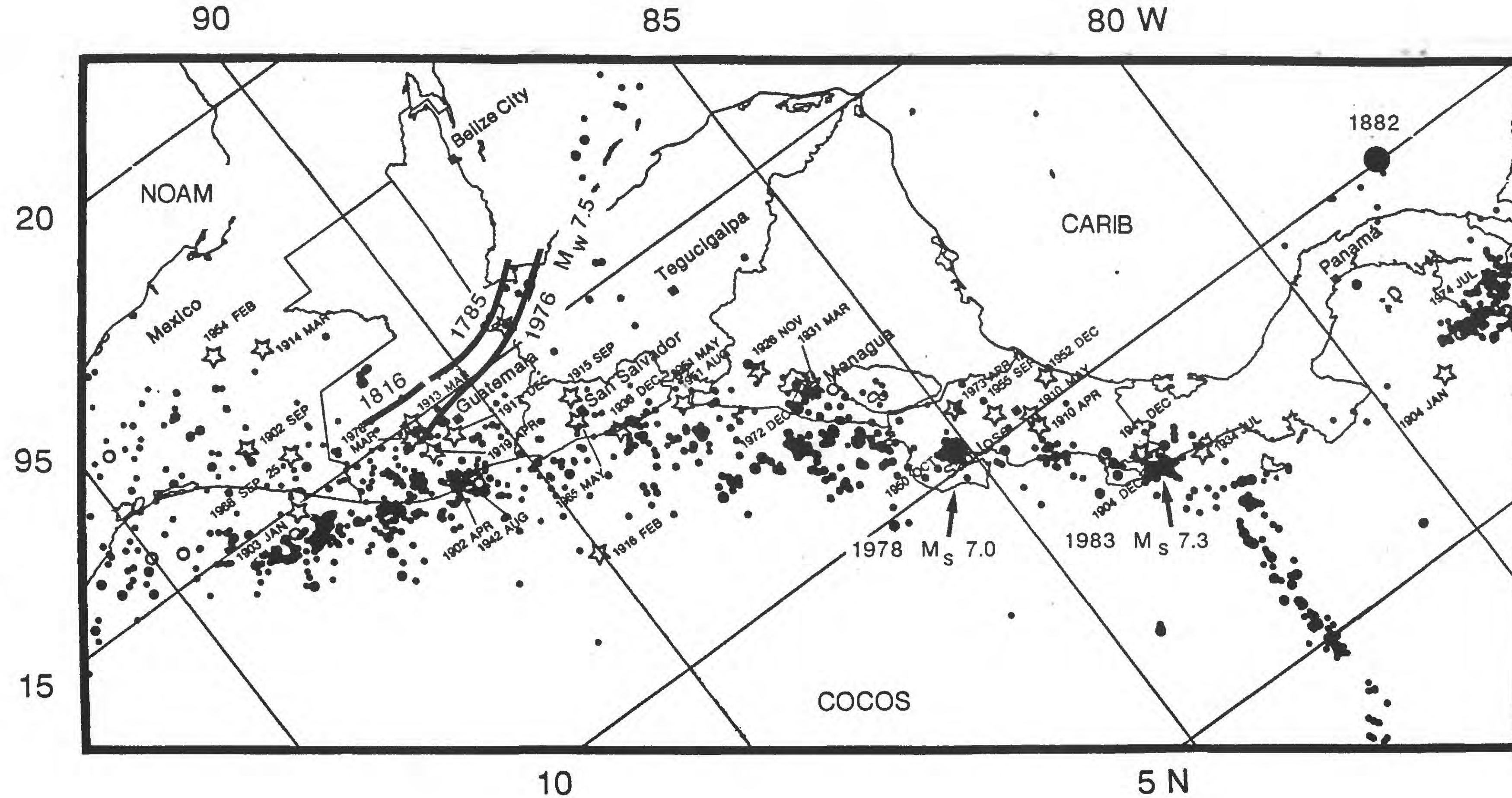

Figure 16. Recent seismicity along the Central American seismic zone (modified from Rinehart et al., 1982). Epicenters of earthquakes with M_S greater than 3.9 from 1900 through 1979 are shown. Stars are those events with either M_S greater than 7.7 or associated with more than 10 recorded deaths. Additional events discussed in the text are also indicated. NOAM, COCOS, and CARIB refer to the North American, Cocos, and Caribbean tectonic plates. Note the striking contrast in seismicity between Panama and the rest of the Central American seismic zone.

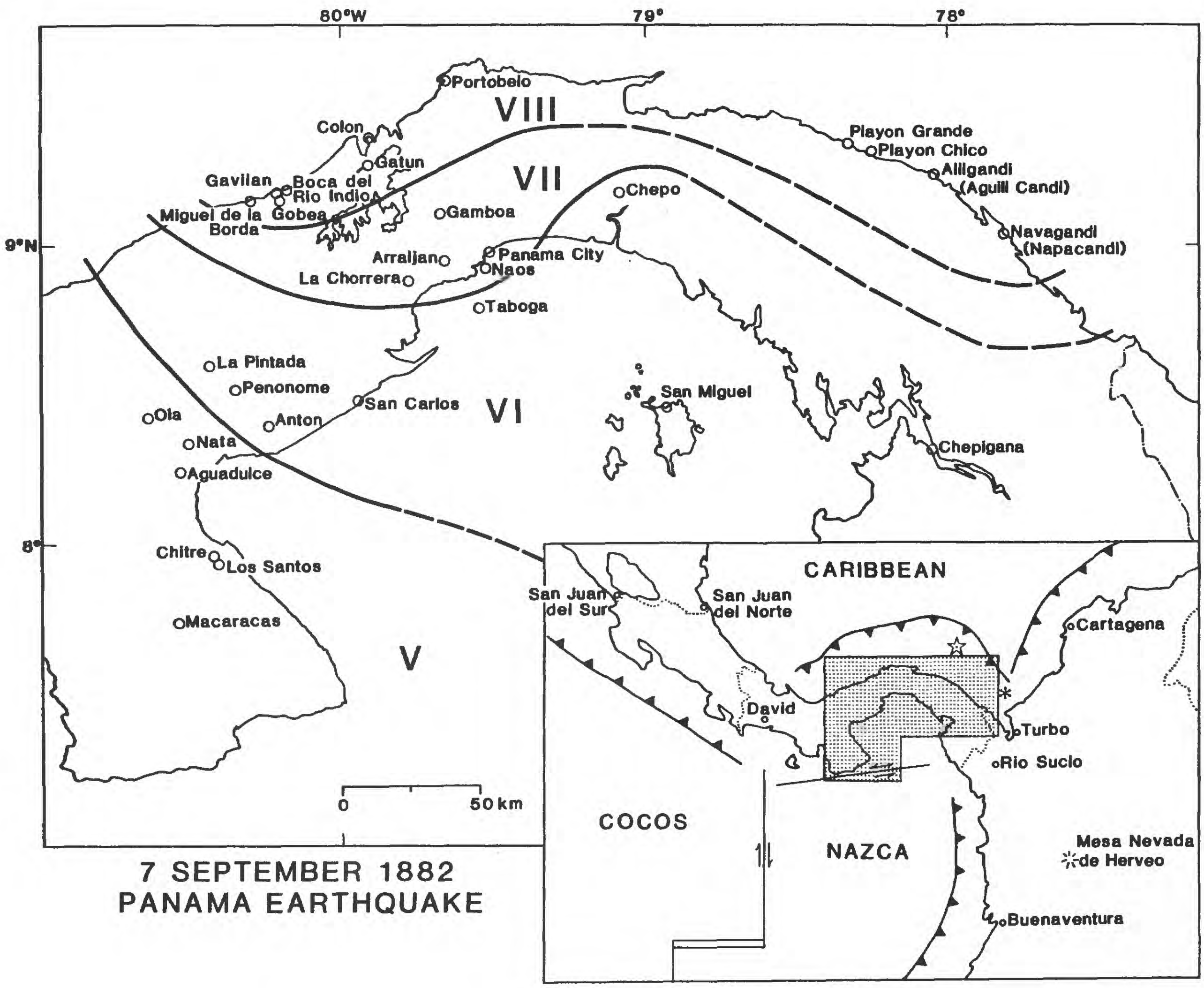

Figure 17. Intensity map for the 7 September 1882 Panama earthquake. Contour lines (dashed where inferred) seperate zones of equal Modified Mercalli intensity associated with the 1882 event. Principal tectonic features presently known for the Panama region are shown in the inset map. Barbed lines represent zones of plate convergence. The intensity data indicate that the star, centered at 10° N, 78° W, is the most probable location of the 1882 event, and suggest that this event may be related to convergence between the Caribbean plate and the Panama microplate (from Mendoza and Nishenko, 1989).

and south coast appear to have higher rates of seismic activity.

Costa Rica

Montero (1986) has divided the west coast of Costa Rica into 4 primary segments based on the seismic history from 1800 to the present. These are the Papagayo, Nicoya, Quepos, and Osa segments. A number of significant tectonic features are present along the Costa Rican portion of the Middle American trench, including changes in the dip of the Benioff zone, and the subduction of topographic features on the Cocos plate. Northwest of the Nicoya peninsula, the Benioff zone is deeper and has a steeper dip, and then gradually shallows beneath the Nicoya and Osa peninsulas. The change in dip of the Benioff zone southeast of the Nicoya peninsula has been suggested as representing a contortion in the subducted Cocos plate. Farther to the southeast, the Osa peninsula is the site of a ridge-trench collision between the Cocos ridge and the Middle American Trench.

CR-1. *Papagayo*, 87°-86° W. Only two major earthquakes are associated with the Papagayo segment by Montero (1986), 18 February 1840 and 27 February 1916 (M_S 7.5). There are, however, uncertainties as to the exact location of the 1840 event. If the 1840 earthquake is the predecessor to the 1916 event, we estimate the probability for a similar event in the next 10 years to be at the 31% level. An earlier event in 1750 caused widespread damage from the Nicaragua-Costa Rica border to San Jose, Costa Rica (R. White, personal comm., 1988). Too few details are known at present, however, to confidently assign this earlier event to a particular segment.

CR-2. *Nicoya*, 86°-85° W. The Nicoya region is one of the most active seismic zones along the Costa Rican margin, and has had large events on 21 March 1827; 9 August 1853; 12 September 1863, 21 June 1900 (M_S 7.2); 21 December 1939 (M_S 7.3); 10 May 1950 (M_S 7.7); and 23 August 1978 (M_S 7.0). The 24 April 1916 M_S 7.4 event had been assigned to this location by Montero (1986); however, felt intensities and a small tsunami reported by Reid (1917) indicate a location near Almirante, Panama on the Caribbean side of the isthmus.

With the exception of the 1950 event, all of the above listed earthquakes are similar in size to within a factor of about two (i.e. M_S 7.0-7.4). The larger 1950 earthquake may represent a more complex event, or a class of earthquakes with a longer recurrence cycle that has not been well sampled yet. If the above sequence of large earthquakes is representative of the characteristic strain release in this segment, the average ***repeat time*** is 22 $\pm$ 2 years, and the probability for continued activity in the Nicoya region over the next 10 years is at the 43% level.

CR-3. *Quepos*, 85°-84° W. The only large earthquakes associated with this segment are the events of 3 March 1882 and 9 September 1952 (M_S 7.0). Based on this one recurrence time, 70 years, we estimate the probability for another event in the next 10 years to be at the 8% level.

CR-4. *Osa*, 84°-83° W. The Osa peninsula marks the site where the aseismic Cocos ridge is subducting beneath the Caribbean plate. Large events occurring in the Osa segment include 8 May 1822; 4 August 1854; 20 December 1904 (M_S 7.2); 5 December 1941 (M_S 7.5); and 3 April 1983 (M_S 7.3). Both the 1941 and 1983 events were studied in detail by Adamek et al.(1987) who showed that while both were similar, the 1941 event exhibited more complexity in the source time functions and had a slower rupture initiation. Based on these data, the average *repeat time* for large events in the Osa peninsula segment is 40 $\pm$ 4 years, and we estimate the probability for recurrence to be at the $\leq$1% level.

Nicaragua and El Salvador

The Pacific coast of central El Salvador and Nicaragua can be divided into three primary segments based on the occurrence of large earthquakes between 1898 and 1926. These segments are Central El Salvador, ES-1 (28 February 1926, M_S 7.2); Western Nicaragua, N-1 (28 March 1921, M_S 7.4); and Eastern Nicaragua, N-2 (29 November 1898 M_S 7.0 and 30 December 1907 M_S 7.2). Unfortunately, few reports exist for 19th century and earlier earthquakes in this area. Those that do exist do not provide enough spatial coverage to estimate earthquake location or rupture extent. Hence, recurrence estiamtes similar to others made in this study are difficult at this time.

We do note, however, that the time elapsed since the previous episode of large plate boundary earthquakes, 63 to 91 years, is equal to or longer than average recurrence times for adjacent segments of the Central American trench. This region then should be regarded as having a significant but unknown seismic potential. Clearly, more work needs to be done to better constrain the hazard from large plate boundary earthquakes in this region.

Guatemala

The two principal seismic regions in Guatemala that are covered by this report are 1) the strike-slip Chixoy-Polochic-Motagua fault system that defines the North American-Caribbean plate boundary in central and northern Guatemala, and 2) the convergent boundary between the Caribbean and Cocos plates along the west coast of Guatemala and the Middle or Central American trench. Hence, within Guatemala and neighboring Chiapas, Mexico there exists a diffuse triple junction between the North American, Caribbean and Cocos plates. The following earthquake hazards estimates are based on analysis by Schwartz (1985), Schwartz et al. (1979), White (1984, 1985), and White and Cifuentes (1989).

Transform Faults: The Chixoy-Polochic and Motagua faults represent the principal strike-slip structures within a broad zone of deformation that defines the western portion of the Caribbean-North American plate boundary in Central America. While these faults have been the most active historically, there are insufficient data to evaluate the potential of other faults within this diffuse zone of deformation. During the time interval 1538 to 1983, White (1988) has documented 2 or possibly 3 active periods for the combined

Chixoy-Polochic-Motagua fault system. These active periods, which typically are terminated by large earthquakes on either the Chixoy-Polochic or Motagua fault systems, have had durations of 50 to 100 years and are separated by quiet periods of about 120 years duration.

G-1. *Motagua Fault*, 88.3°-91° W. Geologic investigations, following the 4 February 1976 (M_W 7.5) Motagua earthquake, indicate that the previous large event occurred around 1280 A.D. (Schwartz, 1985; Schwartz et al., 1979). Given that the last large event was in 1976, the probabilities for a similar event on the Motagua fault in the near future are negligible (i.e. $\leq 1\%$). In addition, White (1984) suggests that the 1976 event has probably terminated the current active period in this region which began in 1945.

G-2,3. *Chixoy-Polochic Fault*, 89°-91.5° W. Previous events that are associated with the eastern portion of the Chixoy-Polochic fault, based on both geologic and historic investigation, occurred in 600 A.D., 938, 1538 (?), and 1785. The average recurrence time is about 250 years, and the estimated probability for the eastern Chixoy-Polochic segment is at the 8% level. For the western segment of the Chixoy-Polochic fault, only one event in 1816 is presently documented (White, 1985). Given the temporal coupling of earthquakes on the eastern and western segments in the last cycle (1785-1816), we qualitatively estimate that the chances of a future large event on the western portion of the Chixoy-Polochic are similar to those for the eastern segment.

Convergent margin: The convergent margin of Guatemala can be subdivided into 3 principal segments based on the historic analysis of White and Cifuentes (1988), which covers the time interval 1526 to 1987. Rupture zones for earlier events are determined from the location of the Modified Mercalli (MM) VII intensity contour. These 3 segments are termed the northwestern, central and southeastern portions.

G-4. *Northwestern*, 92.5°-91.5° W. Prior great earthquakes along the northwestern portion of Guatemala include 24 October 1765, 18 April 1902 (M_S 7.9), and 6 August 1942 (M_S 7.9). The 1902 event was part of a sequence of 3 great earthquakes in western Guatemala and Chiapas, Mexico, from 1902 to 1903 (see also Nishenko and Singh, 1987c). The northwestern segment appears to have a much more variable recurrence history than the central or southeastern segments (see text below). White and Cifuentes (1989) have suggested that this marked variability may reflect complex interactions between the convergent and strike-slip fault systems in the vicinity of the Cocos-North American-Caribbean triple junction. The longest interval between events (1765-1902) occurs during the time span that the western Chixoy-Polochic fault experienced its only known historical rupture (1816). While the average recurrence time is not well known for this segment, and the nature of fault interactions not well understood at present, we tentatively estimate that the recurrence time is 89 years, and that the probabilities for future great earthquakes throughout this zone during the next 10 years are at the 13% level.

G-5. *Central*, 91.5°-90.5° W. Prior events in the central portion of the Guatemala seismic zone include 29 September 1717, 29 July 1773, 19 December 1862, 3 September 1874 and 6 August 1942 (M_S 7.9). In contrast to the northwestern segment, there appears to be more regularity in the pattern of earthquake occurrence. The average *repeat time* is 66 years, and the probabilities for the next 10 years are at the 23% level.

G-6. *Southeastern*, 89°-90.5° W. This segment also includes the northwestern portion of El Salvador and is located in the area between Guatemala City and San Salvador, El Salvador. Additionally, this area contains the most consistent or regular history of great earthquakes in the catalog of White and Cifuentes (1989). Previous events occurred on 1575, 1658, 5 March 1719, 30 March and 30 May 1776, 19 December 1862, and 6 September 1915 (M_S 7.7). Based on these events, the average *repeat time* is 68 ± 6 years, and the probability for a future event is at the 51% level for the next 10 years. Presently this segment stands out as having the highest hazard along the Guatemala portion of the Middle America Trench. Analysis of the 1915 earthquake indicates that it ruptured the lower portion of the plate interface, between 60 and 80 km, and was not accompanied by a tsunami. Presently, this gap is also associated with zone of seismic quiescence for small and moderate sized earthquakes since 1963 (White and Cifuentes, 1989).

Mexico

The following sections summarize the basic earthquake data for 13 segments along the Mexican subduction zone and are organized by state within the Republic of Mexico. A more complete analysis is presented in Nishenko and Singh (1987a). Place names and a space-time graph illustrating historic rupture zones and the locations of current seismic gaps are shown in Figure 18.

Chiapas

M-1. *Chiapas*, 92.5°-94° W. Previous earthquakes known or thought to have occurred in this region include 1565 or 1591, 1743, 1902 (M_S 7.5, 7.8) and 1903 (M_S 7.7). The average *repeat time* is approximately 162 years, much longer than elsewhere along the Mexican or Guatemalan margin. At present, the probability for another great event in Chiapas appears to be at the 2% level for the next 10 years.

Oaxaca

M-2. *Tehuantepec*, 94°-95.2° W. The Tehuantepec gap is one of two segments along the Mexican margin that are presently distinguished as having no historic record of large or great earthquakes (Kelleher et al., 1973; Kelleher and McCann, 1976; Singh et al., 1981). The location of this gap is coincident with the intersection of the Tehuantepec Ridge with the Middle America Trench, and is near the triple junction of the North American, Cocos, and Caribbean plates.

At present, there are no data with which to base a seismic hazard estimate for this segment. One possible candidate for a prior event in this region is the 5 June 1897 M_S 7.4 earthquake, which had previously been associated with the eastern Oaxaca segment

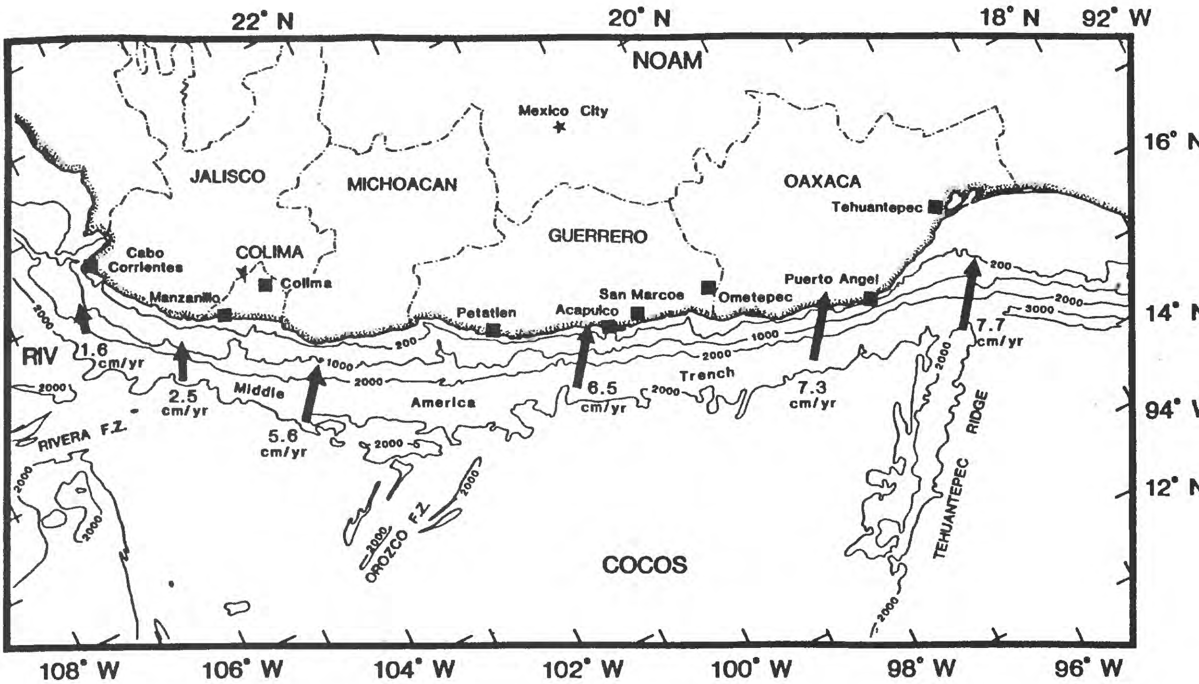
22° N
20° N
18° N
92° W
NOAM
Mexico City
16° N
JALISCO
MICHOACAN
OAXACA
Tehuantepec
GUERRERO
Cabo Corrientes
COLIMA
Colima
Manzanillo
Petatlan
Acapulco
San Marcos
Ometepec
Puerto Angel
14° N
RIV
1.6 cm/yr
2.5 cm/yr
Middle
America
Trench
5.6 cm/yr
6.5 cm/yr
7.3 cm/yr
7.7 cm/yr
94° W
RIVERA F.Z.
OROZCO F.Z.
TEHUANTEPEC RIDGE
12° N
COCOS
108° W
106° W
104° W
102° W
100° W
98° W
96° W

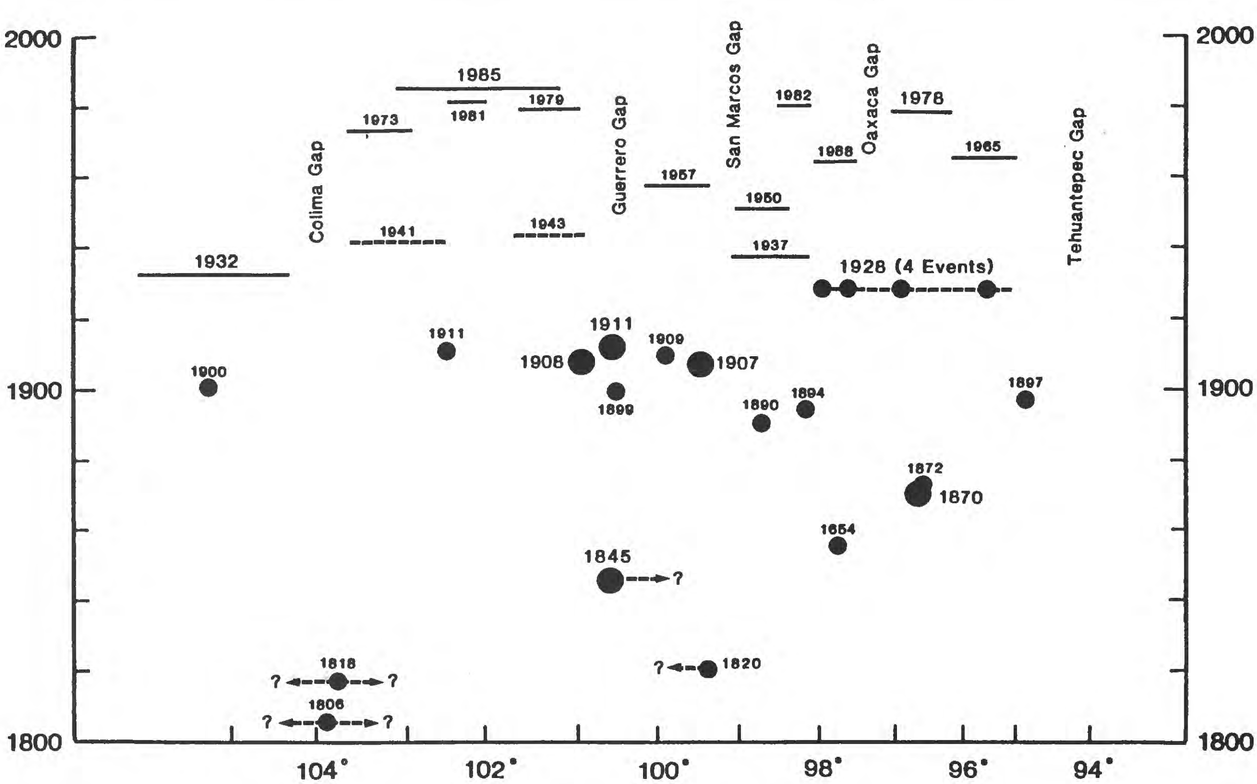
2000
1900
1800
Colima Gap
Guerrero Gap
San Marcos Gap
Oaxaca Gap
Tehuantepec Gap
1985
1973
1981
1979
1982
1978
1988
1965
1957
1950
1941
1943
1937
1932
1928 (4 Events)
1911
1908
1909
1907
1900
1899
1890
1894
1897
1872
1870
1854
1845
1818
1806
1820
104°
102°
100°
98°
96°
94°

Figure 18. (*Top*) Location of Mexican states, cities, and major bathymetric features. Bathymetry from Chase et al. (1970), contour interval: 1000 m. Solid arrows indicate the direction and relative rates of convergence between the North American (NOAM), and Cocos (COCOS) or Rivera (RIV) plates [convergence vectors after McNally and Minster (1981) and Eissler and McNally (1984)]. (*Bottom*) Space-time diagram of historic and recent earthquakes along the Mexican subduction zone, and locations of current seismic gaps. Large circles represent earthquakes with $M_S \geq 7.7$. Small circles are events with $M_S \geq 7.0$. Dashed horizontal lines indicate the lateral extent of rupture zones since 1928, based on aftershock studies and are dashed where less well-determined.

(Singh et al., 1981). Based on the dimensions of the Tehuantepec gap (125 km length, 80 km width) this region may be capable of producing an event of M_W 8.0 (M_O 1 x 10^{28} dyne-cm). This region should be regarded as having a poorly known seismic potential, and should be the target of future research to better constrain both the earthquake history and the hazard level.

M-3. *Eastern Oaxaca*, 95.2°-96.4° W. Previous large earthquakes that are known to have occurred within this segment include: 22 March 1928 (M_S 7.7) and 23 August 1965 (M_S 7.8). The observation of similar body waveforms (Chael and Stewart, 1982; Singh et al., 1984), and comparable magnitudes for both events indicate that the characteristic earthquake model may be appropriate in this region. Based on the one available recurrence time, 1965-1928 or 37 years, the corresponding estimates of conditional probability for the next 10 years are at the 35% level.

M-4. and M-5. *Central Oaxaca*, 96.4°-97.7° W. Previous large and great earthquakes that have occurred along these segments of the margin include: 11 May 1870 (M_S 7.9); 27 March 1872 (M_S 7.4(?)); 17 June 1928 (M_S 8.0); 9 October 1928 (M_S 7.8); and 29 November 1978 (M_S 7.8). The Central Oaxaca regions contains two segments or source zones, one between 96.4° and 97.3° W (Zone M-4) and a second between 97.3° and 97.7° W (Zone M-5).

In general there is good agreement between the earlier intensity data and the instrumental data that the 1870, 17 June 1928 and 1978 earthquakes ruptured the same segment of the plate boundary (Zone M-4). As in the case of the eastern Oaxaca segment (M-3), the observation of simple body waveforms, and comparable magnitudes indicates that the observed 54 $\pm$ 8 year average repeat time appears to represent a reliable recurrence estimate for this region. Based on these data, the conditional probability for the next 10 years appears negligible (i.e. $\leq$ 1%).

In contrast, the adjacent segment (97.3° to 97.7° W, zone M-5), which last ruptured on 9 October 1928, has not had a repeat since that time and is presently considered to have a high probability for recurrence. The historic record is not clear as to what events ruptured this segment prior to 1928, or whether this segment is capable of rupturing independently. Hence, well constrained recurrence estimates, similar to others in this study are not possible at this time. Based on the size of this gap (55 km length, 80 km width), the estimated seismic moment of an event that would fill this region is approximately 2 x 10^{27} dyne-cm (equivalent to M_S 7.7, or approximately the size of the 9 October 1928 earthquake). One possible candidate for a previous event is the 27 March 1872 earthquake. Using the interval 1928-1872 or 56 years, as a recurrence time estimate, the estimated conditional probability is at the 45% level for the next 10 years. For comparison, a recurrence time of 44 years is suggested based on the sizes and times of events occurring in adjacent segments (M-4 and M-6). While the absolute values are not well-constrained, these estimates are significantly higher than the estimates for the adjacent regions in the state of Oaxaca.

M-6. *Western Oaxaca*, 97.7°-98.2° W. Previous large earthquakes that have occurred in this segment include 5 May 1854 (M_S 7.7); 2 November 1894 (M_S 7.4); 4 August 1928 (M_S 7.6); and 2 August 1968 (M_S 7.4). As in the case of the other Oaxaca segments (M-3, M-4), comparable body waveforms and magnitudes indicate that all events are essentially identical, and that the observed 38 $\pm$ 5 year average *repeat time* is a reliable recurrence time estimate. Accordingly, the probability estimates for the next 10 years are at the 21% level.

Guerrero

M-7. *Ometepec*, 98.2°-99.3° W. Previous large earthquakes that are known or suspected to have occurred in this segment include: 2 December 1890 (M_S 7.5); 15 April 1907 (M_S 7.9); 23 December 1937 (M_S 7.5); 14 December 1950 (M_S 7.3); and 7 June 1982 (M_S 6.9,7.0). This segment has been classified as a seismic gap by Singh et al. (1981) on the basis of the amount of time elapsed since a prior large earthquake. During this century, the recurrence history along the Ometepec segment has been somewhat anomalous when compared to the adjoining segments in Oaxaca. Earthquakes in Ometepec exhibit both simple and complex modes of rupture, with large variations in both magnitude and interevent times. For example, the 1937 event was followed 13 years later, in an almost identical location, by the 1950 event. Nishenko and Singh (1987b) argue that this sequence may not represent a true recurrence, but rather a complex mode of rupture that took 13 years to complete. In contrast, Gonzalez-Ruiz and McNally (1988) suggest that the Ometepec segment is characterized by randomly occurring large events. According to their interpretation, the best recurrence probabilities would be based on a Poisson type model, which gives estimates of 30 to 40% for the next 10 years. For comparison, the lognormal model gives slightly higher estimates of 47% for the same time interval.

M-8. *Acapulco-San Marcos*, 99.3°-100° W. Previous large and great earthquakes that are associated with this segment include: 4 May 1820(?) (M_S 7.6); 7 April 1845 (M_S 7.9); 15 April 1907 (M_S 7.9); and 28 July 1957 (M_S 7.7). Estimates of the seismic potential for this segment have been discussed by Singh et al. (1982) based on the assumption that both the 1907 and 1957 events ruptured the same segment of plate interface. The seismic moment of the 1907 event is approximately twice that of the 1957 earthquake, and based on the above assumption and the time-predictable model, a possible recurrence time of 28 years was suggested. Nishenko and Singh (1987), on the other hand, suggest that the 1907 event may have ruptured both the Acapulco and Ometepec segments (M-7 and M-8). Hence the difference in seismic moment may reflect the fact that the 1957 shock only ruptured half of the 1907 zone.

Based on historic observations of great shocks in the Acapulco-San Marcos region, there are two possible candidates for a predecessor to the 1907 event: 1820 and 1845. The average *repeat times*, depending on which event actually occurred in this segment, range from 56 to 68 years. In spite of this present uncertainty, the current probability estimates are low for the next 10 years (i.e. 13%).

M-9. *Central Guerrero*, 100°-101° W. Previous earthquakes of $M_S \geq 7.5$ known or estimated to have occurred in this segment include: 7 April 1845(?) (M_S 7.9); 24 December 1899 (M_S 7.7); 26 March 1908 (M_S 7.8); 30 July 1909 (M_S 7.5); and 16 December 1911 (M_S 7.8). With the exception of the 1845 event, there are no presently well-documented earthquakes for this region prior to 1899, owing to low population densities during the 19th century and perhaps longer than average *repeat times*. Hence, recurrence estimates for this segment are speculative at best.

This segment may be capable of producing a single event of M_W 8.0 (M_O 1 x 10^{28} dyne-cm) based on the physical dimensions of the gap (100 km length, 80 km width). The summation of moment release during the 1899-1911 sequence is approximately 1.5 x 10^{28} dyne-cm, and suggests that while the exact locations of these earlier events are poorly known, most probably all contributed to filling in the entire gap.

While no historic recurrence times are available, we can estimate recurrence times by extrapolating the known recurrence behavior in Oaxaca. This comparison suggests recurrence times of approximately 60 to 70 years for M_S 7.7 to 7.8 events, and 50 years for M_S 7.5 earthquakes. These estimates are in relatively good agreement with a postulated 54 year recurrence time, if the 1854 event is actually located in the Central Guerrero gap. While these estimates are shorter than the amount of time that has already elapsed since the previous series of large and great shocks at the turn of the century, we note that the Central Guerreo gap stands out as having a significantly higher potential (30–40%) than the surrounding regions.

M-10. *Petatlan*, 101°-101.8° W. Previous shocks in this region include 22 February 1943 (M_S 7.7) and 14 March 1979 (M_S 7.6). In contrast to the earthquakes in Oaxaca, there appears to be much more variability in the mode of rupture for this region. Based on the observation that the interval 1979-1943 represents a recurrence interval for this segment, the conditional probability for the next 10 years is negligible (3%).

Michoacan

M-11. *Michoacan*, 101.5°-103° W. This segment, like the Tehuantepec gap, is coincident with the intersection of a bathymetric feature, the Orozco fracture zone. Kelleher and McCann (1976) and LeFevre and McNally (1985) have suggested that collisions of this sort may locally modify the subduction process, resulting in longer than average repeat times. The occurrence of the great 19 September 1985 earthquake in this gap appears to support the model of infrequent great shocks with longer than average *repeat times*. An earlier event 7 June 1911 (M_S 7.9) has been relocated in this gap on the basis of locally recorded S-P times and similarities in intensity with the 1985 event (Eissler et al., 1986). Hence, while still poorly known, a recurrence time of 74 years appears to be appropriate for this segment, and the hazard estimate for the recurrence of a great event within this gap in the next 20 years is small ($\leq$ 1%).

M-12. *Colima* 103°-103.7° W. Previous large earthquakes associated with this segment include: 15 April 1941 (M_S 7.9) and 30 January 1973 (M_S 7.5). Comparison of locally recorded S-P times and felt intensities indicate that the rupture zone of the 1941 event was larger than the 1973 event, and may have extended into the 1985 Michoacan rupture zone (UNAM Seismology Group, 1986). These variable rupture patterns illustrate the current difficulties in exactly forecasting future earthquake activity. Nevertheless, if we base our forecast on the observed interval 1973-1941, the conditional probability is at the 25% level for the next 10 years.

Colima

M-13. *Colima gap*, 103.7°-104.5° W. The Colima gap is defined on the basis of relocations of aftershocks of the great 3 June 1932 Jalisco earthquake (Singh et al., 1985) and covers a zone approximately 60 km long between the 1932 and 1973 Colima rupture zones. The Colima gap is approximately coincident with the coastal extension of the Colima graben - the arm of an incipient triple junction in Jalisco (Luhr et al., 1985). The lack of any major shocks in this region during the last 80 years may indicate the existence of a modified stress regime in this area. Given this, any further discussion is outside of the scope of this study. with the exception of noting that the Jalisco graben system is also capable of producing large earthquakes (i.e. 11 February 1875, Guadalaraja (M_S 7.5))

Jalisco

M-14. ***Jalisco***, 104.3°-105.7° W. Previous large and great earthquakes that have occurred in or near the state of Jalisco include: 25 March 1806 (M_S 7.5); 31 May 1818 (M_S 7.7); 20 January and 16 May 1900 (M_S 7.6 and 7.1); and 3 and 18 June 1932 (M_S 8.1 and 7.8). The 3 June 1932 earthquake is one of the largest events to have occurred in Mexico during this century. Analysis of intermediate-period body waves, relocations of locally recorded aftershocks and compilation of intensity data (Singh et al., 1984; Singh et al., 1985) indicate that this was a complicated event that ruptured a 220 km portion of the Rivera plate. Low population densities along the coast of Jalisco, however, makes positive identification of older rupture zones difficult. One or both of the 1806 and 1818 events may have ruptured either the Jalisco or Colima segments. Singh et al. (1985) estimate a recurrence time of 77 years, based on the long-period seismic moment and rupture areas of the 3 and 18 June events. This direct estimate is shorter than the historically suggested intervals of 114 to 126 years, if either of these events did actually rupture this segment of the margin. The corresponding conditional probabilities range from 2-18% for the next 10 years.

Additionally, we have no information about the recurrence of large (i.e. $7 < M_S < 7.7$) events, like the 20 January 1900 earthquake for this region. Hence, recurrence time and probability estimates for large shocks in the state of Jalisco are not possible at this time.

Figure 19. Seismic potential of the San Andreas fault and Washington-Oregon seismic zone: 1989-1999. Colors portray the level of conditional probability for occurrence of large and great (M_S 7.0 and larger) earthquakes during the next 10 years, 1989-1999, and range from dark blue, 0-20%; green, 20-40%; yellow, 40-60%; and red, 60-100%. Light blue regions are those areas with no historic record of large or great earthquakes. Specific dates and magnitudes refer to areas with incomplete historic records. See Figure 6 for additional symbols and information.

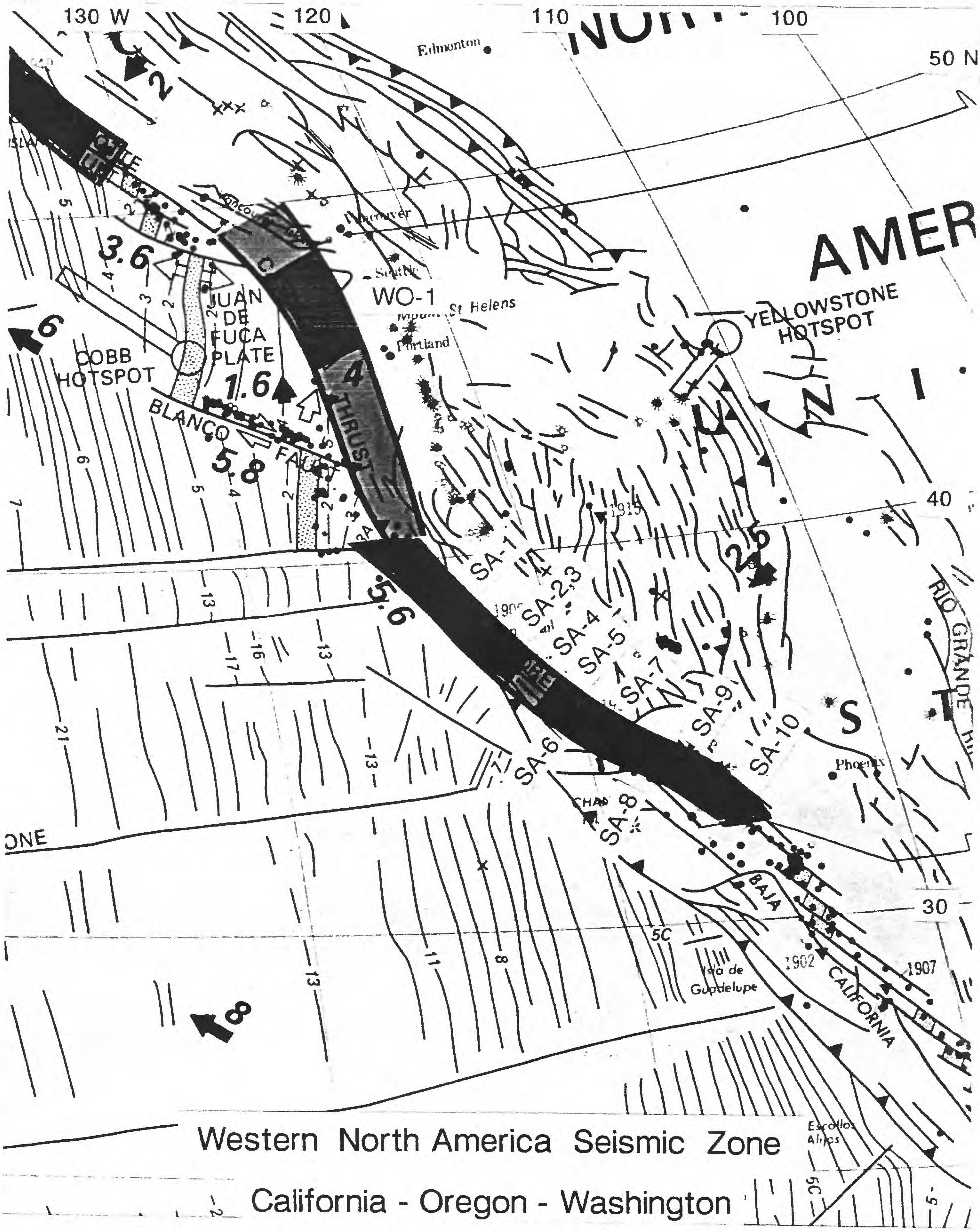

Western North America Seismic Zone

California - Oregon - Washington

(p. 61 follows)

NORTH AMERICA

California

The San Andreas fault system represents the primary locus of plate motion between the North American and Pacific plates in the western United States. The following discussion summarizes the results of the Working Group on California Earthquake Probabilities (1988) and is focused primarily on the San Andreas fault proper. The 10 year forecast (1989-1999) is shown in Figure 19, and the 30 year (1988-2018) forecast of the Working Group is shown in Figure 20. Discussion of other faults that comprise the San Andreas fault system can be found in the Working Group report.

Primary segmentation of the San Andreas fault is based on the rupture zones of great through moderate sized earthquakes that have occurred within the last 300 years and are thought to define characteristic segments along the fault trace. From north to south these primary segments include the 1906 San Francisco rupture, the Central Creeping Zone, the 1966 Parkfield-Cholame, the 1857 Fort Tejon, the 1812(?) San Bernardino, and the 1680 Coachella Valley earthquake ruptures. Within each of these rupture zones, subdivisions have been made, reflecting spatial variations in the amount of observed coseismic displacement associated with a particular rupture. These subdivisions will be discussed within the overall discussion of the primary segmentation.

SA 1-3. *Northern San Andreas Fault*, 36.8°- 40.4° N. The northern San Andreas fault segment is defined by the rupture zone of the great 1906 San Francisco earthquake, and extends from Punta Gorda south through the San Francisco Peninsula and terminates near San Juan Bautista. Over the 485 km long rupture zone, the average amount of slip in 1906 reaches a maximum of 4 to 7 meters (from Punta Gorda to Olema) and steadily decreases in the San Francisco Peninsula region from 3 to less than 1 meter before terminating near San Juan Bautista.

The long term rate of fault motion for the northern (Olema) and San Francisco Peninsula segments (1.6 cm/yr), and the amounts of displacement in 1906 indicate recurrence times of 303 and 169 years, respectively. Hence, probabilities for a great earthquake in the immediate future appear quite low (i.e. $\leq 1\%$ and 5%, respectively). For the southern terminus of the 1906 break, however, estimates are more equivocal, and are highly dependent on interpretation of available data (see Scholz, 1985; Sykes and Nishenko, 1984; Thatcher and Lisowski, 1987). Using coseismic displacement values of 2.5 and 1.5 meters, and a slip rate of 1.6 cm/yr, the estimated return times for the Peninsula segment (SA-2) range between 156 and 94 years, respectively, and corresponding probabilities range between 5% and 16%. This segment then stands out as having the highest potential along the 1906 break, and could produce a large (i.e. M_S 7) earthquake. The Santa Cruz segment (SA-3) also has a relatively higher potential for the occurrence of a moderate sized event (M_S 6.5).

SA-4. *Central Creeping Zone*, 36°-36.8° N. The 130 km long Central Creeping segment has exhibited continuous or quasi-continuous slippage, with a rate of creep that is similar to that of the long-term geologic rate of fault motion. Since all or the majority of fault motion is being accounted for by creep, it does not appear that this segment is accumulating strain for release in a large or great earthquake.

SA-5. *Parkfield-Cholame*, 36°- 35.7° N. South of the central creeping zone is the Parkfield-Cholame segment which historically has ruptured in moderate (M 6.0) earthquakes about every 22 ± 2 years. The last event occurred in 1966, and the next event is expected in a 5 year window centered on 1988. Currently this segment is the site of the Parkfield Earthquake Prediction Experiment (Bakun and Lindh, 1985), and has a high probability (i.e. 93%) for recurrence within the next 10 years.

SA 6-8. *Central San Andreas Fault*, 35.7°-34.3° N. The rupture zone of the great 1857 Ft. Tejon earthquake defines the Central San Andreas fault, and like the 1906 break can be divided into subsegments along its 300 km length. The three principal subdivisions are the Cholame, Carrizo and Mojave segments. The Cholame segment lies at the northern end of the 1857 rupture and exhibits a decrease in displacement from 9 meters to less than 1 meter over a distance of about 55 km. Application of existing methods for estimating recurrence time is difficult due to the gradational nature of the displacement. A best estimate, using the median value for slip on this segment, is 159 years and the corresponding probability over the next 10 years is at the 11% level. The Carrizo segment has surface displacements that range from 6 to 10 meters in 1857, and at 3.4 cm/yr, indicate recurrence times of 296 years or probabilities of 1% for the next 10 years. Hence, the possibility for a great earthquake in central California involving the Carrizo segment of the San Andreas fault appears to be negligible over the next 10 years. The Mojave segment contains the southern terminus of the 1857 rupture, and has surface displacements of about 3 to 5 meters. Pallet Creek, in the Mojave segment, has been extensively studied (Sieh et al., 1989), and offset sediments dated by ^{14}C indicate recurrence intervals that range from 44 to 332 years. The lack of well defined periodicity in the Pallett Creek data is puzzling at present and may indicate overlap of adjacent rupture zones in this region (i.e. Carrizzo and Coachella-San Bernardino). Based on interpretation of data at face value, the average recurrence time is 131 years, and probability over the next 10 years is at the 7% level. If we use the direct method to estimate a *repeat time*, with an average slip of 4.5 meters, and rate of fault motion of 3.0 cm/yr, the estimated recurrence time is 162 years, and the probability is at the 11% level for the next 10 years.

SA 9,10. *Southern San Andreas*, 34.3°-33.0° N. The southern San Andreas is comprised of two primary segments, San Bernardino and Coachella Valley. Palesoseismic investigations of the Coachella Valley segment indicate a sequence of 4 events during the period 1000 to 1700 A.D.. The average *repeat time* is 220 years, and the last event occurred in A.D. 1680 ± 20. Given these observations, the probability for a future event is at the 14% level for the next 10 years, and it is felt that this segment will be the site of the next great California earthquake. In contrast, much less is known about the San Bernardino segement. Dendrochronological studies indicate that the last event may have occurred in

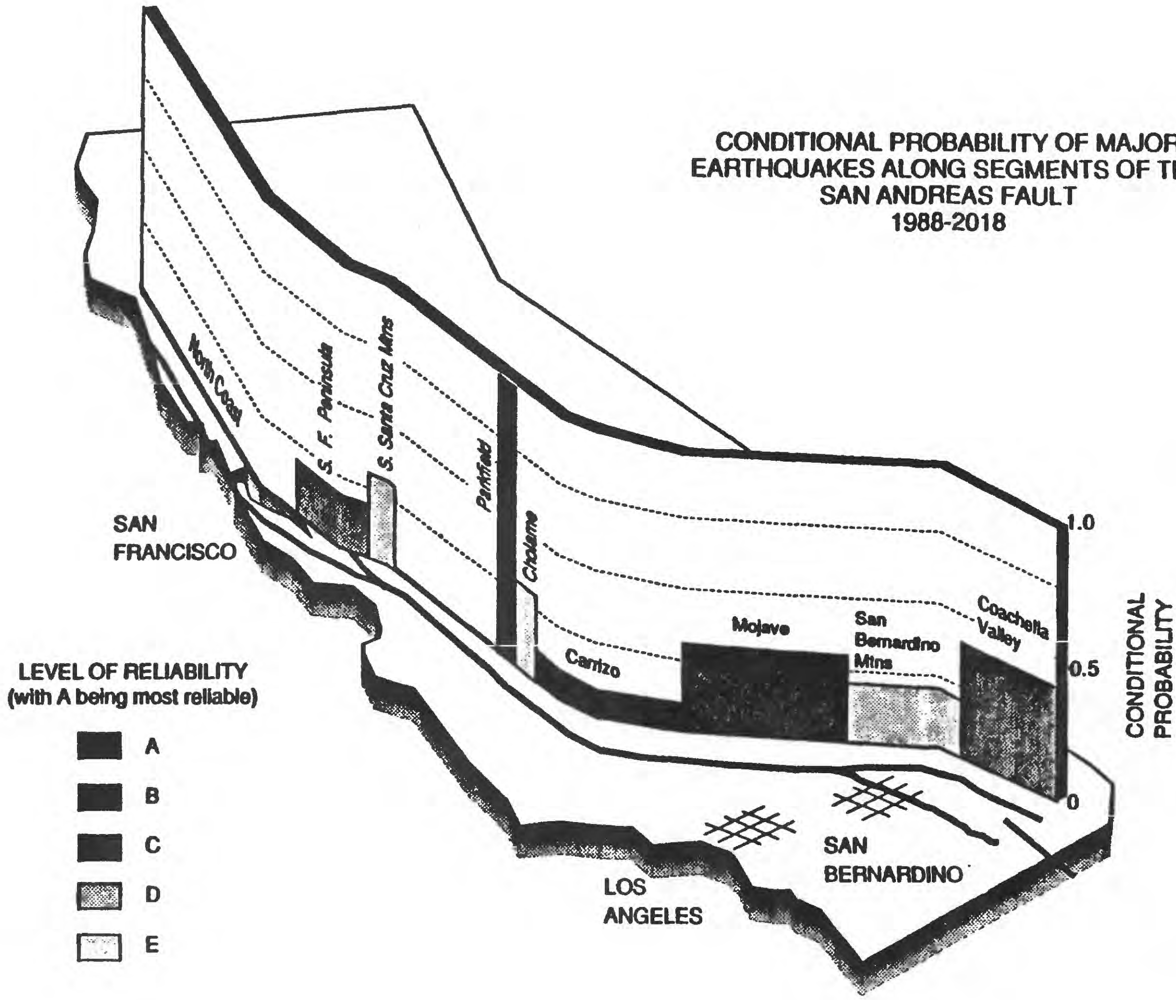

Figure 20. Conditional probability for the occurrence of major earthquakes along the San Andreas fault, in the 30 year interval 1988-2018 (from Working Group on California Earthquake Probabilities, 1988).

1812 (Jacoby et al., 1988), however, the magnitude and extent of rupture at this writing are not well known. In addition, it is not well understood how the San Berardino segment interacts with the adjacent Mojave or Coachella Valley segments. Tentative estimates of the seismic potential for San Bernardino are at the 8% level for the next 10 years.

Washington-Oregon

In recent years, scientific attention has focused on the possibility of great earthquakes occurring along the Washington-Oregon coast of the United States, in association with the subduction of the Juan de Fuca plate (see Heaton and Kanamori, 1984; Heaton and Hartzell, 1986). Most of the arguments for, and appraisals of, the seismic potential of the Cascade subduction zone have been made on the basis of tectonic analog with other convergent margins that are presently subducting young oceanic lithosphere, and have produced great earthquakes (see for example, discussions for Jalisco, Mexico, and Ecuador-Colombia). At present, the only firm evidence for recurring, large scale tectonic events is based on observations of subsided coastal marsh deposits by Atwater (1987) and Atwater et al. (1987, 1989). While these data indicate widespread subsidence or submergence events, it is not clear at this writing that these are unequivocally related to the occurrence of great earthquakes. Preliminary ^{14}C dating of buried wetland soils indicate an average return period of 500 to 600 years. These intervals, however, are not strictly periodic and individual inter-event times range from 100 to 1000 years. The last event has been dated at A.D. 1618-84 by dendrochronological methods (Yamaguchi, 1989) and suggests that we are still in the middle of the recurrence cycle. Based on these ^{14}C dates and the apparent aperiodic nature of the inter-event times, a Poisson model for recurrence indicates a probability of 2% for the next 10 years and is approximately equal to the time-dependent estimate. Consequently, the hazard over the next 10 years appears to be small. One caveat, however, is that if these submergence events are related to earthquakes, they only describe the effects of great (i.e. M_W 8.0+) events, and say little or nothing about the the occurrence of large (i.e. M_S 7.-7.7) interplate or intraplate events in this region (Spence, 1989).

(p. 66 follows)

Figure 21. Seismic potential of the Queen Charlotte-Alaska-Aleutian seismic zone: 1989-1999. Colors portray the level of conditional probability for occurrence of large and great (M_S 7.0 and larger) earthquakes during the next 10 years, 1989-1999, and range from dark blue, 0-20%; green, 20-40%; yellow, 40-60%; and red, 60-100%. Light blue regions are those areas with no historic record of great earthquakes. Specific dates and magnitudes refer to areas with incomplete historic records. See Figure 6 for additional symbols and information.

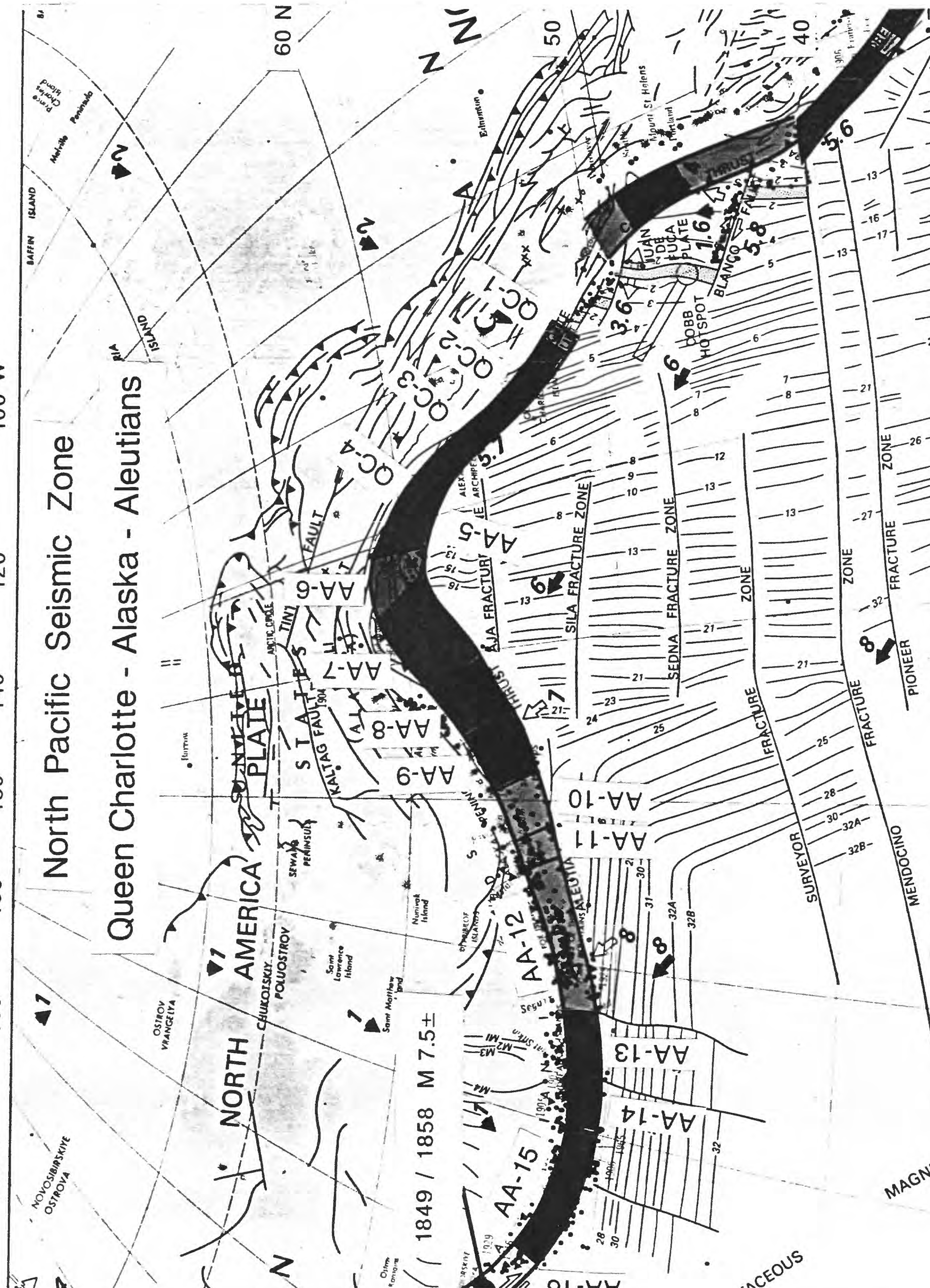
North Pacific Seismic Zone
Queen Charlotte - Alaska - Aleutians
(1849 / 1858 M 7.5±)
140 E
160
180
160
140
120
100 W
60 N
50
40
NORTH AMERICA
PLATE
JUAN DE FUCA PLATE
COBB HOTSPOT
BLANCO
THRUST
KALTAG FAULT
SEWARD PENINSULA
CHUKOTSKIY POLUOSTROV
OSTROV VRANGELYA
NOVOSIBIRSKIYE OSTROVA
Saint Lawrence Island
Nunivak Island
Saint Matthew Island
Mount St Helens
Portland
Edmonton
SILA FRACTURE ZONE
SEDNA FRACTURE ZONE
SURVEYOR FRACTURE ZONE
PIONEER FRACTURE ZONE
MENDOCINO FRACTURE ZONE
ALEUTIAN
QC-1
QC-2
QC-3
QC-4
AA-5
AA-6
AA-7
AA-8
AA-9
AA-10
AA-11
AA-12
AA-13
AA-14
AA-15
AA-16

(p. 69 follows)

NORTH PACIFIC

Queen Charlotte-Alaska-Aleutians

The Queen Charlotte-Alaskan-Aleutian (QC-A-A) seismic zone extends north from the Juan de Fuca spreading center offshore British Columbia through southern Alaska and west to the Aleutian and Kommandorski Islands in the northwest Pacific. Throughout the more than 5000 km long zone of interaction between the Pacific and North American plate, 5 distinct tectonic regimes are recognized to comprise the QC-A-A seismic zone. These include 1) a predominately strike-slip regime along the Queen Charlotte-Fairweather fault zone, 2) a zone of transition between strike-slip and underthrust motion in southeast Alaska, 3) a continental-type subduction regime in southern Alaska grading into 4) island arc type subduction in the Aleutian Islands and 5) a regime of oblique subduction-transform motion in the Kommandorski Islands. The rates of relative plate motion vary from about 5.5 cm/yr along the Queen Charlotte Islands to about 9 cm/yr near the Kommandorski Islands. The following discussion is based on work by Nishenko and Jacob (1989), and Figure 21 summarizes the seismic forecast for this region for the time interval 1989-1999. Place names along the Queen Charlotte-Alaska- Aleutian seismic zone and the locations of recent earthquake rupture zones are shown in Figure 22.

QCAA-1. *Cape St. James*, 51.7°-52.4° N. Relocation of earthquakes ($M \geq 7$ since 1900, $M \geq 6$ since 1917) on or near the Queen Charlotte fault by Rogers (1986) indicates the existence of a 75 km long segment (south of the 1949 M_W 8.1 Queen Charlotte Island shock, QCAA-2) which has no history of large earthquakes since 1898. Comparison with other areas along strike of the Queen Charlotte fault indicate that this area may be capable of independently producing large earthquakes. The estimated size of a future event that would fill this gap is approximately M_S 7.5-7.6. The strain accumulation since 1900 is estimated to be about 4.8 meters and is equivalent to a M_S 7.6 earthquake. Unfortunately, information about recurrence intervals are lacking for this segment. Using the interval 1900-1987 as a minimum estimate, the probability for the next 10 years is estimated to be at the 22% level. While poorly constrained, this segment stands out as presently having the highest probability along the Queen Charlotte-Fairweather fault zone, and deserves further study.

QCAA-2. *Queen Charlotte Islands*, 52.4°-56° N. The 22 August 1949 (M_W 8.1) Queen Charlotte Islands earthquake is estimated to have had a rupture length of approximately 490 km. Based on seismological studies, the majority of seismic moment release (and hence, coseismic displacement) appears to have been released in a zone extending 265 km north of the epicenter. This suggests that smaller amounts of displacement may have occurred in the adjacent northern and southern segments (55.5°-56° N and 52.5°-53.5° N, respectively).

An estimate of the average coseismic displacement in 1949 ranges from 4 to 7.5 meters depending on the length of faulting chosen. Dividing these estimates by the rate of fault motion indicates a recurrence time of 70 to 130 years. The historic and geologic record of

Figure 22. (*Top*) Bathymetry, major tectonic features, and place names along the Queen Charlotte-Alaska-Aleutian seismic zone. F.F. and Q.C.F. are the Fairweather and Queen Charlotte fault zones, respectively. Contour interval for marine bathymetry is 1000 fm (after Naval Oceanographic Office, 1978). (*Bottom*) Rupture zones of large and great earthquakes: 1917-1986 (from Nishenko and Jacob, 1989). M_S and M_W values refer to the 20 sec surface wave and ultra-long period magnitude scales. Directions of relative plate motion between the Pacific and North American plates indicated by arrows. Rates of relative plate motion (in cm/yr) after Minster and Jordan (1978).

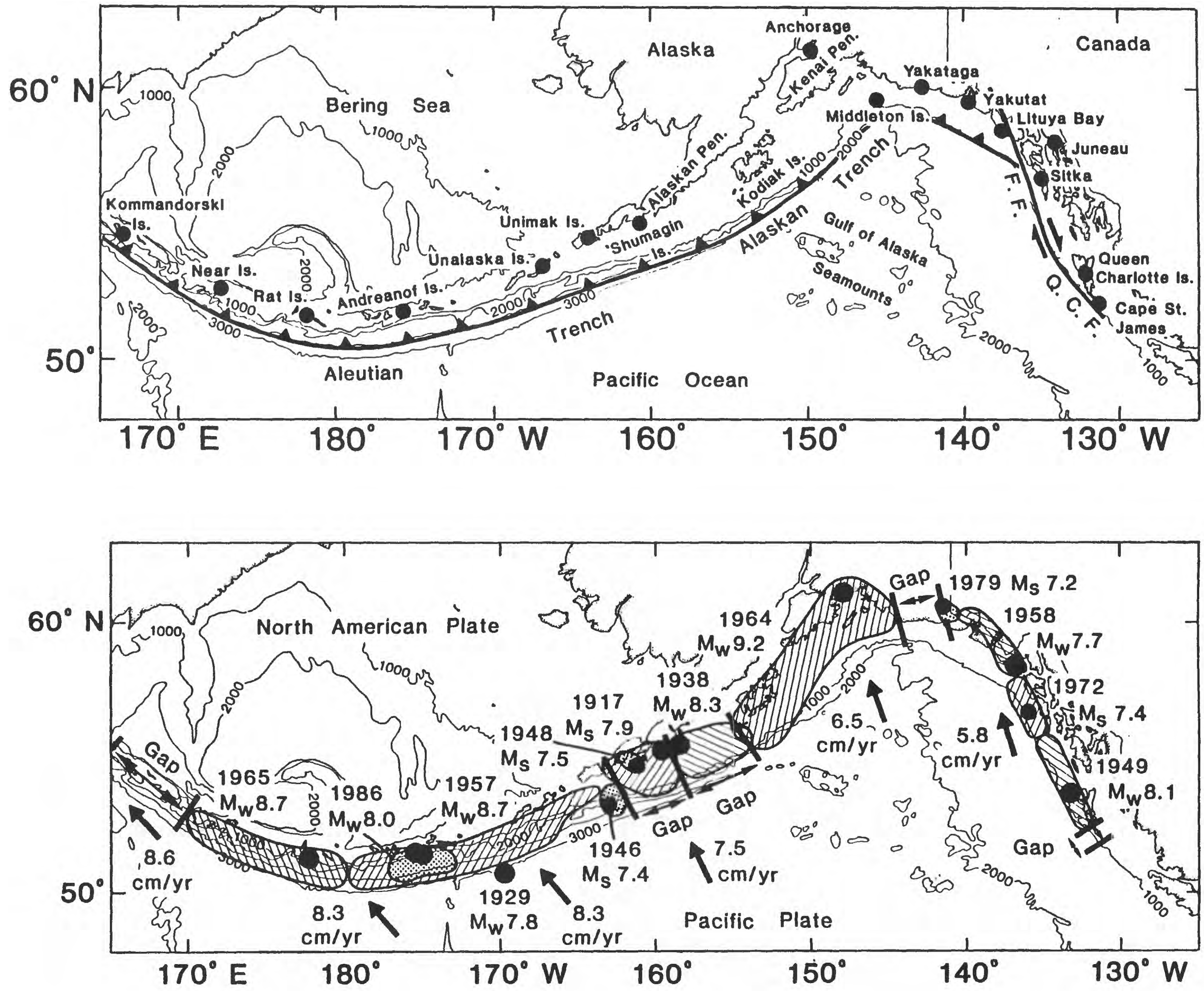
Alaska
Canada
Anchorage
Kenai Pen.
Yakataga
Yakutat
Middleton Is.
Lituya Bay
Juneau
Sitka
F. F.
Queen Charlotte Is.
Cape St. James
Q. C. F.
Bering Sea
Alaskan Pen.
Kodiak Is.
Trench
Kommandorski Is.
Unimak Is.
Shumagin Is.
Alaskan
Gulf of Alaska
Seamounts
Near Is.
Rat Is.
Unalaska Is.
Andreanof Is.
Trench
Aleutian
Pacific Ocean
60° N
50°
170° E
180°
170° W
160°
150°
140°
130° W
North American Plate
1979 Ms 7.2
1958
Mw 7.7
1964
Mw 9.2
1938
Mw 8.3
1917
Ms 7.9
1948
Ms 7.5
1972
Ms 7.4
1949
Mw 8.1
1965
Mw 8.7
1986
Mw 8.0
1957
Mw 8.7
1946
Ms 7.4
1929
Mw 7.8
Gap
6.5 cm/yr
5.8 cm/yr
7.5 cm/yr
8.6 cm/yr
8.3 cm/yr
Pacific Plate

prior great earthquakes along this segment of the plate boundary is poorly known. Hence, independent estimates of recurrence time are not available at present. Using the average of the estimates, 108 years, and considering the recency of faulting, the probabilities for a M_W 8.0 event over the next 10 years are at the 4% level.

Note that this discussion deals with great M_W 8.0 events. The observation that significant variations in displacement may exist along strike may also define smaller fault segments that may rupture independently in large earthquakes (i.e. M_S 7-7.5) and have recurrence times shorter than 100 years. At present there are no data with which to constrain a recurrence time for these smaller segments.

QCAA-3. *Sitka*, 56°-58° N. Previous earthquakes that are either known or suggested to have occurred along this segment of the plate boundary include: 26 November 1880; 24 October 1927 (M_S 7.1); and 30 July 1972 (M_S 7.6). If all three events ruptured the same segment of plate boundary, the observed average *repeat time* is 46 ± 7 years. However there is a large variation in the magnitude of the last two earthquakes (7.1 and 7.6). Given the recency of faulting, both *repeat times* indicate negligible probabilities (2%) over the next 10 years.

QCAA-4. *Lituya Bay*, 58°-60.5° N. The Fairweather fault is the only historically active transform fault in this region that is exposed on land, and hence accessible for direct measurement of rate of fault motion and coseismic displacement. Observations following the 10 July 1958 (M_S 7.9) earthquake indicate a maximum coseismic displacement of 6.5 meters at Crillion Lake and smaller offsets (2.5 to 3.5 meters) elsewhere. Dividing the maximum offset by the rate of fault motion gives a recurrence time estimate of 125 years. The long term geologic rate of fault motion gives estimates of about 110 years for 6.5 meter events or 60 years for 3.5 meter events. For comparison, dividing the average coseismic displacement (4.5 meters) by the rate of fault motion gives an estimate of 85 years. Given the range of recurrence time estimates for this segment of the QC-A-A seismic zone, 85 to 125 years, the probability for the repeat of a M_W 8.2 earthquake is negligible (4%) over the next 10 years.

QCAA-5,6. *Yakutat and Yakataga*, 139°-145° W. Both the Yakutat and Yakataga segments define a complex transitional zone between predominately strike-slip motion along the Fairweather fault system and underthrusting along the Alaskan trench. Between these two simple fault systems, thrust faulting along the east-west trending Chugach-St. Elias fault zone, and evidence of active faulting offshore within the exotic Yakataga block (i.e the Pamplona zone) indicate the existence of a complex and diffuse plate boundary in this region. In other words, plate motion does not appear to be concentrated along a single throughgoing structure, and hazards estimates made for this segment may be less reliable.

Prior great earthquakes in this region occurred on 4 and 10 September 1899 (M_W 8.2 and 8.1, respectively). Estimation of recurrence intervals for these two events however is highly dependent on the interpretation of the type of faulting involved. Estimates for the 10

September event range from 80 years for an interplate event to 380 years for an intraplate event. While there is doubt as to the type of faulting involved in the 10 September event, there is little doubt that the 4 September event was an interplate event that involved faulting along the Chugach-St. Elias fault zone. For this event the estimated coseismic displacement ranges from 2.5 to 5 meters (McCann et al., 1980), and the average *repeat time* is about 90 years. While poorly constrained, the conditional probability for this gap is at the 21% level for the next 10 years.

QCAA-7. *Prince William Sound-Gulf of Alaska*, 145°-156° W. The 24 March 1964 Prince William Sound earthquake (M_W 9.2) is the largest earthquake to have occurred along the QC-A-A seismic zone in historic time. Estimates of the average coseismic displacement, based on seismologic and geodetic information range from 14 to 30 meters, and the estimated recurrence time ranges from 230 to 460 years. Hence the probability of another great earthquake in this zone is negligible ($\leq$ 1%) for the immediate future.

The recurrence estimates for M_W 9.0 earthquakes indicate little about the possibility of smaller great earthquakes (i.e. M_W 8.0) occurring in this area. Relocations of great events on 14 July 1899 and 9 October 1900 in this segment indicates that the region also has the potential for other destructive earthquakes in addition to the largest ones. Unfortunately, the hazard associated with these events is not well understood, and the probability for these events to occur cannot be dismissed by virtue of the fact that the probability for M_W 9.0 events may be low in the future.

QCAA-8. *Kodiak Island*, 150°-155° W. The area in and around Kodiak Island is distinguished by having one of the longest, and presumably most complete earthquake histories along the entire QC-A-A seismic zone. Reports of large earthquakes felt on Kodiak Island during the last 200 years suggest a recurrence interval of about 60 years between periods of increased activity that may last as long as 10 years. The identification of specific fault segments is difficult, however, given the sparse distribution of felt reports. For this reason, we feel it appropriate to use a Poisson-based description of probability for the Kodiak Island region. In other words, we have sampled the strain release in a volume surrounding Kodiak Island, not just the behavior of a single fault or plate boundary segment. Using a Poisson model and the observed 58 year recurrence interval the probability for the next 10 years is at the 16% level. Since this is a Poisson based probability estimate, it is static and will not change as a function of time.

QCAA-9. *Alaskan Peninsula*, 156°-158.5° W. Previous large and great earthquakes that are known to have ruptured this segment include 22 July and 7 August, 1788; 16 April 1847; 20 September 1880; and 10 November 1938 (M_W 8.2). These events indicate recurrence times between 49 and 75 years for this segment of the QC-A-A seismic zone. Additionally, the historic record indicates that during the last 200 years, the mode of rupture in this region has changed from a series of great shocks in 1788 and 1847 (with estimated rupture lengths of 400 to 600 km) to a sequence of relatively smaller events in 1880, 1917 (see next section) and 1938 which independently ruptured the Shumagin and

Alaskan Peninsula segments. Hence, while we are able to estimate recurrence times for this region, we cannot quantitatively assess the likelihood that these two segments will break independently or simultaneously. Based on the average recurrence time of 75 ± 11 years, the conditional probability for the next 10 years is at the 18% level.

QCAA-10. *Shumagin Islands*, 158.5°-161.7° W. Previous great earthquakes located in the Shumagin Island region include 22 July and 7 August 1788; 16 April 1847; and 31 May 1917 (M_S 7.9). As in the case of the Alaskan Peninsula gap, there is an indication that the region exhibits a variable mode of rupture. Based on the 1788, 1847 and 1917 events, the average *repeat time* is 65 ± 10 years, and the probability for recurrence over the next 10 years is at the 48% level.

QCAA-11. *Unimak Island*, 161.7°-164° W. This segment is defined on the basis of the 1 April 1946 (M_S 7.4, M_t 9.3) earthquake which produced one of the largest tsunamis recorded during this century. The size of the tsunami, however, is not in agreement with the seismologically observed size of the earthquake, and it has been suggested that the tsunami was triggered by submarine landsliding at the time of the earthquake. Based on the size of the earthquake, M_S 7.4, we estimate a recurrence time of about 25 years. Locations of prior earthquakes in this region are poorly known. One event in 1905 is located on the eastern edge of the 1946 aftershock zone, and may indicate a longer 41 year recurrence interval. Due to the amount of time elapsed, both the 25 and 41 year estimates indicate probabilities for the occurrence of a large (i.e. M_S 7-7.5) events at the 43-55% level over the next 10 years. The unusual circumstances surrounding the tsunami, however, indicate that the next Unimak Island earthquake does not necessarily have a high potential for producing a great tsunami.

QCAA-12-14. *Central Aleutians*, 165°-180° W. The Aleutian Islands portion of the QC-A-A seismic zone provides an excellent example in documenting variations in the mode of subduction. At the turn of the 20th century, a series of large earthquakes ruptured this region within a interval of 10 years. Following this episode of subduction, the great (M_W 8.7) 9 March 1957 Andreanof Islands earthquake and its aftershocks ruptured this entire plate boundary within a few days. The occurrence of another great earthquake on 7 May 1986 (M_W 8.0) appears to represent the return to a more segmented mode of earthquake recurrence in this region. Based on the analysis of the 1957 shock and the occurrence of the 1986 event, it is possible to divide the Aleutian Islands portion of the QC-A-A seismic zone into three segments: Fox Islands (165°-173° W); Andreanof Islands (173°-177° W); and the Delarof Islands segments (177°-180° W). The locations of these segments appear to controlled by the presence of fracture zones on the subducted Pacific plate (Amlia FZ 173° W, Adak FZ 177° W) as well as major structural discontinuities within the Aleutian Ridge and forearc regions: Adak canyon, Bowers ridge, Hawley ridge.

QCAA-12. *Fox Islands*, 164°-173° W. This segment includes the Unalaska gap of House et al. (1981). Following the 1957 mainshock, the Fox Island segment exhibited a gradual expansion of the aftershock area, over a period of three days, in contrast to the more rapid 24 hour expansion in the Andreanof and Delarof segments. All evidence suggests that the rupture characteristics changed dramatically in the region east of the Amlia fracture zone (173° W). In conjunction with the arrested rupture propagation of the 1957 event, it is noteworthy that a great normal faulting earthquake occurred seaward of this segment on 7 March 1929 (M_W 7.8). The occurrence of such an event is suggested by Kanamori (1972) as evidence of partial decoupling of the plate interface in this area. A number of large earthquakes have been located in this segment during the 20th century, suggesting that the normal mode of strain release in this segment may characteristically occur as large, rather than great, earthquakes every 20 to 50 years. Based on the historical seismicity and estimates of displacement in this region in 1957 (approx 240 cm, or a 30 year recurrence time) we estimate the probability for large (i.e. M_S 7-7.5) events in this segment to be at the 44% level for the next 10 years.

QCAA-13. *Andreanof Islands*, 173°-177° W. This segment contains both the epicenter of the 1957 event and the rupture zone of the 1986 earthquake. Both earthquakes nucleated in approximately the same area, just east of Hawley Ridge, suggesting that this forearc feature may play a significant role in the earthquake process there. Based on the short instrumental record for this region, the only great earthquakes known to have occurred are 1957 and 1986. A great event in 1906 is located near 180°, and may have ruptured either to the east or to the west. Hence the two return periods for this segment of the QC-A-A seismic zone are 29 and $\geq$ 51 years. Given these two intervals, the average return time is at least 40 years, and the conditional probability for the recurrence of a great earthquake is at the $\leq$ 1% level.

QCAA-14. *Delarof Islands*, 177°-180° W. As in the case of the Fox and Andreanof Islands segments, the seismological record for this century indicates a history of large earthquakes, with an apparent return period of 20 to 30 years, punctuated by the 1957 event. This segment has been a gap for large earthquakes since 1957, and the conditional probability for the recurrence of a large earthquake in this region is at the 85% level.

QCAA-15. *Rat Islands*, 180°-171° E. Previous large and great earthquakes are only known from the instrumental record and include 29 June 1898, 17 August 1906, 2 September 1907, 17 December 1929 and 4 February 1965. While the exact locations of these earlier events are not well constrained, these events suggest recurrence times of 21 to 59 years.

Within this segment, the QC-A-A seismic zone is composed of 4 distinct tectonic crustal blocks: Rat, Buldir, Near and Stalemate (Spence, 1977). The boundaries of these blocks are well defined by submarine canyons that are of tectonic rather than erosional origin. The sequence of large events at the turn of the century indicate that these individual blocks ruptured separately, but within a few years of one another. In 1965 all 4 blocks ruptured simultaneously. Hence, within the last 90 years there have been two modes of strain release in this segment.

Recurrence estimates based on the size of the 1965 event range from 58 to 83 years and indicate a low probability (4%) over the next 10 years.

QCAA-16. *Kommandorski Islands,* 171°-165° E. The motion of the Pacific plate is parallel to the Aleutian Arc along the Kommandorski Islands segment of the QC-A-A seismic zone, and terminates in underthrusting at the Kurile Trench along the east coast of Kamchatka. Within the Kommandorski segment, motion is accommodated by a broad zone of strike-slip deformation which includes vertical strike-slip motion along the Bering Sea flank, and horizontal strike-slip motion along the southern or Pacific flank of the Aleutian Ridge.

Few large shocks have been located in this segment during this century. As discussed by McCann et al. (1979) there is evidence for large or great shocks along the southern flank in 1849 and 1858. Uncertain size and poorly known rupture dimensions for these shocks makes estimation of *repeat times* difficult at this time.

(p. 78 follows)

Figure 23. Seismic potential of the Western Pacific, including Kamchatka, the Kuriles, Japan, Izu-Bonin, and the Mariana arcs: 1989-1999. Colors portray the level of conditional probability for occurrence of great (M_S 7.7 and larger) earthquakes during the next 10 years, 1989-1999, and range from dark blue, 0-20%; green, 20-40%; yellow, 40-60%; and red, 60-100%. Light blue regions are those areas with no historic record of great earthquakes. Specific dates and magnitudes refer to areas with incomplete historic records. See Figure 6 for additional symbols and information.

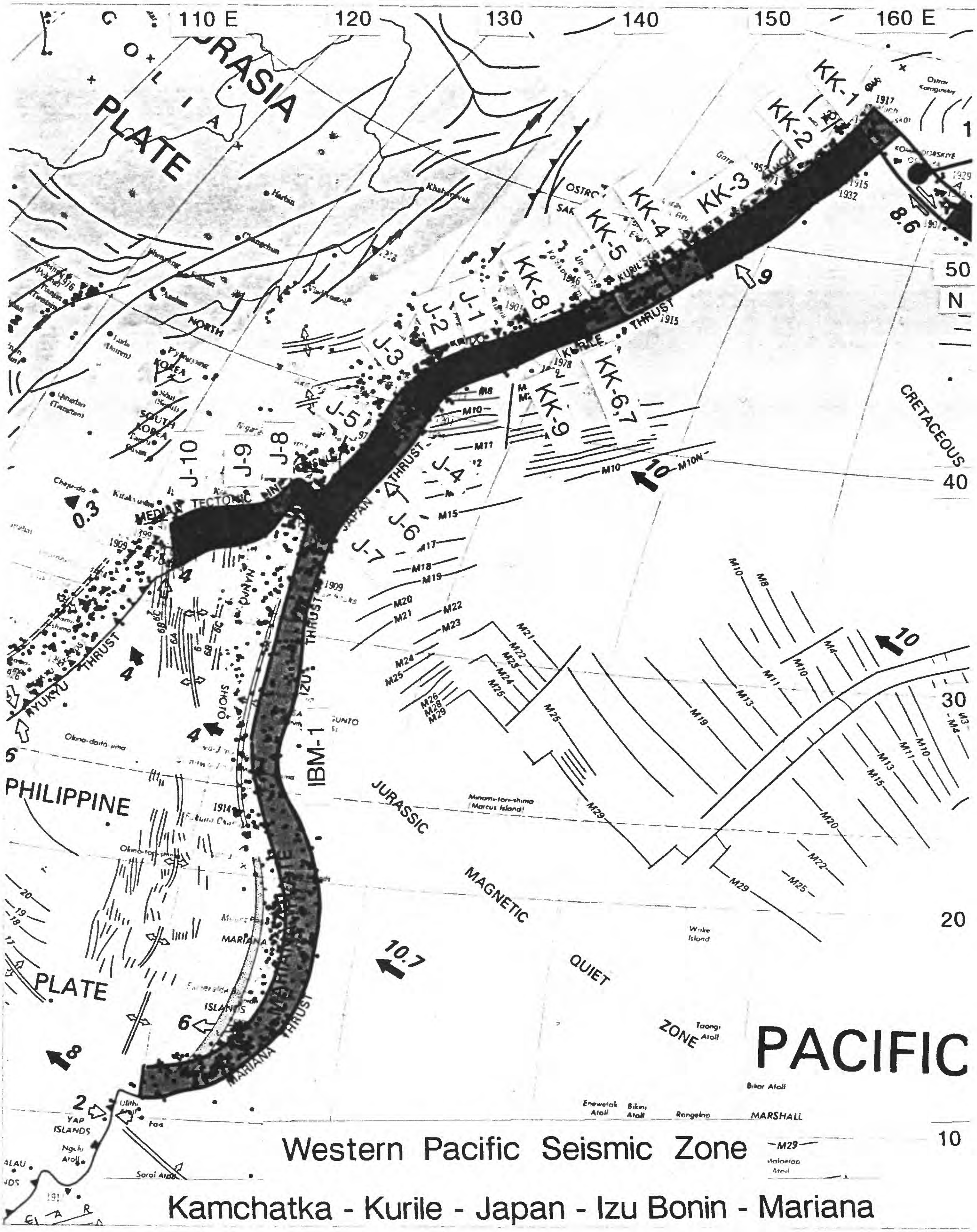
Western Pacific Seismic Zone
Kamchatka - Kurile - Japan - Izu Bonin - Mariana
EURASIA PLATE
PHILIPPINE PLATE
PACIFIC
JURASSIC MAGNETIC QUIET ZONE
CRETACEOUS
110 E
120
130
140
150
160 E
50 N
40
30
20
10

WESTERN PACIFIC

The western Pacific seismic zone extends south from Kamchatka through the Kurile, Japan, Izu-Bonin and Mariana trenches, and represents the zone of convergence between the Pacific and the Asian and Philippine Sea plates. Along this zone, the rates of northwesterly plate convergence vary from 8.5 cm/yr to 11 cm/yr, from north to south. Variations in the rate and size of shallow thrust earthquakes that occur along the western Pacific seismic zone reflect changes in the plate interface geometry and other geophysical parameters that influence the tectonic regime and earthquake potential of a particular segment of plate boundary. Seismic hazards estimates for the western Pacific seismic zone are shown in Figure 23.

Kamchatka and the Kurile Islands

In contrast to the lengthy Japanese earthquake history discussed in the next section, much less is known about the earthquake history of the Kurile and Kamchatka seismic zones. Along the Kurile Islands there are few sites for observation and the generally low population densities have resulted in a sparse earthquake record prior to the advent of instrumental recording. Hence, the majority of recurrence estimates for this portion of the circum-Pacific are based on only one or two observed ***repeat times***, and have large uncertainties. In the southern Kurile Islands, the identification of segmentation and recurrence histories are further complicated by overlapping rupture zones and interacting asperities. The following discussion summarizes work by Fedotov (1965), Fukao and Furumoto (1979), Kondorskaya and Shebalin (1982), Fedotov et al. (1982), Schwartz and Ruff (1985, 1987), Beck and Ruff (1987), and Schwartz et al. (1989). Figure 24 shows recent earthquake rupture zones along the Kurile-Kamchataka seismic zone.

KK-1. *Kamchatsky Peninsula*, 55°-57° N. Two large events have occurred in this segment during this century, 13 November 1936 (M_S 7.1) and 15 December 1971 (M_S 7.5). The latter event is distinguished on the basis of its having been anticipated by Fedotov (1965) using the basic concepts of seismic gaps. Based on this apparent 35 year recurrence, the probability within the next 10 years for another large event is at the 23% level.

KK-2. *Northeastern Kamchatka*, 53°-55° N. Previous great earthquakes that have affected the Pacific coast of northeast Kamchatka occurred on 22 August 1792 (M 8.4) and 3 February 1923 (M_W 8.3, M_t 8.8). Based on this single 131 year ***repeat time***, the probability for another great event in this northeastern zone is at the 3% level for the next 10 years.

KK-3. *Southeastern Kamchatka and Paramushir Is.*, 49°-53° N. Prior great earthquakes that are located in this segment include 17 October 1737 (M 8.3), 6 May 1841 (M_t 9.0), 25-27 June 1904 (M_S 7.2-7.4), and 4 November 1952 (M_W 9.0). Descriptions of the 1737 event (Kondorskaya and Shebalin, 1982) indicate that this was a great earthquake

Figure 24. Major tectonic features, active volcanoes (solid triangles), and recent earthquake rupture zones (cross hatched areas) along the Kamchatka-Kurile-Japan-Izu Bonin-Mariana trench system (after Kelleher and McCann, 1976). Note the relatively smooth ocean floor, large earthquake rupture zones, and the nearly continious line of active volcanoes to the north (Kamchatka-Kurile-Japan). Contrast this with the absence of great earthquakes, the irregular distribution of active volcanoes, and the rougher ocean floor bathymetry to the south along the Bonin and Marianas trenches. Bathymetry from Chase et al. (1970).

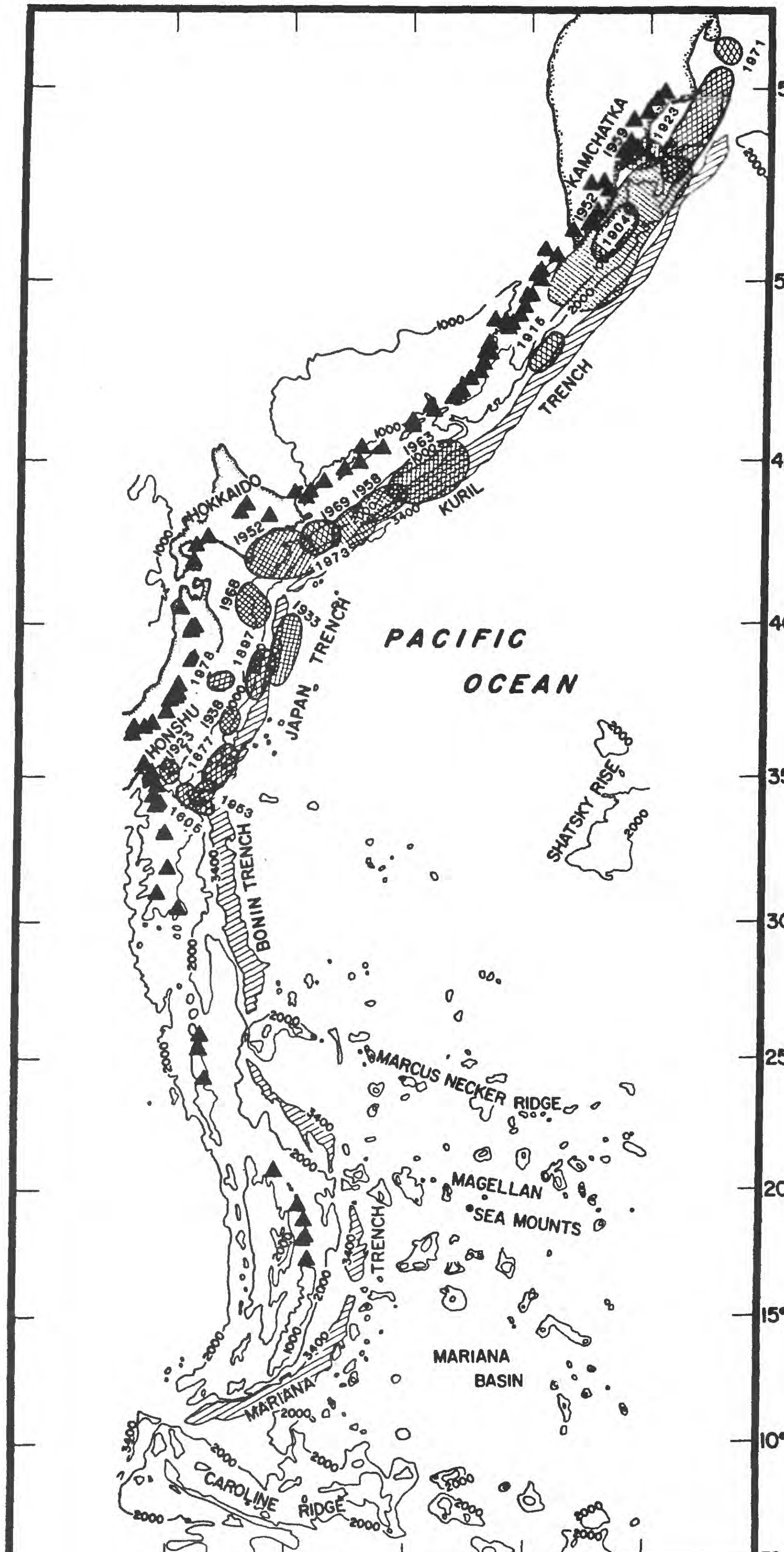
KAMCHATKA
KURIL
TRENCH
HOKKAIDO
HONSHU
JAPAN TRENCH
PACIFIC
OCEAN
SHATSKY RISE
BONIN TRENCH
MARCUS NECKER RIDGE
MAGELLAN
SEA MOUNTS
TRENCH
MARIANA
BASIN
MARIANA
CAROLINE
RIDGE
1971
1923
1959
1952
1904
1918
1963
1958
1969
1952
1973
1968
1933
1897
1978
1938
1923
1677
1953
1605
55°
50°
45°
40°
35°
30°
25°
20°
15°
10°
5°
140°
145°
150°
155°
160°

with a rupture zone comparable to that of the 1952 event. Descriptions of the 1841 earthquake however, do not provide as clear a comparison. The primary information about the size of the 1841 event comes from a comparison of tsunami waves recorded at Hilo, Hawaii (1841, 4.6 m and 1952, 3.7 m), and Abe (1979) has assigned a M_t of 9.0 to both events (see Figure 5). If the 1737, 1841 and 1952 events all ruptured similar portions of the seismic zone, the average *repeat time* would be 108 ± 16 years, and the probability for another great (i.e. M_W 9.0) event in this region is less than 1% for the next 10 years. If, in fact, only the 1737 and 1952 events are comparable, the recurrence time increases to 215 years. Both recurrence time estimates however, indicate negligible probabilities for the immediate future.

The 1904 events, as depicted by Fedotov (1965) and Fedotov et al. (1982) appear to have ruptured a central portion of the 1952 zone. These events point out the possibility of having large earthquakes occurring within the rupture zones of great earthquakes (see also the discussion for the 1964 Prince William Sound earthquake in the Alaska section). At present, we have no data to quantitatively evaluate the probability for these types of events to occur.

KK-4. *Shiashkotan Is.*, 48°-49° N. Only one event, 1 May 1915 (M_S 8.0), is listed for this segment of the Kurile Islands by Fedotov et al. (1982). Extrapolation of recurrence times for similar sized events along the Kurile arc suggests that intervals of 80 to 100 years may be appropriate, if the 1915 earthquake is an underthrust event. In this case, we tentatively estimate a probability at the 20% level for the next 10 years .

KK-5. *Central Kurile Islands*, 46°-48° N. No large or great shallow earthquakes are known for this segment of the Kurile Island arc during this century. This segment is also coincident with a pronounced discontinuity in the structure of the island arc, between the Bussol and Kruzenshtern Straits, where depths to the Vityaz Ridge increase by 2000+ meters. This unusual island arc structure suggests that the lack of great earthquake activity may be symptomatic of the tectonic regime. Interestingly, a compressional outer rise (COR) event occurred opposite this segment in 1963 (m_b 7.7), and may reflect the presence of compressive stresses in the plate interface zone. At present, lacking both an historic record and knowledge of when the last event occurred, we do not have enough information to quantitatively evaluate the large or great earthquake potential of this zone or assess the intermediate term significance of the COR events. Qualitatively, however, we note that this region should be considered one of high but unknown potential. If this gap ruptured at one time, the physical dimensions indicate that it could produce both a great earthquake and tsunami.

KK-6,7. *Shimushir and Urup Is.*, 149°-153° E. Prior great earthquakes along this section of the Kurile arc include 7 September 1918 (M_t 8.7) and 13 October 1963 (M_W 8.5). While an earlier event in 1780 is also associated with this segment, the completeness of the earthquake catalog during the 19th century is in question (see Sykes and Quittmeyer, 1981). In contrast to many of the other seismic zones around the circum-Pacific, this segment of the Kurile arc has exhibited a substantial degree of overlap between adjacent ruptures in 1918 and 1963. Analysis of the 1918 and 1963 events by Beck and Ruff (1987) show that the 1963 earthquake was a complex event that involved rupture of 3 separate asperities. The southwestern asperity, near the epicenter, appears to have been unbroken since 1780. The remaining 2 northeastern asperities appear to have been ruptured in 1918 and subsequently reruptured in 1963.

Given the uncertain status of the historic record in this area, recurrence times may range from 45 (1963-1918) to 183 (1963-1780) years. The 45 year recurrence estimate indicates probabilities at the 21% level for the next 10 years, and the probabilities based on the 183 year estimate are significantly smaller.

KK-8. *Etorofu Is.*, 148°-150° E. The only great earthquakes located in this segment occurred on 6 November 1958 (M_W 8.3) and 24 March 1978 (M_S 7.6). While separated by 20 years, both events ruptured different portions of the plate interface, and hence, constitute one complete episode of subduction for this segment of the Kurile arc. The great 1958 event was a high stress drop earthquake that exhibited low aftershock activity at shallow depths (i.e. $\leq$ 20 km, Fukao and Furumoto [1979]). The updip portion of this segment was subsequently ruptured 20 years later in 1978. No prior events are known for this segment, and the high stress drop of the 1958 event is suggested to reflect the long interval of strain buildup (Fukao and Furumoto, 1979). Estimates of recurrence time (and future behavior), based on earthquakes in adjacent segments indicate small probabilities (i.e. $\leq$1% for the next 10 years) but are tentative, at present.

KK-9. *Shikotan Is.*, 146.5°-148.5° E. Earthquakes that have occurred along this portion of the arc include are 4 June 1893 and 11 August 1969 (M_W 8.2). According to Scwhartz and Ruff (1987), the 1969 event can be classified as a simple earthquake that involved rupture of a single asperity on the plate interface. The estimated coseismic slip within this asperity region (7.2 meters) equals the strain buildup since the 1893 event (76 years x 9.3 cm/yr). Reconstruction of the tsunami source zones for the 1893 and 1969 events by Hatori (1979) indicates that the 1969 zone may be larger than the 1893 zone (200 vs 150 km, respectively). Hence, if the 1969 event, in addition to having a larger source zone, also had a larger amount of coseismic slip, then the recurrence time may be slightly longer than the 76 year interval indicated by the historic record. Both estimates, however, indicate small probabilities for recurrence in the immediate future (i.e. $\leq$ 1% for 1989-1999)

Eastern Japan- Eastern Honshu and Hokkaido

The earthquake history of the Japanese islands spans 1300+ years, and represents one of the longest historic records in the circum-Pacific region. The period of complete reporting, however, is confined to the period from the 17th century to the present. This interval includes a number of repeats for individual segments and hence, provides us with reasonably well constrained recurrence time and forecast estimates. The hazard estimates for the Japanese seismic zone are based primarily on data summarized in Wesnousky et al. (1984). The ten year forecast is shown in Figure 23 and the locations of recent rupture zones are shown in Figure 24.

Based on this long historic record, a large variation in *repeat times* from Hokkaido to southern Honshu has been noticed (Kanamori, 1977). While the rates of plate convergence vary by 10% from northern Hokkaido to southern Honshu, the observed recurrence times for great earthquakes vary by a factor of 10. This large temporal variation is suggested to reflect a decrease in the plate coupling from north to south and an increase in the amount of apparent aseismic slip.

J-1. *Nemuro-Oki*, 146.5°-147° E. Previous large events known to have occurred in this segment include 22 March 1894 and 17 June 1973 (M_W 7.8). The 1973 event was anticipated on the basis of the seismic gap hypothesis (Fedotov, 1965; Shimazaki, 1974). Based on this single 79 year repeat, we estimate the probability during the next 10 years to be at the $\leq$ 1% level.

J-2. *Tokachi-Oki*, 144.5°-146.5° E. Previous great earthquakes include 1843 (?) and 4 March 1952 (M_W 8.1). This single recurrence indicates a probability at the $\leq$ 1% level for the next 10 years.

J-3. *Tokachi-Oki*, 142°-144° E. This segment has a well known history of great earthquakes that include 13 April 1677 (M_S 8.1), 11 March 1763 (M_S 7.7), 23 August 1856 (M_S 7.7), and 16 May 1968 (M_W 8.2). This sequence of events indicates an average *repeat time* of 96 $\pm$ 12 years, and the probability for next great earthquake is at the $\leq$ 1% level for the next 10 years.

J-4. *Sanriku-Oki*, 37.7°-39° N. Previous events related to underthrusting along this portion of the Japan trench include 2 December 1611 (M_S 8.1), 17 February 1793 (M_S 7.1), and 5 August 1897 (M_S 7.6). The average *repeat time* is 143 $\pm$ 21 years, and probability for an event in the next 10 years, based on these data, is at the 7% level. Reconstruction of tsunami source zones for the 1897 and 1793 events indicate that both were of similar size and ruptured the same portion of the plate boundary (Hatori, 1976); however, the coseismic displacements in both events were not comparable, and the 1897 event appears to be smaller than the 1793 event. Application of the time-predictable model by Wesnousky et al. (1984) indicates a recurrence time of 93 years. Based on this shorter recurrence time estimate, the probability in the next 10 years would increase to the 21% level.

This section of the Honshu coast is also effected by great normal faulting earthquakes (e.g. the great 1933 Sanriku earthquake) that occur in the trench outer rise region and generate destructive tsunamis. These earthquakes appear to be rare events and are outside the scope of this study.

J-5. *Miyagi-Oki*, 37.5°-39° N, 142° E. The Miyagi-Oki region of Honshu has been site of a series of earthquakes over the last 350 years that exhibit remarkable regularity in recurrence time (see Wesnousky et al., 1984; and Nishenko and Buland, 1987) . The last event occurred in 1978 (M_S 7.4), and based on the observed 40 ± 3 year periodicity, the probability for an event during the next 10 years is at the ≤ 1% level.

J-6. *Shioya-Oki*, 36°-38.5° N. A series of five large and great (M_S 7.1-7.7) earthquakes ruptured this portion of the plate boundary in 1938. These appear to be the only events to have occurred in this region within the last 1000 years (Abe, 1977, Wesnousky et al., 1984). Based on this observation, the probability for future events in the next 10 years appears to be negligible (i.e. ≤ 1%).

J-7. *Boso Peninsula*, 35°-36° N. The last major earthquakes that ruptured the northern portion of the Sagami Trough and the Boso peninsula occurred on 31 December 1703 (M_S 8.2) and 1 September 1923 (M_W 7.9). The combined coseismic uplift of both events, which comprises the Genroku terrace in this area, matches the height of the highest Holocene terrace (Numa terrace) in the area. This equivalence has led to recurrence time estimates for 1703-1923 type events to be on the order of 800-1700 years. More direct estimates based on the size of the 1923 earthquake indicate recurrence times of 200 years (Scholz and Kato, 1978). Based on these recurrence time estimates, we calculate negligible (≤ 1%) probabilities for this segment of the Boso peninsula.

Infrequent large and great events are noted to occur farther southeast along the Boso peninsula and near the junction of the Japan and Izu-Bonin trenches. The 3 February 1605 (M_S 7.9) and 26 September 1953 (M_S 7.5) events occurred southeast of the 1703 rupture. Lacking further information, Wesnousky et al. (1984) used the interval between the 1953 and 1605 events as a recurrence time estimate. The 4 November 1677 (M_S 7.4) earthquake occurred along the Japan Trench, in an area with no known predecessors. Given the length of the Japanese record in this region, recurrence times on the order of 1000 years seem appropriate, and the resulting probabilities are low for the immediate future.

Southwestern Japan- Western Honshu

J 7-10. *Nankai Trough*, 133°-139° E. The Nankai Trough marks the zone of interaction between the Philippine Sea and Eurasian plates in southwestern Japan. While the historic record of great earthquakes exists since A.D. 684, it is incomplete prior to A.D. 1707. Ando (1975) and Ishibashi (1981) have divided the margin into a number of distinct segments or blocks which have ruptured either simultaneously or within a few days to years of one another. Previous great earthquakes (and the segments ruptured) include 28 October 1707 (M 8.4, ABCDE), 23 and 24 December 1854 (M 8.4, AB and CDE), 7 December 1944 (M_W 8.1, CD, segment J-9), and 20 December 1946 (M_W 8.1, AB, segment J-10). See Figure 25 for the locations of these recent ruptures.

At present, the segment east of the 1944 Tonankai event (E, segment J-8) has been unruptured since 1854. This is segment is called the Tokai gap, and is the present day focus of the Japanese earthquake prediction program (Ishibashi, 1981; Mogi, 1981). Prior to 1707, the rupture history of the Tokai gap is poorly known. During the the 1707 Hoeii

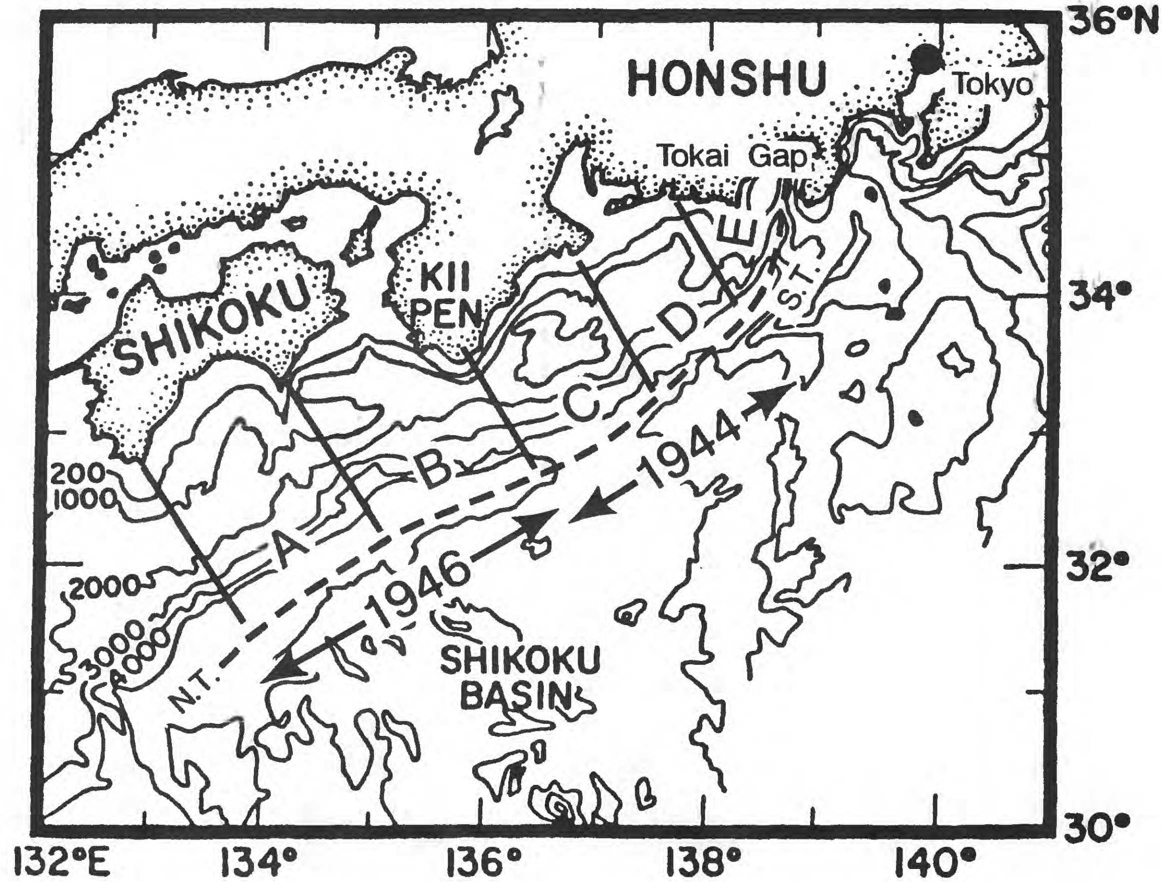

Figure 25. Geographic place names, major tectonic features, and great earthquake source zones along southwest Japan (modified from Nishenko and McCann, 1979). A, B, C, D, and E refer to the principal tectonic segments along the Nankai trough (after Ishibashi, 1981). Segments A, B, C, D, and E all ruptured within 32 hours of one other in 1854. During this century, segments A and B ruptured in 1946, C and D in 1944, and E (the Tokai gap) has not reruptured since 1854. The Tokai gap is currently the focus of the Japanese earthquake prediction program (see Mogi, 1981). N.T. is the Nankai trough and S.T. is the Suruga trough.

and 1854 Ansei earthquakes, the Tokai region appears to have ruptured in conjunction with blocks C and D. Hence, it is not known if block E can rupture independently. Based on the one available recurrence interval that involved this block, 1707-1854 or 147 years, the probability for an event in the Tokai gap is at the 16% level for the next ten years. For comparison, the shorter recurrence histories for Kii and Nankai segments (blocks AB and CD, respectively), suggest a probability at the 31% level. Probabilities for the Kii and Nankai regions (which last ruptured in 1944 and 1946, respectively) are at the $\leq$ 1% level for the next 10 years.

Izu-Bonin and Mariana arcs

IBM-1 *Izu Bonin and Mariana*, 34°-10° N. The Izu-Bonin and Mariana arcs form the eastern edge of the Philippine Sea plate and the zone of interaction with the Pacific plate. Neither Gutenberg and Richter (1954) nor Rothé (1969) report any shallow earthquakes of magnitude greater than 7.3 along these arcs between latitudes 10° and 35° S. The absence of great earthquakes, and the small number of reported large shocks, along this margin have been discussed by McCann et al. (1979) and Kanamori (1977).

Large shocks do occasionally occur along this boundary. The event on 22 September 1902 was originally listed as M=8.1 by Richter (1958) and has been revised to M_S 7.5 by Abe and Noguchi (1983). With the exception of this event, both the instrumental and short historic record of the Marianas and Izu-Bonin arcs give no indication of the frequent occurrence of large thrust events that are typical of other subduction zones with narrow plate interfaces. Based on these observations, we qualitatively assign this segment a low probability for the occurrence of great earthquakes during the next 10 years.

Figure 26. Seismic potential of the southwest Pacific, including New Britain, Solomon Islands, Vanuatu and Tonga-Kermadec: 1989-1999. Colors portray the level of conditional probability for occurrence of large and great (M_S 7.0 and larger) earthquakes during the next 10 years, 1989-1999, and range from dark blue, 0-20%; green, 20-40%; yellow, 40-60%; and red, 60-100%. Light blue regions are those areas with no historic record of great earthquakes. Specific dates and magnitudes refer to areas with incomplete historic records. See Figure 6 for additional symbols and information.

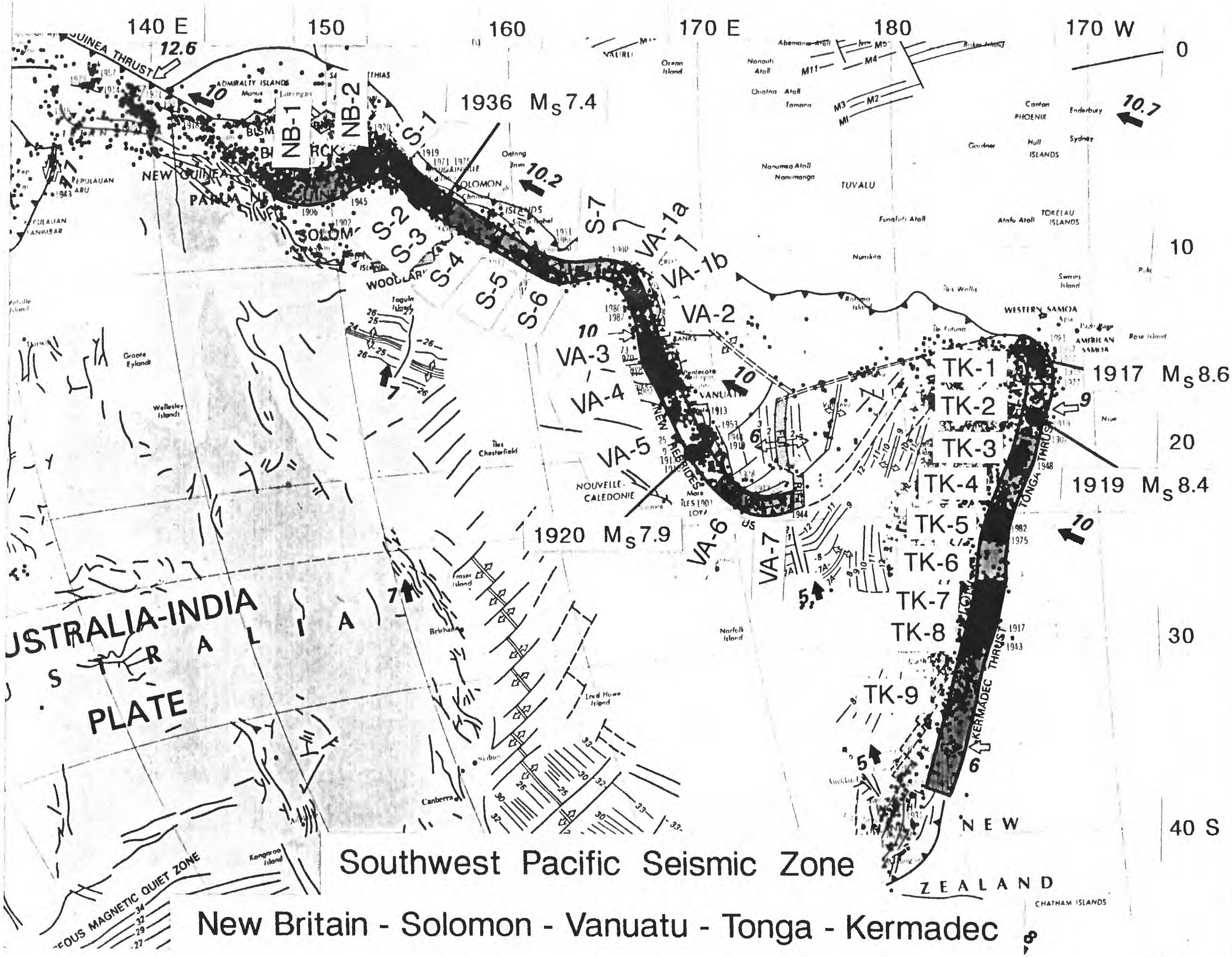

Southwest Pacific Seismic Zone

New Britain - Solomon - Vanuatu - Tonga - Kermadec

(p. 93 follows)

SOUTHWEST PACIFIC

The tectonics of the southwest Pacific region are in response to the convergent motions of the Pacific and Australian plates. Subduction of the Pacific plate along a westerly dipping seismic zone extends from the southern Kermadec arc to the northern end of the Tonga Islands. Transform and extensional tectonics characterize the region between the northern end of the Tonga arc and the southern portion of the New Hebrides subduction zone. The Australian plate is subducted at the New Hebrides seismic zone, which dips to the east. To the west, the Solomon arc subducts both Australian lithosphere and the smaller Solomon plate. Along the northern coast of New Guinea, the plate motion is generally east-west, though a well defined seismic zone is not present.

The rates of plate motion in this region range from a low of 5 to 6 cm/yr in the Kermadec region to near 10 cm/yr in the northern portion of the Tonga arc. Along the New Hebrides region, plate motion may be as high as 11 cm/yr, while plate motions near the New Guinea-Solomon region may be 10 cm/yr. The following discussion of the seismic potential of the southwest Pacific is based on McCann and Nishenko (1989), and is summarized in Figure 26 for the time interval 1989-1999.

New Guinea

The northern coast of New Guinea , east of 138° E, experienced few large earthquakes in the first part of the 20th century. Of the 20 large earthquakes located along the coast since 1900, only six have magnitudes of 7.5 or larger. Seismic activity from 138° to 143° E, when taken over the last 75+ years, indicates a rather broad zone of large earthquake activity, perhaps as wide as 250 km. The higher rate of activity in the region from 138° to 143° E when compared to the adjacent region to the east, appears to stem from differences in tectonic regime and therefore, may persist indefinitely into the future.

The region from 140° to 143° E was not the site of large shocks from 1935 to 1987, and thus may be considered a likely site for large earthquakes in the future. Few reports for large shocks exist prior to 1900 exist for the New Guinea region.

New Britain & Solomon Islands

This region can be divided into three distinct tectonic elements: east-northeast trending New Britain, northwest trending Bougainville, and the Guadalcanal-San Cristobal region. The junction of the New Britain and Bougainville arc segments is one of the most seismically active regions in the Pacific (see Figure 27), and is a good site for earthquake prediction research during the next 10 years.

NB-1. *Western New Britain*, 148°-151° E. The section of the seismic zone near western New Britain and the Huon Peninsula has not been ruptured by earthquakes of magnitude 7.5 or greater since 28 December 1945 M_S (7.9) and 6 May 1947 (M_S 7.7). An event on 14 September 1906 (M_S 7.7) is located in this area, but could not be reliably

Figure 27. Geographic place names and locations of large and great earthquakes along the New Guinea-New Britain-Solomon seismic zone. (*Top*) Major geographic features of the New Guinea-Solomon Islands region. Bathymetry from Chase et al. (1970), contour interval: 1000 m. Stippled regions are deeper than three thousand fathoms. Solid triangles are active volcanoes (after Katsui, 1971). (*Bottom*) Shallow earthquakes larger than M_S 7.5 from 1900 to 1987. Each event is labelled with date and magnitude. Open circles are location from Gutenberg and Richter (1954) or Richter (1958). Solid circles are either relocated or taken from the National Earthquake Information Center Hypocentral Data File. Hachured areas are aftershock zones of more recent earthquakes. From McCann and Nishenko (1989).

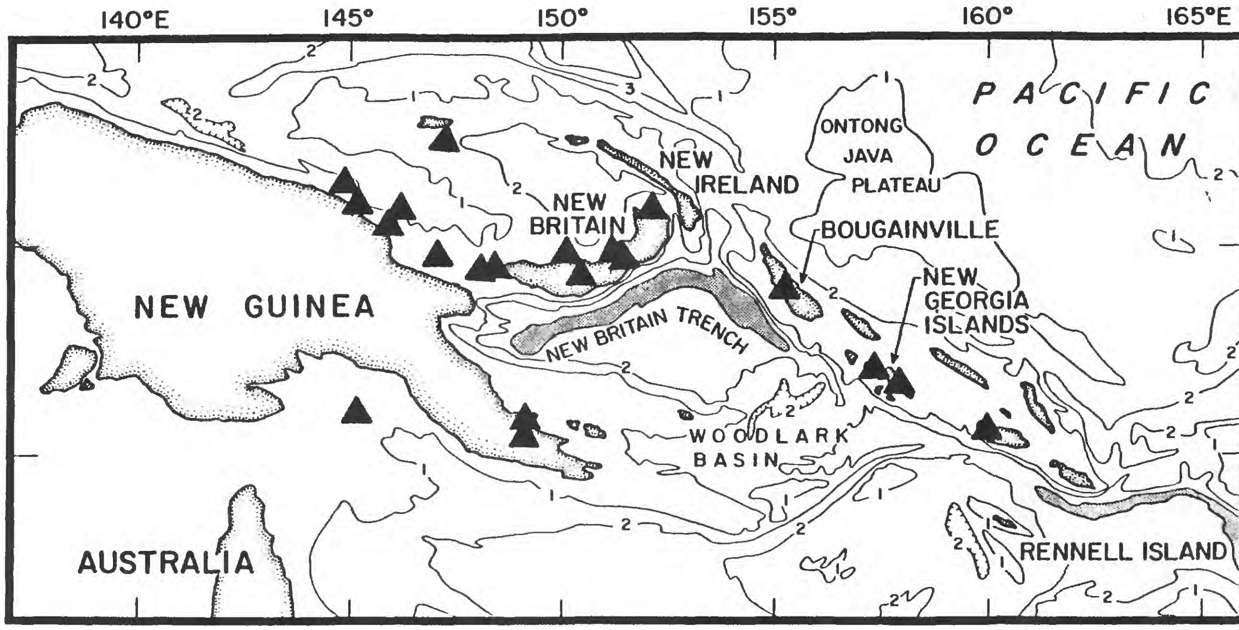
140°E
145°
150°
155°
160°
165°E
5°S
10°
PACIFIC OCEAN
ONTONG JAVA PLATEAU
NEW IRELAND
NEW BRITAIN
BOUGAINVILLE
NEW GEORGIA ISLANDS
NEW GUINEA
NEW BRITAIN TRENCH
WOODLARK BASIN
AUSTRALIA
RENNELL ISLAND

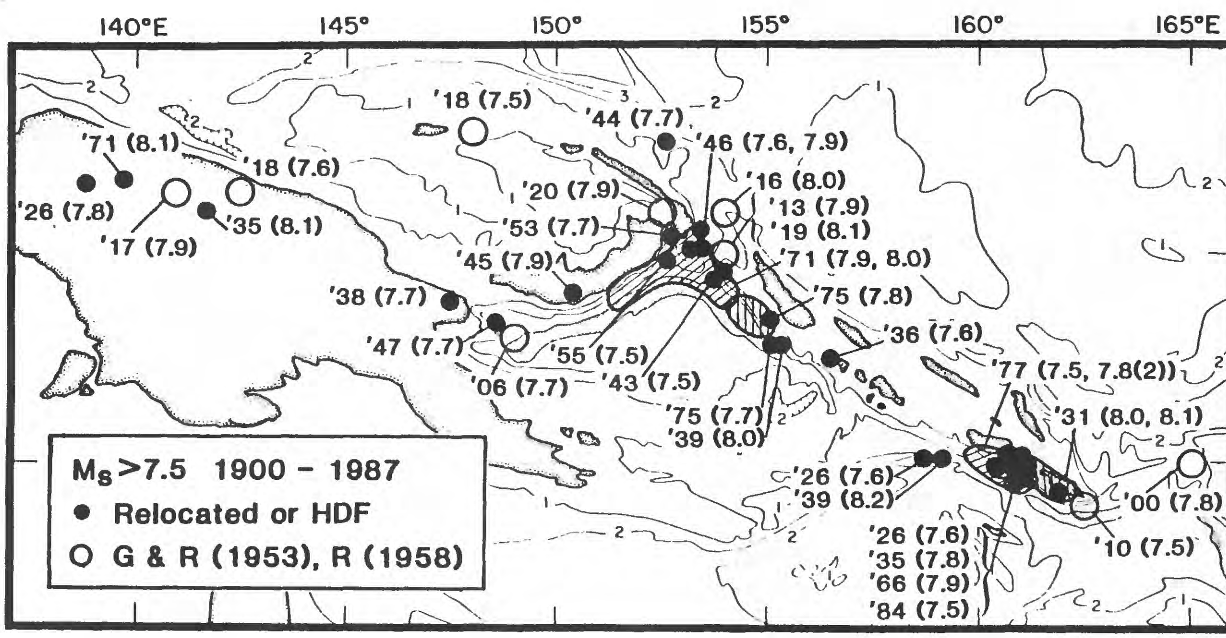
140°E
145°
150°
155°
160°
165°E
5°S
10°
'18 (7.5)
'44 (7.7)
'46 (7.6, 7.9)
'71 (8.1)
'18 (7.6)
'16 (8.0)
'20 (7.9)
'13 (7.9)
'26 (7.8)
'35 (8.1)
'53 (7.7)
'19 (8.1)
'17 (7.9)
'45 (7.9)
'71 (7.9, 8.0)
'38 (7.7)
'75 (7.8)
'36 (7.6)
'47 (7.7)
'55 (7.5)
'06 (7.7)
'43 (7.5)
'77 (7.5, 7.8(2))
'75 (7.7)
'39 (8.0)
'31 (8.0, 8.1)
'26 (7.6)
'39 (8.2)
'00 (7.8)
'26 (7.6)
'35 (7.8)
'66 (7.9)
'84 (7.5)
'10 (7.5)
Ms>7.5 1900 - 1987
Relocated or HDF
G & R (1953), R (1958)

relocated. If we assume that this earlier event was the predecessor to the events in the 1940's, the *repeat time* is approximately 40 years. Given this estimate, the tentative probability for recurrence within the next 10 years is at the 58% level.

Two compressional outer rise (COR) events occurred in this region in 1966 and 1973, and indicate that the trench outer rise region has been accumulating compressive stress over the last 25 years (Christensen and Ruff, 1989). Presently, western New Britain stands out as the only segment along the New Britain-Solomon arc that has produced a COR event.

NB-2. *Eastern New Britain*, 151°-153° E. In eastern New Britain, earlier sequences of events (2 February 1920 (M_S 7.9); 29 September 1946 (M_S 7.7), 23 April 1953 (M_S 7.6); and 26 July 1971 (M_S 7.7)) have repeatedly ruptured substantial portions of the plate boundary, and *repeat times* appear to be as short as 25 ± 5 years. Given that the last event occurred in 1971, and the relatively short *repeat time*, the probability is at the 59% level for the next 10 years.

S-1. *Northern Bougainville*, 153°-154.5° E. The northern Bougainville segment has ruptured in a series of great earthquakes that are closely linked in space and time with those in the eastern New Britain segment (1 January 1916 (M_S 8.0); 6 May 1919 (M_S 8.1); 29 September 1946 (M_S 7.9); and 14 July 1971 (M_S 7.8). Like segment NB-2, the occurrence of events in 1971 and the relatively short 25 year recurrence time indicates a high conditional probability of 53% over the next 10 years.

S-2. *Southern Bougainville*, 154.5°-155.5° E. Previous events in this segment occurred on 30 January 1939 (M_S 8.0) and 20 July 1975 (M_S 7.5, 7.6). Based on this single 36 year recurrence, we estimate the probability over the next 10 years to be at the 10% level.

Tensional outer rise (TOR) events occurred in regions NB-2, S-1 and S-2 following gap filling events in 1978, 1974 and 1975 and reflect the relaxation of compressive stress in the plate interface region . Given the relatively short recurrence time for great earthquakes in the New Britain-Bougainville area, monitoring for changes in stress in the trench outer rise region will be of great use for narrowing the time windows of future earthquake forecasts. As of this writing, a moderate size event has recently occurred in the trench outer rise region between segments NB-2 and S-1 on 23 July 1988 (M_S 6.8). Analysis of this event indicates it to be a TOR event, and indicates that stresses in this region have not yet changed in preparation for the next episode of great underthrust earthquakes.

S-3. *New Georgia*, 155.5°-157° E. A large event appears to have broken this segment of the plate boundary on 19 April 1936 (M_S 7.4). Its position between the seismically active Bougainville and inactive Woodlark segments of the Solomon arc suggest that this is a transitional region. Comparison of magnitudes and *repeat times* for other regions in the Solomon arc indicate that this region should have reruptured since 1936, if this was an underthrust earthquake. At present not enough information is available to explain this discrepancy or to confidently estimate a recurrence time.

S-4. *Woodlark Basin*, 157°-159.5° E. Within the Woodlark Basin lies the boundary between the Solomon Sea and Australian plates. The entire Woodlark Basin, a region of extensional tectonics, has not had large events since the turn of the century, and is considered to have a low potential for such events. The segment of the Solomon arc that is subducting this young seafloor (region S-4) has also maintained its quiescent nature for large and great earthquakes since 1900. Based on the lack of large or great earthquakes during this century, and the unique tectonic setting, we qualitatively assign region S-4 a low probability for large earthquake occurrence.

S-5. *Guadacanal*, 159°-161° E. This segment of the Solomon plate boundary exhibits a clear cluster or source for epicenters that have only been observed to propagate to the northwest. When taken as a whole, the Guadacanal region has seen two episodes of high earthquake activity, 1926-1935 and 1977 to the present (1988). Therefore recurrence times appear to be about 50 years, or about twice that of the New Britain-Bougainville segments. Given the estimated similarity in convergence rates (about 10 cm/yr) and in the sizes of earthquakes in both regions, this difference may indicate that more aseismic slip is occurring along the southern portion of the Solomon arc.

Because of our uncertainty in the location and mechanism of this earlier sequence of earthquakes, it is not apparent if the present sequence of earthquakes in this region has terminated. For comparison, the cumulative seismic moment release in the interval 1926-1935 is approximately 2.3 x 10^{28} dyne-cm, while the moment release in the current sequence is about 33% of the earlier (i.e. 7.5 x 10^{27} dyne-cm). Hence, the end of the current sequence may still lie in the future. Continued activity in this region on 10 August 1988 (M_S 7.5) is consistent with this pattern. Accordingly, we estimate the probability for future activity to be at the 45% level.

S-6. *San Cristobal*, 161°-163° E. The San Cristobal region last ruptured in a great earthquake on 3 October 1931 (M_S 8.0). No recurrence intervals have been observed for this segment during this century. We have used the recurrence time from the adjacent Guadacanal region (S-5), 50 years, as an estimate for this region. Based on this extrapolation, we estimate the probability to be at the 45% level for the next 10 years.

S-7. *SE Solomons*, 163°-165° E. The far southeastern portion of the Solomon island arc defines the transition zone between the Solomon and Vanuatu plate boundaries, and has been nearly aseismic for large earthquakes during the last 30 years. One event is located in this region on 29 July 1900 (M_S 7.6), but the uncertainty in location is large and cannot be confidently assigned to this region. A more detailed understanding of the nature of this region will be necessary before we can reliably estimate the seismic potential.

Santa Cruz & Vanuatu Islands

VA-1a,b. *Santa Cruz and Vankolo Is.*, 11°-13° S. Events on 18 July 1934 (M_S 8.3); 31 December 1966 (M_S 8.1); and 17 July 1980 (M_S 7.9) have ruptured similar segments

Figure 28. Geographic place names and locations of large and great earthquakes along the New Hebrides - Vanuatu seismic zone. (*Left*) Major geographic features of the New Hebrides - Vanuatu Islands region. Bathymetry from Chase et al. (1970), contour interval: 1000 m. Stippled regions are deeper than three thousand fathoms. Solid triangles are active volcanoes (after Katsui, 1971). (*Right*) Shallow earthquakes larger than M_S 7.5 from 1900 to 1987. Each event is labelled with date and magnitude. Open circles are location from Gutenberg and Richter (1954) or Richter (1958). Solid circles are either relocated or taken from the National Earthquake Information Center Hypocentral Data File. Hachured areas are aftershock zones of more recent earthquakes. From McCann and Nishenko (1989).

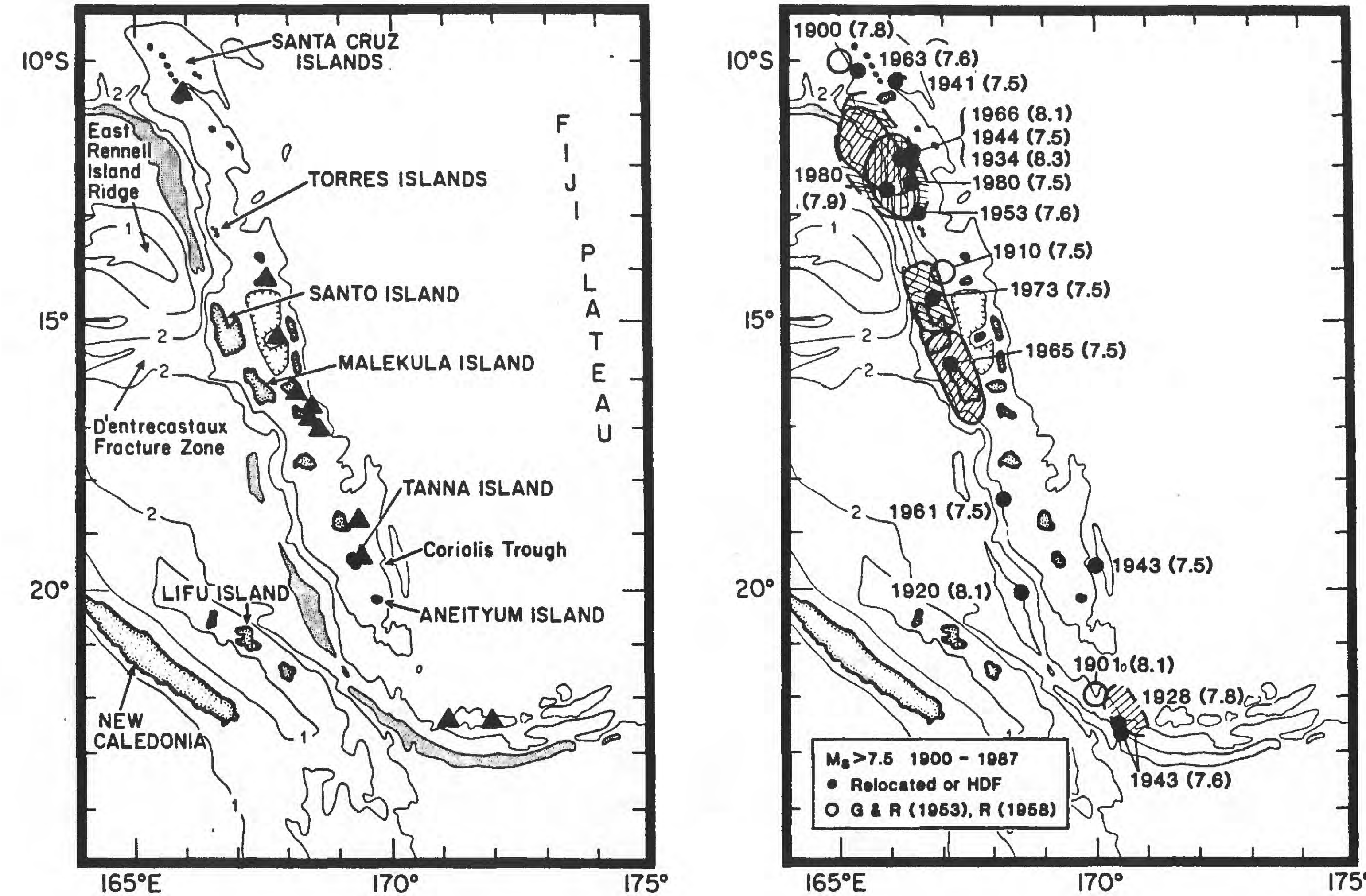

10°S
15°
20°
165°E
170°
175°
SANTA CRUZ ISLANDS
TORRES ISLANDS
East Rennell Island Ridge
SANTO ISLAND
MALEKULA ISLAND
D'entrecastaux Fracture Zone
TANNA ISLAND
Coriolis Trough
ANEITYUM ISLAND
LIFU ISLAND
NEW CALEDONIA
FIJI PLATEAU
1900 (7.8)
1963 (7.6)
1941 (7.5)
1966 (8.1)
1944 (7.5)
1934 (8.3)
1980 (7.5)
1980 (7.9)
1953 (7.6)
1910 (7.5)
1973 (7.5)
1965 (7.5)
1961 (7.5)
1943 (7.5)
1920 (8.1)
1901 (8.1)
1928 (7.8)
1943 (7.6)
Ms>7.5 1900 - 1987
Relocated or HDF
G & R (1953), R (1958)

of the arc (see Figure 28), but display different details in the rupture process. Events in 1934, 16 November 1944 (M_S 7.3) and 1966 have nearly identical epicenters suggesting similarities in the initiation of rupture at 11.9° S. This region is named the Vankolo asperity by McCann and Nishenko (1989), and appears to spawn major earthquakes every 10 to 20 years. If the adjoining segments of plate boundary have stored enough strain energy, then rupture of the Vankolo asperity may spread into the adjoining region resulting in a great rather than a large earthquake. Based on this pattern, we would expect the Vankolo asperity to rupture in an event of at least M_S 7.5 before the year 2000, and estimate the conditional probability at 83%. The recurrence time for larger events appears to be about 30 years, hence the next failure may initiate a rupture similar to that in 1966, and conditional probability for a great event is at the 48% level.

VA-2. *Torres Islands*, 13°-14° S. While no earthquake activity is known for the Torres Islands segments during this century, the occurrence of a COR event in 1985 (Christensen and Ruff, 1989) may provide a basis for qualitatively upgrading the hazard in this segment.

VA-3. *North Santo Island*, 14.°-15.3° S. Emerged corals on northwest Santo Island indicate that at least one event in 1865 ± 6 occurred prior to the 23 December 1973 (M_S 7.5) earthquake (Taylor et al., 1988; Edwards et al., 1987). The amount of uplift in this earlier event is twice that of the 1973 event (0.6 vs 1.2m), suggesting that the 1865 event was twice the size, or that there is a missing event. Hence recurrence times for this segment of the Vanuatu arc range from 54 to 108 years. Due to the recency of faulting, both estimates indicate relatively low probabilities for this region over the next 10 years ($\leq$ 1%).

VA-4. *South Santo and Malekula Island*, 15.3°-16.3° S. The boundary between the north and south Santo seismic zones coincides with the region where the D'Entrecasteaux ridge intersects the New Hebrides trench. Two large earthquakes on 5 January 1946 (7.3, 7.0) appear to have ruptured similar segments of south Santo Island that broke during events in 11 August 1965 (M_S 7.5) and 27 October 1971 (M_S 7.1). The distribution and amounts of coral emergence on south Santo suggest that the 1946 events are most similar to the combined effects of the 1965 and 1971 events. Hence, the probability for the occurrence of M_S 7 events, based on the historic record is at the 60% level. Taylor et al. (1988) note that this observed 19-25 year recurrence is shorter, by a factor of two, than the recurrence inferred from dividing the average coseismic uplift (0.28 m) by the long-term uplift rate (5.5 mm/yr). In the latter case, the estimated recurrence time is 51 years and the corresponding probability is at the 9% level.

In addition to the 1946-1965/71 events on South Santo Island, coseismic uplift during the 1965 earthquake also occurred on Malekula Island. The next highest coral terrace on Malekula has ^{230}Th dates of 1718-1729 A.D., and is locally uplifted by an amount similar to the 1965 event. The coral data suggest long (240 year) recurrence times for 1965 sized events along this portion of the Vanuatu arc, and is in good agreement with the estimated recurrence time based on rates of uplift. Consequently, the probability for future events is relatively low over the next 10 years ($\leq 1\%$).

VA-5. *Central Vanuatu*, 17°-20° S. To the south there are fewer large shocks along the plate boundary, and the principal mode of plate motion may be by aseismic processes. Little is known about the great 20 September 1920 (M_S 7.9) earthquake. It is located near the trench, and may be a normal faulting earthquake, signifying reduced coupling in this area. No specific forecasts for future behavior are available at this time.

VA-6. *Loyalty Islands*, 20°-23° S. In contrast to central Vanuatu, the Loyalty Islands portion of the Vanuatu arc exhibits frequent large earthquakes. Prior events on 16 March 1928 (M_S 7.6); 14 September 1943 (M_S 7.4); and 25 October 1980 (M_S 7.2) indicate a short recurrence time of about 24 $\pm$ 4 years. In addition, an event on 9 August 1901 (M_S 7.9) is also located near this segment, however, this epicenter needs to be verified. Based on the pattern of occurrence of post-1901 events, the probability for a large event in this segment over the next 10 years is at the 22% level.

VA-7. *Hunter Is.*, 171°-174° E. This segment is bounded by the Loyalty Islands segment to the west and the Fiji rift to the east. As shown in Figure 28, there is no history of great earthquakes in this segment, and hazards estimates similar to others in this study cannot be made at this time.

Tonga & Kermadec Islands

In contrast to many of the other subduction zones covered in this study, large areas of the Tonga and Kermadec arcs are distinguished by the lack of demonstrable repeats of shallow interplate earthquakes during this century. Both Tonga and northern Kermadec were sites of a series of great earthquakes from 1907 to 1919. These events are poorly located, their focal mechanisms are not known, and if assumed to be interplate events, cannot cover the entire plate boundary. Given the present incomplete state of knowledge for this region, we will attempt to single out those areas where recurrence estimates can be made. Other areas will have to, for the present, be regarded as suspect. These areas include Tafahi Is. (TK-1), Eua Is. (TK-2), Ata Is. (TK-4), and the junction of the Tonga and Kermadec trench systems (TK-6). Place names and recent rupture zones are shown in Figure 29.

TK-3. *Tongatapu*, 20°-22° S. Of the seismic gaps in the Tonga arc, the region from 20° to 22° S is clearly identified as one of high seismic potential by the observations of a) one recurrence interval (2 January 1907 (M_S 7.6) or June 1913 (M_S 7.7) to 8 September 1948 (M_S 7.8), 35-41 years) and the fact that 40 years has elapsed since the last event, b) three compressional outer rise events (1982-1986) and c) an area of high level background seismicity. On the basis of the historic seismicity and estimated 38 year *repeat time*, this area has a probability of 58% over the next 10 years, which appears to be consistent with the observations of other intermediate-term phenomena.

Figure 29. Geographic place names and locations of large and great earthquakes along the Tonga-Kermadec seismic zone. (*Left*) Major geographic features of the Tonga-Kermadec Islands region. Bathymetry from Chase et al. (1970), contour interval: 1000 m. Stippled regions are deeper than three thousand fathoms. Solid triangles are active volcanoes (after Katsui, 1971). (*Right*) Shallow earthquakes larger than M_S 7.5 from 1900 to 1987. Each event is labelled with date and magnitude. Open circles are location from Gutenberg and Richter (1954) or Richter (1958). Solid circles are either relocated or taken from the National Earthquake Information Center Hypocentral Data File. Hachured areas are aftershock zones of more recent earthquakes. From McCann and Nishenko (1989).

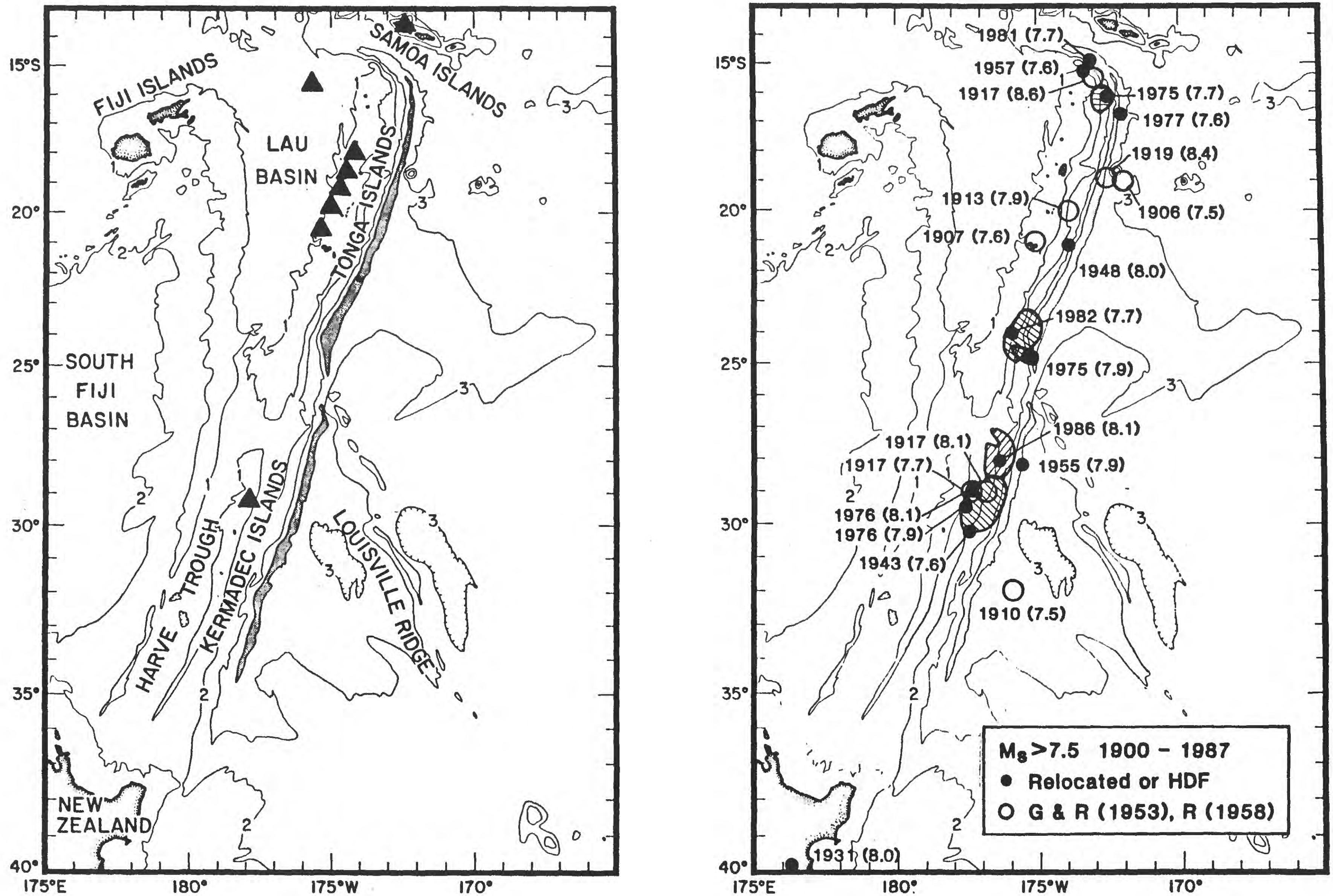

15°S
20°
25°
30°
35°
40°
175°E
180°
175°W
170°
FIJI ISLANDS
SAMOA ISLANDS
LAU
BASIN
TONGA ISLANDS
SOUTH
FIJI
BASIN
HARVE TROUGH
KERMADEC ISLANDS
LOUISVILLE RIDGE
NEW
ZEALAND
1981 (7.7)
1957 (7.6)
1917 (8.6)
1975 (7.7)
1977 (7.6)
1919 (8.4)
1913 (7.9)
1906 (7.5)
1907 (7.6)
1948 (8.0)
1982 (7.7)
1975 (7.9)
1986 (8.1)
1917 (8.1)
1955 (7.9)
1917 (7.7)
1976 (8.1)
1976 (7.9)
1943 (7.6)
1910 (7.5)
1931 (8.0)
M_s >7.5 1900 - 1987
Relocated or HDF
G & R (1953), R (1958)

TK-5. *Louisville Ridge Intersection*, 23°-25° S. Collision with the Louisville Ridge has indented the arc geometry in this area. No great earthquakes are located in this region prior to the great 19 December 1982 (M_S 7.7) event, suggesting that *repeat times* in this region are on the order of 80 years or more. Using 82 years as a tentative *repeat time* estimate, the conditional probability, given the recency of faulting, is less than 1% for the next 10 years.

TK-7,8. *Northern and Southern Kermadec Is.*, 27°-28.5° and 28.5°-30.2° S. The best documented recurrence history in the Tonga-Kermedec region is along the northern Kermadec arc. This region experienced two great events on 1 May (M_S 8.1) and 16 November 1917 (M_S 7.7) and again on 14 January 1976 (M_S 8.1, 7.9, within 50 min) and 20 October 1986 (M_S 8.2). Given the apparent *repeat time* and the recency of faulting, the probability for great earthquakes over the next 10 years is negligible (i.e. $\leq$ 1%).

TK-9. *Southern Kermadec*, 30.2°-38° S. The southern part of the Kermadec arc is distinguished by the lack of large and great earthquakes, and low levels of background seismicity during this century. This segment coincides with the well developed back-arc spreading of the Harve Trough, and the section of the arc with the lowest convergence rate. Uyeda and Kanamori (1979) related the slow subduction of old seafloor to aseismic subduction, and this region may be a good example of that phenomena. Based on these observations we have qualitatively assigned this section of the Kermadec arc a low probability for the occurrence of great earthquakes in the near future.

Summary

We have examined and characterized the seismic potential for 119 seismic gaps around the circum-Pacific region. This report represents the first probabilistic comparison of seismic hazards on this scale, and updates earlier work on seismic gaps by McCann et al. (1979) by explicitely including earthquake *repeat times* and the proximity to the next expected recurrence as a factor in describing earthquake hazards along simple plate boundaries. Variations in observed earthquake magnitudes, recurrence times, and the completeness of the historic record for individual plate boundary segments have resulted in a diverse data set for the circum-Pacific region. The probabilistic framework adopted in this study, in addition to accounting for uncertainties in the individual data, has provided a common base for comparing seismic hazards, and being able to rank gaps in terms of those most likely to rupture in the next 10 and 20 years.

The estimates presented in this study are based on conditional probability and the primary results summarized in Plate 1, Figures 6, 10, 15, 19, 21, 23, 26, and the Appendix cover the time interval 1989-1999, which overlaps the International Decade of Natural Disaster Reduction. The Top Ten list (Table 1) is a ranked list of those gaps with greater than a 50% probability of recurrence within the next 10 years. This list includes 10 zones, or 8% of the total number of gaps examined. The majority of gaps on this list are characterized by relatively short recurrence times and the 10 year interval (1989-1999) covers a substantial fraction of possible recurrence times for those gaps. Note, that this does not preclude other gaps, with less than a 50% chance in 10 years, of also rupturing. Table 2 presents a ranked list of gaps with a greater than 50% probability of recurrence in the next 20 years (1989-2009). This list is quite a bit larger, and includes 30 out of 119 gaps, or 25% of our sample. While many of the gaps in Table 2 have longer *repeat times*, the combination of time elapsed since the last event, and a larger time window (or fraction of possible recurrence times) has resulted in more candidates appearing on this list. Note that many more gaps in Table 2 occur near urban centers. The 20 year list is useful for longer-term forecasting, and may be a more reliable list in that, at this writing, we still do not have an appreciation of what threshold percentage, for a given time interval, constitutes a high or significant hazard level.

One of the basic observations to come from this study is that the variation in repeat times for characteristic, plate boundary earthquakes is proportional to the average repeat time. The implication of varying degrees of temporal resolution impacts the planning of earthquake prediction programs or experiments, hazard mitigation work, and the funding and expected lifetimes of research programs. Given the inherent large uncertainties in many hazards estimates, which in some instances cover decades, research and hazard mitigation programs must be organized with these limitations in mind. Some programs, such as geodetic, strong motion, and seismological monitoring can be instituted and carried out for decades. Hence, the long-term estiamtes presented here can be considered a "blueprint" for future research. Other research programs, which may have shorter life spans, due to logistical or instrumental reasons, should await deployment untill the expectancy of the earthquake matches the lifetime of the project.

Earthquake forecasting is a rapidly developing field, hence in addition to updating these forecasts, due to the time-dependent nature of the problem, advances due to new information and understanding of the earthquake process and the recurrence cycle will be necessary. Further improvements in the direct method of estimating recurrence times are necessary for areas with one or no observed *repeat times.* Accounting for variations in the size of earthquakes from cycle to cycle presently poses a problem. While we are rapidly gaining experience in estimating the time of occurrence and portraying the overall hazard level, specific predictions as to the exact size or rupture dimension of a future event are still uncertain. This uncertainty ultimately effects seismic risk estimates and decisions concerning the type of mitigation effort needed for urban areas near hazardous seismic gaps.

While this study has summarized the seismic potential for a large number of seismic gaps around the circum-Pacific area, there are still a number of geographic and seismo-tectonic regions which need to be included. Additional geographic regions include Indonesia, the Phillipines, New Zealand, and the countries which surround the Caribbean basin. The occurrence of shallow, large earthquakes in volcanic valleys (e.g. El Salvador, Nicaragua, Colombia, and Ecuador) may also be amenable to the techniques used in this study. Earthquakes in these regions pose an even greater risk to life and property due to high population densities.

Tsunamis associated with the occurrence of great, shallow plate boundary earthquakes pose a threat to the entire circum-Pacific community. Knowledge as to when and where great earthquakes can be expected is invaluable towards developing a tsunami forecast for the circum-Pacific. This type of forecast would provide a basis for the development of an active, rather than passive, tsunami mitigation program.

Finally, attention needs to be given to the development of a real-time earthquake warning and advisory system. The time windows for the forecasts presented here need to be narrowed, as additional data become available, to realize the ultimate goal of earthquake forecasting and prediction reasearch, saving lives and property. Advances in the analysis of seismologic data, coupled with satellite communications, provide the opportunity for rapid data collection, interpretation, and evaluation. The development of a global, real-time, seismic hazards network could be a achievement that would outlive the International Decade of Natural Disaster Reduction.

References

Abe, K., 1977, Tectonic implications of the large Shioya-Oki earthquakes of 1938, *Tectonophysics,* **41**, 269–289.

Abe, K., 1979, Size of great earthquakes of 1837-1974 inferred from tsunami data, *Jour. Geophys. Res.,* **84**, 1561–1568.

Abe, K. and S. Noguchi, 1983, Revision of magnitudes of large shallow earthquakes, 1897-1912, *Phys. Earth Planet. Interiors,* **33**, 1–11.

Adamek, S., F. Tajima, and D.A. Weins, 1987, Seismic rupture associated with subduction of the Cocos plate, *Tectonics,* **6**, 757–774.

Adamek, S., C. Frolich, and W.D. Pennington, 1988, Seismicity of the Caribbean-Nazca boundary: constraints on microplate tectonics of the Panama region, *Jour. Geophys. Res.,* **93**, 2053–2075.

Ando, M., 1975, Source mechanisms and tectonic significance of historical earthquakes along the Nankai trough, Japan, *Tectonophysics,* **27**, 119–140.

Askew, B.L. and S.T. Algermissen, 1985, Catalog of earthquakes for South America, Peru, vol. 7, CERESIS, Lima, Peru, 1108 pp.

Atwater, B.F., 1987, Evidence for great Holocene earthquakes along the outer coast of Washington state, *Science,* **236**, 942–944.

Atwater, B.F., A.G. Hull, K.A. Bevis, 1987, Aperiodic Holocene recurrence of widespread, probably coseismic subsidence in southwestern Washington (abs), *EOS, Trans, Amer. Geophys. Union,* **68**, 1468.

Atwater, B.F., S.P. Nishenko, J.B. Phipps, and A.G. Hull, 1989, Extent and timing of probable coseismic subsidence in westernmost Washington state during the past 3500 years, *Jour. Geophys. Res.*, submitted.

Barazangi, M., and B.L. Isacks, 1976, Spatial distribution of earthquakes and subduction of the Nazca plate beneath South America, *Geology,* **4**, 686–692.

Bakun, W.H. and A.G. Lindh, 1985, The Parkfield, California earthquake prediction experiment, *Science,* **229**, 619–624.

Beck, S.L. and L.J. Ruff, 1984, The rupture process of the great 1979 Colombia earthquake: evidence for the asperity model, *Jour. Geophys. Res.,* **89**, 9281–9291.

Beck, S.L. and L.J. Ruff, 1987, Rupture process of the great 1963 Kurile Islands earthquake sequence: asperity interaction and multiple event rupture, *Jour. Geophys. Res.*, **92**, 14123–14138.

Beck, S.L. and S.P. Nishenko, 1989, Variations in the earthquake rupture mode along the central Peru subduction zone, *Geophys. Res. Letters*, submitted.

Beck, S.L. and L.J. Ruff, 1989, Great earthquakes and subduction along the Peru trench, *Phys. Earth Planet. Interiors.*, in press.

Buland, R. and S.P. Nishenko, 1989, Preferred earthquake forecasts and conditional earthquake prediction, *Bull. Seismo. Soc. America*, submitted.

Chael, E.P. and G.S. Stewart, 1982, Recent large earthquakes along the Middle America trench and their implications for the subduction process, *Jour. Geophys. Res.*, **87**, 329–338.

Chase, C.G., 1978, Plate kinematics: the Americas, East Africa, and the rest of the world, *Earth Planet. Sci. Letters*, **37**, 355–368.

Chase, C., H. Menard, and J. Mammerickx, 1970, Bathymetry of the North Pacific, Charts 1-6, Scripps Inst. Oceanogr., Inst. Marine res., La Jolla, CA.

Christensen, D.H. and L.J. Ruff, 1989, Seismic coupling and outer rise earthquakes, *Jour. Geophys. Res.*, in press.

Compte, D., A. Eisenberg, E. Lorca, M. Pardo, L. Ponce, R. Saragoni, S.K. Singh, and G. Suarez, 1986, The 1985 Central Chile earthquake: a repeat of previous great earthquakes in the region?, *Science*, **233**, 449–453.

Dewey, J.W. and W. Spence, 1979, Seismic gaps and source zones of recent large earthquakes in coastal Peru, *Pure Appl. Geophys.*, **117**, 1148–1171.

Edwards, R.L., F.W. Taylor, J.H. Chen, and G.J. Wasserburg, 1987, High-precision thorium-230 dating of corals using thermal ionization mass spectrometry: applications to paleoseismology, in *Proceedings of Conference XXXIX, Directions in Paleoseismology*, edited by A.J. Crone and E.M. Omdahl, *U.S. Geol. Survey Open File Rpt. 87-673*, pp. 30–38.

Eissler, H.K. and K.C. McNally, 1984, Seismicity and tectonics of the Rivera plate and implications for the 1932 Jalisco, Mexico earthquake, *Jour. Geophys. Res.*, **89**, 4520–4530.

Eissler, H., L. Astiz, and H. Kanamori, 1986, Tectonic setting and source parameters of the September 19, 1985 Michoacan, Mexico earthquake, *Geophys. Res. Letters,* **13**, 569–572.

Espinosa, A.F., R. Husid, and S.T. Algermissen, 1975, Seismological and engineering features of the October 3, 1974 Lima earthquake, *Proc. of the 5th European Conf. on Earthquake Eng.*, Chap. 7, Paper 141, 1–7, Istanbul, Turkey.

Espinosa, A.F., R. Husid, S.T. Algermissen, and J. de las Casas, 1977, The Lima earthquake of October 3, 1974; intensity distribution, *Bull. Seismo. Soc. America,* **67**, 1429–1440.

Fedotov, S.A., 1965, Regularities of the distribution of strong earthquakes in Kamchatka, the Kuril Islands, and northeast Japan, *Tr. Inst. Fiz. Zemli Akad. Nauk SSSR,* **36**, 66–93.

Fedotov, S.A., S.D. Chernyshev, and G.V. Chernysheva, 1982, The improved determination of the source boundaries for earthquakes of $M \geq 7\frac{3}{4}$, of the properties of the seismic cycle, and of long-term seismic prediction for the Kurile-Kamchatkan arc, *Earthq. Pred. Res.,* **1**, 153–171.

Fukao, Y. and M. Furumoto, 1979, Stress drops, wave spectra, and recurrence intervals of great earthquakes - implications of the Etorofu earthquake of 1958 November 6, *Geophys. J.R. Astron. Soc.,* **57**, 23–40.

Gonzalez-Ruiz, J.R.G. and K.C. McNally, 1988, Stress accumulation and release since 1882 in Ometepec, Guerrero, Mexico: implications for failure mechanisms and risk assessments of a seismic gap, *Jour. Geophys. Res.,* **93**, 6297–6317.

Gutenberg, B., 1939, Tsunamis and earthquakes, *Bull. Seismo. Soc. America,* **29**, 517–526.

Gutenberg, B., and C.F. Richter, 1954, *Seismicity of the Earth*, 2nd Ed., Princeton Univ. Press, New Jersey, pp. 161–234.

Hatori, T., 1976, Propagation of tsunamis from sources off the Pacific coast of northeast Japan, *Bull. Earthquake Res. Inst., Univ. Tokyo,* **51**, 197–207.

Hatori, T., 1979, Tsunami sources in Hokkaido and southern Kuril regions, *Bull. Earthq. Res. Inst. Tokyo Univ.,* **49**, 63–75.

Heaton, T.H. and H. Kanamori, 1984, Seismic potential associated with subduction in the northwestern United States, *Bull. Seismo. Soc. America,* **74**, 933–941.

Heaton, T.H. and S. H. Hartzell, 1986, Source characteristics of hypothetical subduction earthquakes in the northwestern United States, *Bull. Seismo. Soc. America,* **76**, 675–708.

Herron, E.M., 1981, Chile margin near 38°S: Evidence for a genetic relationship between continental and marine geological features or a case of curious coincidence?, in *Nazca Plate: Crustal Deformation and Andean Convergence*, edited by L.D. Kulm, J. Dymond, E.J. Dasch, and D.M. Hussong, *Mem. Geol. Soc. America,* **154**, 683–702.

House, L.S., L.R. Sykes, J.N. Davies, and K.H. Jacob, 1981, Identification of a possible seismic gap near Unalaska Island, eastern Aleutians, in *Earthquake Prediction, An International Review, Maurice Ewing Ser.*, Vol. 4, edited by D.W. Simpson and P.G. Richards, pp. 81–92, AGU, Washington, D.C.

Ishibashi, K., 1981, Specification of a soon-to-occur seismic faulting in the Tokai district, central Japan, based on seismotectonics, in *Earthquake Prediction, An International Review, Maurice Ewing Ser.*, Vol. 4, edited by D.W. Simpson and P.G. Richards, pp. 297–332, AGU, Washington, D.C.

Jacoby, G.C., P.R. Sheppard, and K.E. Sieh, 1988, Irregular recurrence of large earthquakes along the San Andreas fault: evidence from trees, *Science,* **241**, 196–199.

Jordan, T.H., 1975, The present day motions of the Caribbean plate, *Jour. Geophys. Res.,* **80**, 4433–4439.

Kanamori, H., 1972, Mechanism of tsunami earthquakes, *Phys. Earth Planet. Interiors.,* **6**, 246–259.

Kanamori, H., 1977, Seismic and aseismic slip along subduction zones and their tectonic implications in *Island Arcs, Deep Sea Trenches, and Back-Arc Basins, M. Ewing Ser.* 1, edited by M. Talwani and W.C. Pitman III, AGU, Washington, D.C., 273–284.

Kanamori, H. and K.C. McNally, 1982, Variable rupture mode of the subduction zone along the Ecuador-Colombia coast, *Bull. Seismo. Soc. America,* **72**, 1241–1253.

Katsui, Y. ed., 1971, *List of World Active Volcanoes*, Volcanological Society of Japan, Sapporo, Japan.

Kelleher, J.A., 1972, Rupture zones of large South American earthquakes and some predictions, *Jour. Geophys. Res.,* **77**, 2087–2103.

Kelleher, J.A., L.R. Sykes, and J. Oliver, 1973, Possible criteria for predicting earthquake locations and their applications to major plate boundaries of the Pacific and Caribbean region, *Jour. Geophys. Res.,* **78**, 2547–2585.

Kelleher, J.A. and W.R. McCann, 1976, Buoyant zones, great earthquakes, and unstable boundaries of subduction, *Jour. Geophys. Res.,* **81**, 4885–4908.

Kondorskaya, N.V. and N.V. Shebalin, 1982, New catalog of strong earthquakes in the U.S.S.R. from ancient times through 1977, 608 pp., U.S. Dept. of Commerce, Boulder, CO

LeFevre, L.V. and K.C. McNally, 1985, Stress distribution and subduction of aseismic ridges in the Middle America subduction zone, *Jour. Geophys. Res.,* **90**, 4495–4510.

Lomnitz, C., 1970, Major earthquakes and tsunamis in Chile during the period 1535 to 1953, *Geol. Rundsch.,* **59**, 938–960.

Luhr, J.F., S.A. Nelson, J.F. Allan, and I.S.E. Carmichael, 1985, Active rifting in southwestern Mexico: manifestations of an incipient eastward spreading ridge jump, *Geology,* **13**, 54–57.

McCann, W.R., S. P. Nishenko, L.R. Sykes, and J. Krause, 1979, Seismic gaps and plate tectonics: Seismic potential for major boundaries, *Pure Appl. Geophys.,* **117**, 1082–1147.

McCann, W.R., O.J. Perez, and L.R. Sykes, 1980, Yakataga gap, Alaska: seismic history and earthquake potential, *Science,* **207**, 1309–1314.

McCann, W.R. and S.P. Nishenko, 1989, Seismic potential and seismic regimes of the southwest Pacific, *Jour. Geophys. Res.*, submitted.

McNally, K.C. and J.B. Minster, 1981, Nonuniform seismic slip rates along the Middle America trench, *Jour. Geophys. Res.,* **86**, 4949–4959.

Mendoza, C. and J.W. Dewey, 1984, Seismicity associated with the great Colombia-Ecuador earthquakes of 1942, 1958, and 1979: implications for barrier models of earthquake rupture, *Bull. Seismo. Soc. America,* **74**, 577–593.

Mendoza, C. and S.P. Nishenko, 1989, The Panama earthquake of 7 September 1882: evidence for active underthrusting, *Bull. Seismo. Soc. America*, submitted

Milne, J., 1880, The Peruvian earthquake of May 9th, 1877, *Trans. Seismo. Soc. Japan,* **2**, 50-96.

Minster, J.B. and T.H. Jordan, 1978, Present day plate motions, *Jour. Geophys. Res.,* **83**, 5331–5354.

Mogi, K., 1981, Earthquake prediction program in Japan, in *Earthquake Prediction, An International Review, Maurice Ewing Ser.*, Vol. 4, edited by D.W. Simpson and P.G. Richards, pp. 635–666, AGU, Washington, D.C.

Mogi, K., 1968, Some features of recent seismic activity in and near Japan, *Bull. Earth. Res. Inst. Tokyo Univ.,* **46**, 1225–1236.

Montero, W., 1986, Periodos de recurrencia y tipos de sequencias sismicas de los temblores interplaca e intraplaca en la region de Costa Rica, *Rev. Geol. Amer. Central,* **5**, 35–72.

Naval Oceanographic Office, 1978, Bathymeric atlas of the north Pacific ocean, *N.O. Pub.* 1301-2-3 (S), 176 pp.

Nishenko, S.P., 1985, Seismic potential for large and great interplate earthquakes along the Chilean and southern Peruvian margins of South America: a quantitative reappraisal, *Jour. Geophys. Res.,* **90**, 3589–3615.

Nishenko, S.P., 1989, Earthquakes: hazards and prediction, in *Encyclopedia of Solid Earth Geophysics*, D.E. James, editor, Van Nostrand Reinhold, 260–268.

Nishenko, S.P. and W.R. McCann, 1979, Large thrust earthquakes and tsunamis: Implications for the development of fore arc basins, *Jour. Geophys. Res.,* **84**, 573–584.

Nishenko, S.P. and W.R. McCann, 1981, Seismic potential of the world's major plate boundaries, in *Earthquake Prediction, An International Review, Maurice Ewing Ser.*, Vol. 4, edited by D.W. Simpson and P.G. Richards, pp. 20-28, AGU, Washington, D.C.

Nishenko, S.P. and R. Buland, 1987, A generic recurrence interval distribution for earthquake forecasting, *Bull. Seismol. Soc. America,* **77**, 1382–1399.

Nishenko, S.P. and S.K. Singh, 1987a, Conditional probabilities for the recurrence of large and great interplate earthquakes along the Mexican subduction zone, *Bull. Seismo. Soc. America,* **77**, 2095–2114.

Nishenko, S.P. and S.K. Singh, 1987b, The Acapulco-Ometepec earthquakes of 1907-1982: evidence for a variable recurrence history, *Bull. Seismo. Soc. America,* **77**, 1359–1367.

Nishenko, S.P. and S.K. Singh, 1987c, Relocation of the great Mexican earthquake of 14 January 1903, *Bull. Seismo. Soc. America,* **77**, 256–259.

Nishenko, S.P. and K. Jacob, 1989, Seismic potential of the Queen Charlotte-Alaska-Aleutian seismic zone, *Jour. Geophys. Res.*, in press.

Plafker, G., 1986, Geologic studies related to earthquake potential and recurrence in the "Yakataga seismic gap", in Minutes of the National Earthquake Prediction Council, edited by C.F. Shearer, *U.S. Geol. Survey Open File Rpt.* 86-92, 135–143.

Plafker, G. and J.C. Savage, 1970, Mechanism of the Chilean earthquakes of May 21 and 22, 1960, *Bull. Geol. Soc. America,* **81**, 1001-1030.

Plafker, G., T. Hudson, T. Bruns, and M. Rubin, 1978, Late Quaternary offsets along the Fairweather fault and crustal plate interactions in southern Alaska, *Can. Jour. Earth Sci.,* **15**, 805–816.

Prince, R.A., W.J. Schweller, W.T. Coulbourn, G.L. Shepard, G.E. Ness, and A. Masias, 1980, Bathymetry of the Peru-Chile continental margin and trench, 9 maps, *Map Chart Series MC-34, Geol. Soc. America*, Boulder, CO.

Reid, H.F., 1917, Note on the earthquakes at Almirante, Republic of Panama, in April 1916, *Bull. Seismo. Soc. America,* **7**, 27–30.

Richter, C.F., 1958, *Elementary Seismology*, W.H. Freeman and Co., San Francisco, CA., 768 pp.

Rikitake, T., 1976, Recurrence of great earthquakes at subduction zones, *Tectonophysics,* **35**, 335–362.

Rinehart, W., R. Ganse, P. Teik, E. Arnold, C. Stover, and R.H. Smith, 1982, Seismicity of Middle America, National Geophysical Data Center and National Earthquake Information Service, Boulder, CO.

Rogers, G.C., 1986, Seismic gaps along the Queen Charlotte fault, *Earthq. Pred. Res.,* **4**, 1–11.

Rothé, J., 1969, The seismicity of the Earth, 1953–1965, UNESCO, Paris, 336 pp.

Scholz, C.H., 1985, The Black Mountain asperity: seismic hazard of the southern San Francisco peninsula, California, *Geophys. Res. Letters,* **12**, 717–719.

Scholz, C.H. and T. Kato, 1978, The behavior of a convergent plate boundary: crustal deformation in the south Kanto district, Japan, *Jour. Geophys. Res.,* **83**, 783–797.

Schwartz, D., 1985, The Caribbean-North American plate boundary in Central America: New data on Quaternary tectonics (abs.), *Earthquake Notes,* **55**, p. 28.

Schwartz, D., L.S. Cluff, and T.W. Donnelly, 1979, Quaternary faulting along the Caribbean-North America plate boundary in Central America, *Tectonophysics,* **52**, 431–445.

Schwartz, S.Y. and L.J. Ruff, 1985, The 1968 Tokachi-Oki and the 1969 Kurile Islands earthquakes: variability in the rupture process, *Jour. Geophys. Res.,* **90**, 8613–8626.

Schwartz, S.Y. and L.J. Ruff, 1987, Asperity distribution and earthquake occurrence in the southern Kurile Islands arc, *Phys. Earth Planet. Inter.,* **49**, 54–77.

Schwartz, S.Y., J.W. Dewey, and T. Lay, 1989, Influence of fault plane heterogeneity on the seismic behavior in the southern Kurile Islands arc, *Jour. Geophys. Res.,*in press.

Schweller, W.J., L.D. Kulm, and R.A. Prince, 1981, Tectonics, structure, and sedimentary framework of the Peru-Chile trench, in *Nazca Plate: Crustal Deformation and Andean Convergence*, edited by L.D. Kulm, J. Dymond, E.J. Dasch, and D.M. Hussong. *Mem. Geol. Soc. America,* **154**, 323–350.

Shimazaki, K., 1974, Nemuro-Oki earthquake of June 17, 1973: a lithospheric rebound at the upper half of the interface, *Phys. Earth Planet. Interiors,* **9**, 314–327.

Shimizaki, K. and T. Nakata, 1980, Time-predictable recurrence model for large earthquakes, *Geophys. Res. Letters,* **7**, 279–282.

Sieh, K., M. Stuiver, and D. Brillinger, 1989, A very precise chronology of earthquakes produced by the San Andreas fault in southern California, *Jour. Geophys. Res.,* **94**, 603–623.

Silgado, E., 1985, Destructive earthquakes of South America 1530-1894, *Earthquake Mitigation Program in the Andean Region, Project SISRA*, vol. 10, 315 pp., Lima, Peru.

Singh, S.K., L. Astiz, and J. Havskov, 1981, Seismic gaps and recurrence periods of large earthquakes along the Mexican subduction zone: a reexamination, *Bull. Seismo. Soc. America,* **71**, 827–843.

Singh, S.K., J.M. Espindola, J. Yamamoto, and J. Havskov, 1982, Seismic potential of the Acapulco-San Marcos region along the Mexican subduction zone, *Geophys. Res. Letters,* **9**, 633–636.

Singh, S.K., T. Dominguez, R. Castro, and M. Rodriguez, 1984, P waveforms of large shallow earthquakes along the Mexican subduction zone, *Bull. Seismo. Soc. America,* **74**, 2135–2156.

Singh, S.K., L. Ponce, and S.P. Nishenko, 1985, The great Jalisco, Mexico earthquakes of 1932: subduction of the Rivera plate, *Bull. Seismo. Soc. America,* **75**, 1301–1313.

Spence, W., 1977, The Aleutian arc: tectonic blocks, episodic subduction, strain diffusion, and magma generation, *Jour. Geophys. Res.,* **82**, 213–230.

Spence, W., 1989, Stress origins and earthquake potentials in Cascadia, *Jour. Geophys. Res.,* **94**, 3076–3088.

Sykes, L.R., 1971, Aftershock zones of great earthquakes, seismicity gaps, and earthquake prediction, *Jour. Geophys. Res.,* **76**, 8021–8041.

Sykes, L.R. and R.C. Quittmeyer, 1981, Repeat times of great earthquakes along simple plate boundaries, in *Earthquake Prediction, An International Review, Maurice Ewing Ser.* 4, edited by D.W. Simpson and P.G. Richards, AGU, Washington, D.C., 217–247.

Sykes, L.R. and S.P. Nishenko, 1984, Probabilities of occurrence of large plate rupturing earthquakes for the San Andreas, San Jacinto, and Imperial faults, California: 1983–2003, *Jour. Geophys. Res.,* **89**, 5905–5928.

Taylor, F.W., R.L. Edwards, G.J. Wasserburg, and C. Frolich, 1988, Seismic recurrence intervals and timing of aseismic subduction inferred from emerged corals and reefs of the central Vanuatu (New Hebrides) frontal arc, *Jour. Geophys. Res.*, submitted.

Thatcher, W. and M. Lisowski, 1987, Long-term seismic potential of the San Andreas fault southeast of San Francisco, *Jour. Geophys. Res.,* **92**, 4771–4784.

UNAM Seismology Group, 1986, The September 1985 Michoacan earthquakes: aftershock distribution and history of rupture, *Geophys. Res. Letters,* **13**, 573–576.

Uyeda, S. and H. Kanamori, 1979, Back-arc opening and the mode of subduction, *Jour. Geophys. Res.,* **84**, 1049–1061.

Wesnousky, S.G, C.H. Scholz, K. Shimazaki, and T. Matsuda, 1984, Integration of geologic and seismologic data for the analysis of seismic hazard: a case study of Japan, *Bull. Seismo. Soc. America,* **74**, 687–708.

White, R.A., 1984, Catalog of historic seismicity in the vicinity of the Chixoy-Polochic and Motagua faults, Guatemala, *U.S. Geol. Survey Open File Rpt.* 84–88, ...pp.

White, R.A., 1985, The Guatemala earthquake of 1816 on the Chixoy-Polochic fault, *Bull. Seismo. Soc. America,* **75**, 455–473.

White, R.A. and I. L. Cifuentes, 1989, Seismic history of the Middle America trench spanning the Guatemala triple junction and an earthquake forecast, *Bull. Seismo. Soc. America*, in press.

Winslow, M.A., 1982, The structural evolution of the Magallanes Basin and the neotectonics in the southernmost Andes, *Antarctic Geosci.,* **4**, 143–154.

Working Group on California Earthquake Probabilities, 1988, Probabilities of large earthquakes occurring in California on the San Andreas fault, *U.S. Geol. Survey Open File Rpt.* 88-398, 62 pp.

Yamaguchi, D. K., 1989, Preliminary tree-ring dating of late Holocene subsidence along the Washington coast, *Quaternary Res.*, in press.

Appendix: Summary of Circum-Pacific Probability Estimates

	Location		Date of Last Event	Magnitude	Forecast Window	Conditional Probability 1989-1994	Conditional Probability 1989-1999	Conditional Probability 1989-2009
	SOUTH AMERICA							
	Chile							
C-1	Tierra del Fuego	65°-72°W	1949	7.7	1995-2064	4%	11%	29%
C-2	Chilean Archipelago	46°-52°S	?		No historic	record of	great	earthquakes
C-3	Southern Chile	40°-46°S	1960	9.4	2043-2148	$\leq 1\%$	$\leq 1\%$	$\leq 1\%$
C-4	Concepcion	35°-40°S	1939-1960	7.9-8.3	2002-2078	1%	3%	12%
C-5	Valparaiso	32°-35°S	1985	8.0	2041-2109	$\leq 1\%$	$\leq 1\%$	$\leq 1\%$
C-5a	Pichilemu-Llico	34.5°-35°S	1906	(7.5-8.0)	1990-2044	17%	33%	59%
C-6	Coquimbo-Los Vilos	30°-32°S	1943	8.2	1991-2049	11%	24%	49%
C-7	Atacama	26°-30°S	1922	8.5	2002-2128	2%	4%	10%
C-8	Taltal-Copiapo	25°-27°S	1978	7.3	2005-2038	$\leq 1\%$	$\leq 1\%$	15%
C-9	Paposo	25°-24°S	?		No historic	record of	great	earthquakes
C-10	Arica-Antofagasta	19°-24°S	1877	9.0	(1992-2074)	(10%)	(20%)	(39%)

Appendix con't. Summary of Circum-Pacific Probability Estimates

	Location		Date of Last Event	Magnitude	Forecast Window	Conditional Probability 1989-1994	1989-1999	1989-2009
			SOUTH AMERICA					
	Peru							
P-1	Arica	19°-16.6°S	1868	9.0	(1991-2300)	($\leq$ 1-12%)	($\leq$ 1-23%)	($\leq$ 1-43%)
P-2	Camana	16.6°-15.8°S	1913	7.8	1993-2073	6%	13%	29%
P-3	Nazca	15.8°-14°S	1942	8.2	(2109-2396)	($\leq$ 1%)	($\leq$ 1%)	($\leq$ 1%)
P-4a	Lima-Pisco	12°-14°S	1974	8.0	2028-2097	$\leq$ 1%	$\leq$ 1%	$\leq$ 1%
P-4b	Pisco-Ica	12°-14°S	1813	?	(1991-2079)	(14%)	(28%)	(47%)
P-5	Chimbote-Lima	10°-12°S	1940/1966	8.2,8.1	1996-2089	$\leq$1-3%	$\leq$ 1-8%	1-24%
P-6	Chimbote-Guayaquil	2°-10°S	?		No historic	record of	great	earthquakes
	Ecuador-Colombia							
EC-1	Jama	0.5°S-1.2°N	1942	7.9	(1990-2015)	(41%)	(66%)	(90%)
EC-2	Esmeraldas	1.2°-1.7°N	1958	7.8	1993-2044	8%	19%	46%
EC-3	Tumaco	1.7°-4°N	1979	7.7	2023-2098	$\leq$ 1%	$\leq$ 1%	$\leq$ 1%
EC-4	Buenaventura	4°-7.5°N	?		No historic	record of	great	earthquakes

Appendix con't. Summary of Circum-Pacific Probability Estimates

	Location		Date of Last Event	Magnitude	Forecast Window	Conditional Probability 1989-1994	1989-1999	1989-2009
			CENTRAL AMERICA					
	Panama							
P-1	San Blas	77°-79.5°W	1882	7.5±	Incomplete	historic	record	
	Costa Rica							
CR-1	Papagayo	87°-86°W	1916	7.5	(1991-2051)	(16%)	(31%)	(55%)
CR-2	Nicoya	86°-85°W	1978	7.3	1993-2010	9%	43%	93%
CR-3	Quepos	85°-84°W	1952	7.0	1996-2067	3%	8%	25%
CR-4	Osa	84°-83°W	1983	7.3	2010-2041	≤ 1%	≤ 1%	4%
	Nicaragua and El Salvador							
ES-1	C. El Salvador	89°-88°W	1926	7.2	Incomplete	historic	record	
N-1	West Nicaragua	88°-87°W	1921	7.4	Incomplete	historic	record	
N-2	East Nicaragua	87°-86°W	1898-1907	7.0-7.2	Incomplete	historic	record	
	Guatemala							
G-1	Motagua	88.3°-91°W	1976	7.5	2392-3117	≤ 1%	≤ 1%	≤ 1%
G-2	E. Chixoy-Polochic	89.0°-90.5°W	1785	(7.3)	(1996-2207)	(4%)	(8%)	(15%)
G-3	W. Chixoy-Polochic	90.5°-91.5°W	1812	(7.5)	(1996-2207)	(4%)	(8%)	(15%)
G-4	Northwest	92.5°-91.5°W	1942	7.9	(1994-2056)	(5%)	(13%)	(34%)
G-5	Central	91.5°-90.5°W	1942	7.9	1992-2041	10%	23%	50%
G-6	Southeast	89°-90.5°W	1915	7.4	1990-2025	29%	51%	79%

Appendix con't. Summary of Circum-Pacific Probability Estimates

	Location		Date of Last Event	Magnitude	Forecast Window	Conditional Probability 1989-1994	1989-1999	1989-2009
			CENTRAL AMERICA					
	Mexico							
M-1	Chiapas	92.5°-94°W	1902	7.8	(2008-2151)	(1%)	(2%)	(5%)
M-2	Tehuantepec	94°-95.2°W	?		No historic	record of	great	earthquakes
M-3	East Oaxaca	95.2°-96.4°W	1965	7.8	1991-2026	15%	35%	70%
M-4	Central Oaxaca	96.4°-97.3°W	1978	7.8	2013-2060	$\leq$ 1%	$\leq$ 1%	2%
M-5	Central Oaxaca	97.3°-97.7°W	1928	7.8	(1990-2032)	(25%)	(45%)	(72%)
M-6	West Oaxaca	97.7°-98.2°W	1968	7.4	1994-2025	6%	21%	64%
M-7	Ometepec	98.2°-99.3°W	1950	7.3	1990-2030	26%	47%	74%
M-8	Acapulco-San Marcos	99.3°-100°W	1957	7.7	1994-2042	5%	13%	40%
M-9	Central Guerrero	100°-101°W	1899-1911	7.8	(1990-2068)	(16%)	(30%)	(52%)
M-10	Petatlan	101°-101.8°W	1979	7.6	2001-2038	$\leq$ 1%	3%	29%
M-11	Michoacan	101.5°-103°W	1985	8.1	2029-2106	$\leq$ 1%	$\leq$ 1%	$\leq$ 1%
M-12	Colima	103°-103.7°W	1973	7.5	1993-2025	8%	25%	66%
M-13	Colima Gap	103.7°-104.5°W	?		No historic	record of	great	earthquakes
M-14	Jalisco	104.3°-105.7°W	1932	8.2	1992-2129	1-9%	2-18%	7-37%

Appendix con't. Summary of Circum-Pacific Probability Estimates

	Location		Date of Last Event	Magnitude	Forecast Window	Conditional Probability 1989-1994	1989-1999	1989-2009
			NORTH AMERICA					
	California							
SA-1	Olema	40.4°-37.5°N	1906	8.0	2049-2452	$\leq$ 1%	$\leq$ 1%	1%
SA-2	Peninsula	37.5°-36.8°N	1906	(7.0)	(1992-2218)	(2-8%)	(5-15%)	(11-30%)
SA-3	Santa Cruz	37°-36.8°N	1906	(6.5)	(1995-2165)	(5%)	(9%)	(19%)
SA-4	Central Creeping Zone	36.8°-35.7°N	?		No historic	record of	great	earthquakes
SA-5	Parkfield	35.7°-37°N	1966	6.0	1989-2000	70%	93%	$\geq$99%
SA-6	Cholame	35.7°-35.3°N	1857	(7.0)	(1994-2234)	(5%)	(11%)	(20%)
SA-7	Carrizo	35.3°-34.7°N	1857	8.0	2018-2370	1%	1%	3%
SA-8	Mojave	34.7°-34.3°N	1857	7.5	1993-2179	6%	11%	22%
SA-9	San Bernardino	34.3°-33.8°N	1812(?)	(7.5)	(1995-2358)	(4%)	(8%)	(15%)
SA-10	Coachella	33.8°-33.4°N	1680	7.5	1993-2167	7%	14%	26%
	Washington-Oregon							
WO-1	SW Washington	48.3°-45.5°N	1680	(8.0)	(2080-2750)	($\leq$ 1%)	($\leq$ 1%)	($\leq$ 1%)

Appendix con't. Summary of Circum-Pacific Probability Estimates

	Location		Date of Last Event	Magnitude	Forecast Window	Conditional Probability 1989-1994	Conditional Probability 1989-1999	Conditional Probability 1989-2009
			NORTH PACIFIC					
	Queen Charlotte-Alaska-Aleutians							
QCAA-1	Cp. St. James	51.7°-52.4°N	1898(?)	7.6	(1991-2087)	(12%)	(22%)	(41%)
QCAA-2	Queen Charlotte	52.4°-56°N	1949	8.0	2000-2152	2%	4%	11%
QCAA-3	Sitka	56°-58°N	1972	7.3	2002-2042	$\leq$ 1%	2%	22%
QCAA-4	Lituya Bay	58°-60.5°N	1958	8.2	2002-2158	1%	4%	10%
QCAA-5	Yakutat	139°-142°W	1899	8.0	1992-2096	10%	19%	36%
QCAA-6	Yakataga	142°-145°W	1899	8.0	1991-2094	11%	21%	39%
QCAA-7	Pr. William Sound	145°-156°W	1964	9.0	2270-2645	$\leq$ 1%	$\leq$ 1%	$\leq$ 1%
QCAA-8	Kodiak Is.	150°-155°W	1964	(8.0)	(2002-2051)	(8%)	(16%)	(29%)
QCAA-9	Alaskan Penn.	156°-158.5°W	1938	8.0	1993-2051	8%	18%	41%
QCAA-10	Shumagin Is.	158.5°-161.7°W	1917	8.0	1990-2029	27%	48%	75%
QCAA-11	Unimak Is.	161.7°-164°W	1946	(7.4)	(1990-2047)	(25-31%)	(43-55%)	(67-82%)
QCAA-12	Fox Is.	164°-173°W	1957	(7.4)	(1990-2022)	(22%)	(44%)	(78%)
QCAA-13	Andreanof Is.	173°-177°W	1986	8.0	2013-2049	$\leq$ 1%	$\leq$ 1%	1%
QCAA-14	Delarof Is.	177°W-180°	1957	(7.4)	(1989-2004)	(59%)	(85%)	(98%)
QCAA-15	Rat Is.	180°-171°E	1965	8.0	2001-2061	1%	4%	17%
QCAA-16	Kommandorski Is.	171°-165°E	1858	(8.0)	Incomplete		historic	record

Appendix con't. Summary of Circum-Pacific Probability Estimates

	Location		Date of Last Event	Magnitude	Forecast Window	Conditional Probability 1989-1994	1989-1999	1989-2009
			WESTERN PACIFIC					
	Kamchatka							
KK-1	Kamchatsky Pen.	55°-57°N	1971	7.5	1993-2028	7%	23%	61%
KK-2	NE Kamchatka	53°-55°N	1923	8.3	2004-2137	1%	3%	8%
KK-3	SE Kamchatka	49°-53°N	1952	9.0	2021-2116	$\leq$ 1%	$\leq$ 1%	1%
KK-4	Shiashkotan Is.	48°-49°N	1915	8.0	(1992-2075)	(10%)	(20%)	(40%)
KK-5	Central Kurile	46°-48°N	?		No historic	record of	great	earthquakes
KK-6&7	Shimushir/Urup Is.	149°-153°E	1963	8.5	(1993-2037)	(8%)	(21%)	(52%)
KK-8	Etorofu Is.	148°-150°E	1958/78	8.3/7.6	(2011-2080)	($\leq$ 1%)	($\leq$ 1%)	(3%)
KK-9	Shikotan Is.	146.5°-148.5°E	1969	8.2	2015-2093	$\leq$ 1%	$\leq$ 1%	2%

Appendix con't. Summary of Circum-Pacific Probability Estimates

	Location		Date of Last Event	Magnitude	Forecast Window	Conditional Probability 1989-1994	Conditional Probability 1989-1999	Conditional Probability 1989-2009
			WESTERN PACIFIC					
	Hokkaido & E. Honshu							
J-1	Nemuro-Oki	146.5°-147°E	1973	7.8	2020-2102	$\leq$ 1%	$\leq$ 1%	1%
J-2	Tokachi-Oki	144.5°-146.5°E	1952	8.1	2018-2130	$\leq$ 1%	$\leq$ 1%	2%
J-3	Tokachi-Oki	142°-144°E	1968	8.2	2031-2112	$\leq$ 1%	$\leq$ 1%	$\leq$ 1%
J-4	Sanriku-Oki	37.7°-39°N	1897	7.6	1991-2109	3-11%	7-21%	17-39%
J-5	Miyagi-Oki	37.5°-39°N	1978	7.4	2004-2034	$\leq$ 1%	$\leq$ 1%	17%
J-6	Shioya-Oki	36°-38.5°N	1938	7.1-7.7	(2340-4360)	($\leq$ 1%)	($\leq$ 1%)	($\leq$ 1%)
J-7	Boso Pen.	35°-36°N	1703/1923	8.2/7.9	2060-2370	$\leq$ 1%	$\leq$ 1%	$\leq$ 1%
	SW Honshu							
J-8	Tokai	138°-139°E	1854	(8.4)	(1990-2112)	(8-17%)	(16-31%)	(30-53%)
J-9	Kii	136°-138°E	1944	8.1	2018-2120	$\leq$ 1%	$\leq$ 1%	2%
J-10	Nankai	133°-136°E	1946	8.1	2021-2124	$\leq$ 1%	$\leq$ 1%	1%
	Izu Bonin & Marianas							
IBM-1	Izu Bonin-Mariana	34°-10° N	?		No historic record of great earthquakes			

Appendix con't. Summary of Circum-Pacific Probability Estimates

	Location		Date of Last Event	Magnitude	Forecast Window	Conditional Probability 1989-1994	1989-1999	1989-2009
			SOUTHWEST PACIFIC					
	New Britian-Solomon							
NB-1	West New Britain	148°-151°E	1945	7.9	(1990-2021)	(34%)	(58%)	(84%)
NB-2	East New Britain	151°-153°E	1971	7.9	1990-2012	29%	59%	92%
S-1	North Bougainville	153°-154.5°E	1971	8.0	1991-2013	23%	53%	90%
S-2	South Bougainville	154.5°-155.5°E	1975	7.8	1997-2034	2%	10%	44%
S-3	New Georgia	155.5°-157°E	1936	7.4	Incomplete historic record			
S-4	Woodlark Basin	157°-159°E	?		No historic record of great earthquakes			
S-5	Guadalcanal	159°-161°E	1988	7.5	1990-2034	25%	45%	71%
S-6	San Cristobal	161°-163°E	1931	8.0	(1990-2034)	(25%)	(45%)	(71%)
S-7	SE Solomons	163°-165°E	(1900?)		Incomplete historic record			
	Vanuatu							
VA-1a	Santa Cruz	11°-13°S	1966	8.1	1990-2020	23%	48%	82%
VA-1b	Vankolo Is.	11.9°S	1980	7.5	1990-2003	41%	83%	$\geq$ 99%
VA-2	Torres Is.	13°-14°S	?		No historic record of great earthquakes			
VA-3	N. Santo Is.	14°-15.2°S	1973	7.5	2036-2152	$\leq$ 1%	$\leq$ 1%	$\leq$ 1%
VA-4	S. Santo and	15.3°-16°S	1971	7.1	1990-2013	30%	60%	91%
	Malekula Is.	15°-17°S	1965	7.5	2109-2359	$\leq$ 1%	$\leq$ 1%	$\leq$ 1%
VA-5	Central Vanuatu	17°-21°S	?		Incomplete historic record			
VA-6	Loyalty Is.	21°-23°S	1980	7.2	1995-2016	3%	22%	80%
VA-7	Hunter Is.	171°-174°E	?		No historic record of great earthquakes			

Appendix con't. Summary of Circum-Pacific Probability Estimates

	Location		Date of Last Event	Magnitude	Forecast Window	Conditional Probability 1989-1994	Conditional Probability 1989-1999	Conditional Probability 1989-2009
			SOUTHWEST PACIFIC					
	Tonga-Kermadec							
TK-1	Tafahi Is.	15°-17.5°S	1917	8.4	Incomplete		historic	record
TK-2	Eua Is.	17.5°-20°S	1919	8.2	Incomplete		historic	record
TK-3	Tongatapu	20°-22°S	1948	8.0	1990-2020	33%	58%	84%
TK-4	Ata Is.	22°-23°S	?		Incomplete		historic	record
TK-5	Louisville Ridge	23°-25°S	1982	7.7	(2024-2130)	(≤ 1%)	(≤ 1%)	(≤ 1%)
TK-6	C. Tonga-Kermadec	25°-27°S	?		No historic	record of	great	earthquakes
TK-7	N. Kermadec Is.	27°-28.5°S	1986	8.1	2027-2099	≤ 1%	≤ 1%	≤ 1%
TK-8	S. Kermadec Is.	28.5°-30.2°S	1976	7.9	2011-2072	≤ 1%	≤ 1%	3%
TK-9	Southern Kermadec	30.2°-38°S	?		No historic	record of	great	earthquakes

Notes:

Magnitudes are M_S unless otherwise noted.
Forecast window represents the 90% confidence interval about the expected recurrence time, and is conditional upon the event not having occurred by 1989.
All values in parentheses reflect less reliable estimates.